AN ABSTRACT OF THE THESIS OF

Fareed H. A. N. Mohammed for the degree of Doctor of Philosophy in Soil Science presented on July 23, 1992.

Title: Water and Solute Transport : Modeling and Application to Water Conservation in Layered Soil

Redacted for Privacy

Abstract approved: _____
Benno P. Warkentin

Sandy soils are among the least productive soils because of their inability to store adequate water for plant growth. Their high percolation rate not only allows water to move quickly beyond the root zone, but also washes nutrients below the reach of plant roots. High evaporation occurs from the soil surface. Many acres of these soils around the world are left out of crop production. This study is a contribution to bring these soils into production by increasing their ability to hold more water in the root zone. Several promising methods of enhancing these soils were simulated, surface mulch, buried barrier layer, and a combination of both. The effects of varying texture and thickness of these layers and varying evaporative demand were investigated. The impact of such modifications on solute distribution in the soil was also simulated. A simulation model of water and solute transport in layered soils was developed for this purpose.

The Richards equation for one-dimensional water transport in unsaturated soils

was modified to account for the water jump between the layers. The solute transport equation was also modified by implementing the same theory of water infiltration in layered soil to the solute convective transport. The Crank-Nicolson scheme was used to solve the transport equations with the help of the Newton-Raphson iteration method.

The results of the simulation show that the proposed methods increase water content in the sandy soil by up to 45%. The combination of barriers, which decreases leaching and evaporation was the most effective in conserving water. Most of the contribution came from the influence of the mulch layer in suppressing water losses by evaporation. The combination method traps solute in the root zone, and this decreased solute leaching from the soil may limit plant growth in saline soils.

WATER AND SOLUTE TRANSPORT: MODELING AND APPLICATION TO WATER CONSERVATION IN LAYERED SOIL

by

Fareed H. A. N. Mohammed

A THESIS

submitted to

Oregon State University

in partial fulfillment of

the requirements for the

degree of

Doctor of Philosophy

Completed July 23, 1992

Commencement June 1993

APPROVED:

Redacted for Privacy

Professor of Soil Science in charge of major

Redacted for Privacy

Head of Department of Crop and Soil Science

Redacted for Privacy

Dean of the Graduate School

Date thesis is presented: July 23, 1992

Typed by: Fareed H. A. N. Mohammed

ACKNOWLEDGEMENT

I would like to express my appreciation and gratitude to my Professor Dr. Benno P. Warkentin, who has been for me and will remain the teacher, the advisor, the guidance, and the friend. I feel very honored to have worked under his supervision.

I would also like to thank Professor Larry Boersma, whose help I have often sought and have never been denied.

My thanks also extended to Professor James Vomocil, not only for serving on my graduate committee, but also for giving me his valuable time during my study.

I would also like to thank my graduate committee members, Professor Richard Cuenca, Professor Jonathan Istok, Professor Arsalan Mazaheri, and Professor Ronald Neilson.

My deepest thanks and love are for my parents, my wife, and my children for their patience and support during my study.

This dissertation is dedicated to my parents, for whom my education is their dream, to my wife, my children, my sisters, and my brother.

TABLE OF CONTENTS

TABLE OF CONTENTS (continued)

LIST OF FIGURES

LIST OF APPENDIX FIGURES

LIST OF APPENDIX FIGURES (continued)

LIST OF APPENDIX FIGURES (continued)

LIST OF APPENDIX FIGURES (continued)

LIST OF TABLES

WATER AND SOLUTE TRANSPORT: MODELING AND APPLICATION TO WATER CONSERVATION IN LAYERED SOIL

1. INTRODUCTION

1.1 Introduction

Water is the most essential element for all creatures, without which no life is expected. Plants are no exception, they depend totally on water. In an actively growing plant, water constitutes more than 90 percent of its fresh weight. For plants to survive they must supply enough water to satisfy the atmospheric demand, and to maintain enough water in cells to complete the metabolism processes. Regardless of water resource, the main source of water for plants is the soil water. Soils have a great influence on plant survival; storage and conduction of water to plant roots are the limiting factors for plant growth. With adequate water in the soil, plants show no signs of wilting and grow very well. However, soils show great variability in their ability to store and conduct water. The amount of water transmitted or stored in the soil is highly affected by physical properties such as texture and structure.

Some soils can store water for longer periods because of lower transmission while others store water for very short time. Retarded water movement can create drainage problems.

Sandy soils are among the least productive soils because of their inability to

store adequate water for plant growth, and their high percolation rate which not only lets the water move faster beyond the root zone, but also washes nutrients to a zone out of reach of plant roots.

These soils require short irrigation intervals and frequent fertilizer applications, but this increases the production cost and will be feasible only in areas where there is enough water. In arid regions and places short of irrigation water, the problem of sandy soils becomes more serious. That is why many acres of sandy soils are left unused in agricultural production. This problem becomes worse when such soils are in an extremely arid location with very high evaporation rates, rare rainfall, and shortage of irrigation water. Modification of such soils can increase and enhance their productivity.

Many studies have been conducted in past decades to investigate the feasibility of enhancing soils to increase water holding capacity. Some of these studies were concerned with rapid deep percolation of the water. Barrier layers made of compacted soil, plastic sheets, asphalt, or soil conditioners were mainly used to decrease water movement below the soil root zone (Diebold, 1954; Jamison and Kroth, 1958; Eagleman and Jamison, 1962; Miller and Bunger, 1963; Willis, et al, 1963; Erickson, et al, 1968; Hedrick and Mowry, 1952; Unger, 1971; Garber and Zaslavsky, 1977; Miller, 1979; Hemyari and Nofziger, 1981; Tayel, et al, 1981; Tayel and El-Hady, 1981; Kumar, et al, 1984; Johnson, 1984; Baasiri, et al, 1986; and Wallace, et al, 1986).

Other studies were concerned with decreasing evaporation from the soil surface using

different types of mulching (Lemon, 1956; Hanks and Woodruff, 1958; Willis, 1962; Willis, et al, 1963; Greb, 1966; Griffin, et al, 1966; Unger, 1971; El-Hady, et al, 1981; and Hartmann, et al, 1981).

In both cases the studies show significant increases in water content in the soil. Application of such work would solve the problem of sandy soils to a certain degree, depending on the type of application. The response to such applications varies from one soil to another.

Many questions arise in considering modifying a given soil under a given climatic regime. What is a suitable method; would a barrier layer be sufficient, or would a mulch layer alone be sufficient, or both be required; what would be the optimum thickness, density, and porosity of the barrier layer or mulch layer; what would be the optimum depth of the barrier layer for maximum water storage ? Answering all these questions would involve many experiments. For each soil and different climatic regime another set of experiments would be required. Although experiments can give reliable results, they are costly and time consuming.

Where the soil processes are understood, simulation models are very important tools for predicting effects in a short time and with low cost compared with experiments. A good simulation model can answer all those questions in short time with low error.

This study concerns modification of sandy soils to increase their ability to retain water. This can be done by changing structure or physical properties, adding soil conditioners or semi-impermeable layers beneath the root zone, or compacting the

lower layers to decrease the size of macro pores that are responsible for rapid percolation. Also evaporation from the soil surface can be reduced by modifying the soil surface with a soil conditioner or adding a layer of coarser material to break continuity of liquid water conducting to the soil surface.

Soil water determines solute behavior in soils; accordingly, any soil modification that affects water flow will have a direct influence on solute displacement and distribution in the soil. A particular method may increase water content, but at the expense of increasing soil salinity which may threaten plant growth. The method of soil modification must not develop a salinity or drainage hazard.

1.2 The objectives

The primary objective of this study is to simulate and evaluate methods to increase soil water storage by modification of the soil root zone. The consequences on solute behavior will be studied and considered in the evaluation. The work will be achieved in five steps:

1. Model development.

   A mathematical model will be developed to simulate one-dimensional water and solute transport in layered bare soil.

2. Computer program.

   A computer program will be developed to estimate water and solute transport in layered soil.

3. Model verification and calibration.

   One or two sets of measured data (soil hydraulic properties) of a layered soil will be used to calibrate the model. The model will be modified as necessary.

4. Simulation.

   The behavior of the modified soil will be simulated to determine time and quantity aspects of water storage. Several methods will be used to deal with the upper (mulching) and lower (barrier) layers of the soil profile. Details of these methods will be described in the following chapters.

   The impact of a given method of modification on soil salinity will also be modeled and simulated.

5. Evaluation and method selection.

All the methods will be evaluated under given soil and climatic conditions in order to select the optimum one. The optimum method is defined when the balance of all of the following components is accomplished by the method:

a. More water is stored in the root zone for the benefit of the plant.

b. Water remains for a longer time in the root zone for the benefit of the plant.

c. No hazards of solute that may threaten plant growth occur in the root zone.

d. No hazards of drainage problems that may threaten plant growth ere developed in the root zone .

2. WATER MOVEMENT IN SOILS

2.1 Factors affecting water movement

During and after rainfall or irrigation, water penetrates the soil surface and moves downward to lower layers in the soil. Soil physical properties and the atmosphere determine rate and direction of water movement in the soil.

The atmosphere may affect water movement directly through evaporation from the soil surface, causing upward movement of water, or by adding water to the soil through rainfall and initiating downward movement. The effect of the atmosphere also occurs through plant water uptake.

The soil physical properties of soil texture and soil structure control water storage and transmission in the soil. They determine the soil water potential and soil hydraulic conductivity which are the basic parameters of soil water movement.

Soil water moves from places of higher potential to areas of lower potential to reach equilibrium. The difference in water potential between two points is the driving force which causes the movement of water in the soil. Evaporation and water uptake by plants cause decreases in soil water potential, and hence cause water movement to those sites. Due to its continuous movement, soil water in the field rarely reaches equilibrium. The rate of water movement is governed primarily by the hydraulic conductivity of the soil.

2.2 Soil water potential

Soil water potential or total potential of water in the soil, ψ, is the summation of three major components that affect the state of water in the soil, namely, gravitational potential, ψ_g, pressure potential, ψ_p, and osmotic potential, ψ_o.

$$\psi = \psi_g + \psi_p + \psi_o \qquad (1)$$

Gravitational potential is affected by the elevation of a point under study from an arbitrary reference level. The osmotic potential becomes an effective part in the presence of solutes and a membrane, for example, in the interaction zone between plant root and soil or where water vapor moves by diffusion.

The most important part of the total soil water potential is the pressure potential. It is the product of capillarity and adsorption forces between water and soil particles. The relative importance of these two mechanisms depends upon soil texture and soil structure, which determine the pore size distribution and the continuity of the capillary system in the soil. Clay soils exhibit both adsorption and capillarity, while in sandy soils, the capillarity is dominant.

At higher values of water potential (0 to -1 bar), the amount of water retained in the soil depends mainly on capillarity and hence pore size distribution; therefore it is highly influenced by soil structure. At lower water potential, water is retained in the soil primarily due to adsorption, which is affected mainly by soil texture, (Hillel, 1982). Clay soils tend to retain more water than sandy soils at various levels of water potential. This is due to a number of reasons. Clay soils have more surface for

absorption than sandy soils, which allow them to retain more water at very low levels of water potential. Second, sandy soils contain macro pores, which are the first to be emptied at a given potential, while clay soils contain mainly micro pores in a more uniform size distribution.

Changing soil structure will affect water retention, for instance, compaction of sandy soil will decrease the number of large pores. Although the amount of water at saturation will be decreased, compaction will also reduce the initial water content loses when soil water is subject to a small negative potential.

The soil water potential is related to soil water content as illustrated in the soil moisture characteristic curve. The relationship between both is highly nonlinear and affected by hysteresis. The shape of the curve which describes the relationship between pressure potential and water content of the soil depends on the direction of water flow in the soil. During the infiltration (wetting) process, the values of water content for a given pressure potential, at equilibrium, is less than that in the redistribution (drying) process.

2.3 Hydraulic conductivity

The soil hydraulic conductivity is defined as the ratio of water flux to the hydraulic gradient. When the soil is saturated, the entire volume of soil pores conducts water. At this point the hydraulic conductivity is maximal and is called saturated conductivity. As water content decreases and the larger pores empty, water exists in the small pores

and in envelopes surrounding soil particles. In this situation, water is conducted through the small pores and between the envelopes, accordingly, water conductivity decreases and is said to be unsaturated.

The hydraulic conductivity is influenced by soil factors such as pore size distribution, total porosity, and tortuosity. Other factors are fluid dependent, such as viscosity and density. Temperature affects hydraulic conductivity through changes in viscosity and the density of the fluid, and accordingly will change the hydraulic conductivity. Entrapped, released, or dissolved air during water flow will also change the measured hydraulic conductivity (Yong and Warkentin, 1975, Hillel, 1982, Iwata et al, 1988).

For a given soil, the unsaturated hydraulic conductivity strongly depends on the water content, the relationship between conductivity and water content is highly non linear. The soil hydraulic conductivity reaches its maximum magnitude at saturation and as water content decreases, the hydraulic conductivity decreases rapidly. This relation varies from soil to soil and is affected by hysteresis.

In fine-grained soils such as clay soils, the hydraulic conductivity is very low due to the narrow water conducting pores, but these pores are continuous at low level of water content compared to coarser-grained soils. Sandy soils which have a large number of macro pores tend to have higher conductivity at saturation than clay soil. But as water content decreases, the conductivity of sands decreases more rapidly than in finer grained soils owing to the emptying of large pores which are responsible for the rapid water movement.

2.4 Governing equations of water flow in soils

The equation of water flow in porous media was first introduced by Darcy, 1856, in his study on water filtration through sand beds. The form of his equation, known as Darcy's Law, may be written as:

$$q = K \frac{\Delta \psi}{L} \qquad (2)$$

where:

q = water flux, L T^{-1}

K = hydraulic conductivity, L T^{-1}

ψ = hydraulic head, L

L = length of soil column, L

The assumptions for this equation are that the flow is steady and saturated in a uniform soil. The relationship between the hydraulic gradient and the flux is linear, and the slope of the line represents the hydraulic conductivity. Therefore, average variables of hydraulic head and hydraulic conductivity along the flow path are sufficient to calculate the flux using this equation.

Obviously these assumptions rarely occur in the field. Most likely, the soil water in the field is neither steady nor saturated, and therefore, water content, water potential, and hydraulic conductivity vary along the flow path. Accordingly, generalized variables such as averaging over hydraulic head and conductivity will not

be suitable to be used in the field conditions. Localized variables are more suitable to be used in conditions where flow is transient and unsaturated such as under field condition.

Richards, (1931), considered these conditions when he extended the Darcy equation to describe water flow in unsaturated conditions. The form of his equation for one-dimensional downward flow may be written as:

$$q = - K(\psi_p) \frac{\partial \psi}{\partial z} \qquad (3)$$

where z is soil depth. In this equation, the hydraulic conductivity is no longer a single value of the soil, but is a function of pressure potential.

By combining the Darcy equation with the continuity equation, the general water flow equation for one-dimensional transient condition can be written as (Richards, 1931):

$$\frac{\partial \theta}{\partial t} = - \frac{\partial}{\partial z} q \qquad (4)$$

where t is time and θ is water content. By substituting Equation.3 into Equation.4 for vertical flow, it becomes:

$$\frac{\partial \theta}{\partial t} = - \frac{\partial}{\partial z} \left(K(\psi_p) \frac{\partial \psi}{\partial z} \right) \qquad (5)$$

As mentioned earlier, soil water potential, ψ, is a summation of pressure potential, ψ_p, and gravitational potential, ψ_g, (neglecting the osmotic potential, ψ_o). Therefore Equation.5 becomes:

$$\frac{\partial \theta}{\partial t} = \frac{\partial}{\partial z}\left(K(\psi_p)\ \frac{\partial \psi_p}{\partial z} \right) - \frac{\partial K(\psi_p)}{\partial z} \qquad (6)$$

This form of Richards equation neglects the hysteresis in the function $K(\psi_p)$. Therefore, application of this equation in situations where wetting and drying processes occur (redistribution) will be affected by hysteresis (Miller and Miller, 1956). However, the hydraulic conductivity as a function of water content, $K(\theta)$ is less hysteretic than $K(\psi_p)$ (Hillel, 1982), therefore Equation.6 could be written as:

$$\frac{\partial \theta}{\partial t} = \frac{\partial}{\partial z}\left(K(\theta)\ \frac{\partial \psi_p}{\partial z} \right) - \frac{\partial K(\theta)}{\partial z} \qquad (7)$$

To simplify Equation.7, the flux could be related to either soil water content, θ, or soil water pressure potential, ψ_p. To solve for water content, the pressure potential gradient must be replaced by moisture gradient by using the chain rule as follows:

$$\frac{\partial \psi_p}{\partial z} = \frac{d\psi_p}{d\theta}\ \frac{\partial \theta}{\partial z} \qquad (8)$$

then Equation.7 will be:

$$\frac{\partial \theta}{\partial t} = \frac{\partial}{\partial z}\left(K(\theta)\ \frac{d\psi_p}{d\theta}\ \frac{\partial \theta}{\partial z} \right) - \frac{\partial K(\theta)}{\partial z} \qquad (9)$$

If the hydraulic diffusivity term, $D(\theta)$, is applied, the two dependent variables (ψ_p and θ) in Equation.9 can be reduced to one. $D(\theta)$ is defined as:

$$D(\theta) = K(\theta) \frac{d\psi_p}{d\theta} \qquad (10)$$

The values of $d\psi_p/d\theta$ can be found from soil moisture characteristic curves. Then Equation.9 becomes:

$$\frac{\partial \theta}{\partial t} = \frac{\partial}{\partial z}\left(D(\theta) \frac{\partial \theta}{\partial z} \right) - \frac{\partial K(\theta)}{\partial z} \qquad (11)$$

To solve Equation.7 for water potential, the following form may applied:

$$\frac{d\theta}{d\psi_p} \frac{\partial \psi_p}{\partial t} = \frac{\partial}{\partial z}\left(K(\psi_p) \frac{\partial \psi_p}{\partial z} \right) - \frac{\partial K(\psi_p)}{\partial z} \qquad (12)$$

Again, the values of $d\theta/d\psi_p$ can be found from soil moisture characteristic curves.

Although Equation.11 is less subject to hysteresis than Equation.12, application of these equations in highly hysteretic soils will not be free from error. Equation 11 and 12 can be used to solve unsaturated transient flow in uniform soils only.

Soils in the field are uniform neither in the material nor in properties. The soil profile typically consists of different layers, and each layer has its own properties. Accordingly, water content, water potential, and hydraulic conductivity vary with distance (different layers may have different characteristics). Water flow in such soils is unlike that of homogeneous soil. Each layer has its own relationship for flowing water, and the least permeable layer controls the other layers when they are combined in one domain.

Therefore, Equation.11 and 12 cannot be applied in layered soils. Modifications with respect to soil heterogeneity must be added to these equations in order to make

them suitable to solve water flow problems in layered soils. More details about this will be provided in the next chapters.

3. FLOW RETARDATION AND WATER CONSERVATION

When rain or irrigation stops, water stored in the soil starts to decrease due to evaporation, drainage, and plant use. The rates of these processes of redistribution determine the amount of water stored in the soil for a given time, and are very important in the water supply for plants.

The parameters which affect soil water storage are identified in the general water balance equation:

$$\Delta S = P + I - R - D - E - T \qquad (13)$$

where ΔS is the change of water storage in the soil, P rainfall, I irrigation, R runoff, D drainage, E evaporation, and T is the transpiration. If it is assumed that there is no runoff and the amount of water which is depleted by the plant (transpiration) is the purpose of soil water storage, then the undesirable losses of water from the soil would be through evaporation and drainage. Therefore, to maintain an adequate level of water in the soil, the processes of evaporation and drainage must be eliminated or decreased in a way that the desired amount and quality of stored water in the root zone is achieved.

This type of water conservation was recognized and studied by many researchers, among them Hide (1954); Lemon (1956); Jamison (1960); Eagleman and Jamison (1961, 1962); Willis (1962, 1963); Miller and Gardner (1962); Miller and Bunger (1963); Griffin, et al (1966); Greb, et al (1967); Corey and Kemper (1968);

Erickson, et al (1968); Bond and Willis (1969); Miller (1979); and Unger (1971). Some of these studies concerned limiting the evaporation from soil, others were involved in decreasing deep and rapid percolation. Most of the studies show encouraging results toward the application of such practices for water conservation, specially in arid regions.

3.1 Inhibition of drainage processes

Water draining below the root zone to deeper soil layers in which the plant roots don't grow, is considered lost. Elimination or delay of water movement beyond the root zone will increase soil water storage.

As reviewed earlier, water movement in soil is affected mainly by soil texture and structure, through the effect on soil water retention and hydraulic conductivity. It was also mentioned that fine-grained soils retain water through both capillary forces and adsorption forces between water and soil particles, while in coarse-grained soils capillarity is dominant. As a result, fine-grained soils tend to retain more water at a given suction. Water flow at close to saturation is much slower in fine-textured soils than in coarse-textured soils, due to the large pores in the later. But as water content decreases, the conductivity in coarse-grained soils decreases more rapidly than in fine-grained soils.

This behavior of the soils can be used to favor soil water conservation, specially in sandy soils. For instance, in a situation where fine-textured soil overlays

coarse-textured soil, and under unsaturated water flow conditions, the initial water infiltration is controlled by the upper soil. When water reaches the interface, the infiltration rate may decrease since the wetting front is under high suction, which does not allow entry into the large pores of the lower soil. When the suction decreases sufficiently at the interface, due to pressure head build up, then water enters the lower soil (Hillel, 1982). Thus, water is conserved in the upper layer due to the delay of water movement, and plants could benefit from this water.

The effect of soil profile heterogeneity on water infiltration has been studied by many researchers. Alway and McDole (1917), found that with an interrupting (coarse-textured) layer of sand or gravel, the amount of water in the upper soil increased by 6% when compared to soil without an interrupting layer.

Miller and Gardner (1962) conducted extensive experiments on water movement from fine-textured to a coarse-textured soil. They observed that the infiltration was temporarily inhibited when the wetting front reached the interface. After water accumulated and the suction of the soil decreased sufficiently, water entered the coarser layer. The degree to which water flow is retarded was related to the differences of the pore size of the layers. As pore size of the coarser layer increases, the degree of flow retardation increases. The effect of gravity on the infiltration into coarser material was also studied. They found that upward infiltration was retarded for a longer time than downward infiltration. The water did not enter the coarser layer in upward infiltration during 15 hours of observation when 77% of the pores consist of 0.2 to 0.6 mm in size. Water entered the coarse layer in 303 second

for downward infiltration.

Miller and Bunger (1963) studied the effect of thickness and depth of the layer of coarse sand and gravel layers on water retention in the soil profile. They reported that a coarse-textured layer increased the water retention of the finer overlaying layer. They also observed that soils tend to retain more water with a gravel layer than with a sand layer.

Eagleman and Jamison (1962), tested the effect of soil layering on unsaturated water flow. When they placed fine-textured soil on top of coarse-textured soil, the top layer restricted the drainage to the lower layer. They found a very small decrease of water content (from 0.44 to 0.40 $cm^3.cm^{-3}$) of the top layer over 26 days after saturation . They observed that when water had to move to the lower layer, from small to large pores, the suction of the lower layer had to be as great as that of upper layer. The soil moisture characteristic curves of fine and coarse-textured soils showed that fine-textured soil would retain more water at the same suction when compared to coarse-textured soil. Stroosnijder, et al (1972) obtained similar results with a fine sand layer overlaying a coarse sand layer.

Sandy soils exhibit high percolation rate, the excess water from rainfall or irrigation moves downward rapidly and away from the reach of the roots. This water could be retained by placing a barrier layer in the soil. Erickson, et al (1968), studied this phenomenon using an asphalt barrier in sandy soil. Their report showed that water content of the soil was increased, and as a result, the yield of crops growing in the soil was increased significantly.

Another approach to increase soil water storage is the utilization of soil conditioners. Numerous studies where conducted. Hedrick and Mowry (1952) observed an increase in soil moisture content when the soil was treated with synthetic polyelectrolyte. They concluded that the treatment enhanced the soil structure and the effect was not an association of water with the polymer itself. Miller (1979) found that a polymer "super slurper" increased the water content of sandy soil to the level of loam and silt loam soils. He also observed a reduction of infiltration rate. The polymer had little effect on fine-textured soils. The same result was reported by Hemyari and Nofziger (1981). Tayel, et al (1981); Baasiri, et al (1986); and Johnson (1984b) found similar results with gel-forming polyacrylamide (PAM). However, the effect of soil conditioners and their water absorption properties may significantly decrease when the soil or irrigation water contains dissolved salts (Johnson, 1984a).

"Super gel" enhances soil water holding capacity. Tayel and El-Hady, (1981) found that the soil porosity and water retention was increased, while the rapidly drained pores, hydraulic conductivity, mean pore diameter, and evaporation was decreased when the soil is treated with "super gel".

The application of manure to sandy soil may enhance its hydraulic properties. A study by Kumar, et al (1984) has shown that manure increases soil water retention and decreases the hydraulic conductivity of sandy soils.

3.2 Inhibition of evaporation processes

Evaporation is an important component of water balance in soil. In arid regions, evaporation is considered to be the largest loss of water from the soil. The rate at which water evaporates from the soil depends mainly on two factors. The first factor is controlled by soil properties, which determine the amount of water that can be transmitted to the evaporating surface, which is in turn controlled by soil water potential and hydraulic conductivity of the soil. The second factor is the atmospheric condition, which includes the amount of energy supplied for evaporation and the vapor pressure gradient between the evaporating site and the atmosphere.

When the soil surface is wet, evaporation rate is initially constant and determined by the atmospheric demand. This is the first stage of evaporation. The second stage starts when the soil dries sufficiently and water transmission to the surface is decreased. The evaporation rate declines substantially in this stage. When the soil surface becomes dry and liquid water supply to the surface has ceased, water moves by the vapor diffusion process, which is very slow compared to liquid water. This is the third stage of evaporation. (Hide, 1954; Lemon, 1956; Hillel, 1982).

The greatest water loss occurs during the first stage of evaporation, where the maximum rate of evaporation occurs. This process lasts as long as water is supplied to the surface, with the assumption that the atmospheric evaporative demand is continuous. While the duration of this stage is generally short when compared to the second and third stages, significant amounts of water can be saved if this stage is

terminated rapidly.

Suppressing evaporation from soil surface has received the attention of Hide (1954) and Lemon (1956). Hide (1954) studied the moisture exchange between soil surface layers and the atmosphere. He indicated that there are at least three ways to decrease soil water evaporation: (1) decrease water movement to the soil surface before any drying occurs; (2) decrease the driving force for evaporation through decreasing the temperature of soil surface; and (3) increase the resistance to vapor diffusion by increasing the thickness of soil-atmosphere boundary layer.

Lemon (1956) reviewed the possibilities of decreasing losses of soil water by evaporation. His review included his work and Russian research work, as well as other studies. He said about these possibilities:

> " The potentialities for decreasing soil moisture evaporation lie in the first two categories of the loss process. These potentialities group themselves roughly into three divisions: (a) decreasing the turbulent transfer of water vapor above the ground surface; (b) decreasing the capillary conductance of water to the surface by decreasing capillary continuity; and (c) decreasing the capillary conductance of water to the surface by the application of surfactants."

Attempts to suppress evaporation due to turbulent transfer include limiting wind speed over the soil surface. Several methods have been employed to slow wind speed, including standing stubble, application of mulch material, trees or other obstacles as wind breaks, and increasing soil roughness. Hanks and Woodruff (1958) investigated the effect of wind on water vapor transfer for different mulches including soil, gravel, and straw. They found that as wind increases evaporation increases. This is due to increase in vapor diffusion as wind speed increases. Evaporation was

increased up to 2-6 times when wind increased from 0 to 25 mile/h for mulch treatments, while in no mulch treatment evaporation increased by 10 times. They have shown that soil mulch is more efficient to reduce evaporation than gravel or straw mulch especially at high wind speed. Under gravel and straw mulch evaporation was higher than under soil mulch. Gravel or straw mulch may, therefore, not be effective in reducing evaporation in windy regions. Benoit and Kirkham (1963) conducted similar experiments with addition of varying radiation. They obtained similar results as Hanks and Woodruff (1958) except that gravel mulch was found to be superior in evaporation reduction to straw and dust mulches. No explanation was given for this difference.

Suppression of evaporation by reduction of wind speed may not be effective, specially in warm regions. Poor wind circulation causes an increase in soil temperature which results in an increase in evaporation. Also, plant residue mulch may increase soil temperature and serve to retain heat especially at night when soil releases heat to the atmosphere (Lemon, 1956). Radiation effect on soil water evaporation is greater than wind effect (Hanks et al, 1967).

Interruption of continuity of liquid-water flow to the soil surface may serve as a barrier to upward water flow, when moisture flow to the surface is forced to be in the form of vapor diffusion, which is a much slower process when compared to liquid flow. The thickness of this barrier has a great influence on vapor diffusion. Lemon (1956) indicated that the maximum effect of the barrier appears at the first inch of its thickness, after that, the barrier thickness effect diminishes. Hanks and Woodruff

(1958) indicated that about 96% reduction in evaporation was observed when the mulch depth increased from 0 to 0.25 inch. Greb, et al (1967) found that the higher application of straw mulch results in less water loss due to evaporation. Hillel and Berliner (1974) found that when the depth of a hydrophobic aggregate layer increases the evaporation suppression increases. Similar effects were also found when the size of the aggregates was increased.

Lemon (1958) referred to experiments conducted by Kolasew (1941) to test the effect of soil stratification on the losses of soil moisture. The sequence of the layers, from top, was compacted-loose-compacted-loose. It was found that the soil water loss was decreased with the stratification. Lemon (1958) reported that Kolasew (1941) interpreted this reduction as due to two factors. The loose soil isolated the compacted layers, and accordingly, capillary continuity was minimized; also, less vapor conductance through compacted layers occurred because of the reduction of porosity.

Willis (1960) placed a coarse-textured layer over fine-textured soil. He found that evaporation was decreased even with the presence of a water table. Evaporation was also affected by the thickness of the coarse layer.

Modaihsh, et al (1985) obtained remarkable results when they applied sand mulch to suppress evaporation from the soil surface. The effect of thickness and texture of sand mulch under two different evaporation demands were examined in their study. They reported that a sand mulch layer of 6 cm thick was superior in reducing evaporation in all cases when compared with layers of 2 and 0 cm thick. The effect of texture was generally significant for both thickness of mulch layer and evaporative

demand. However the effect of the texture ranked second in importance.

Greb (1966) showed that straw mulch significantly reduced water loss via evaporation. Up to 70% reduction at the early evaporating stage was observed. However, when the soil water is depleted the effect of straw mulch diminishes. He reported that the effect of the mulch increased when the amount of mulch was increased. Similar results were obtained by Bond and Willis (1969) with rye straw mulch; Daisley, et al (1988) with grass mulch; and Bristow and Abrecht (1989) with coconut fiber as mulch.

Hanks, et al (1961) tested net radiation, soil temperature and evaporation as affected by surface cover including straw, black gravel, aluminum-painted gravel , and plastic. They reported that the highest net radiation was observed under black gravel, while soil temperature was highest under clear plastic. All of the treatments suppressed evaporation, however, differences between the mulches were not significant in the evaporation treatments.

The use of chemical additives as soil conditioners has shown reasonable success in decreasing evaporation from a soil surface. Hillel and Berliner (1974) found that hydrophobic aggregates reduced evaporation significantly. Callebaut, et al (1979); and El-Hady, et al (1980) obtained similar results. Callebaut, et al (1979) indicated that a great reduction in evaporation occurs in the first stage. Hartmann, et al (1981) found that water loss can be decreased by 50 % when the soil surface is treated with soil conditioners to form aggregates. Kowsar, et al (1969) showed an increase in soil water content with the application of petroleum mulch. They concluded that the mulch

prevented loss of water vapor from soil surface layer. Unger and Stewart (1974) observed reduction in evaporation from a soil surface treated with feedlot waste. Kumar, et al (1984); and El-Asswad and Groenevelt (1985) found that manure significantly reduced evaporation, again a great reduction found to be during the first stage of evaporation.

Rapid drying of the soil surface is another approach to decrease evaporation from the soil surface (Penman, 1941). This procedure is based on reaching the critical point at the end of the first stage and the beginning of the second stage of evaporation. Significant reduction of evaporation depends on how fast the critical point can be reached. This is the third potential process for decreasing evaporation according to Lemon (1956). Numerus research studies have been conducted. Kolasew (1941), quoted by Lemon (1956), treated a soil surface with hydrophobic material. He found that the treated soil dried more rapidly and reached the critical point at higher water content. After that point, the evaporation rate was slower for the treated soil.

Several other methods for suppressing evaporation from soil surface have been used. Willis, et al (1963) tested the effect of surface and subsurface plastic film as a mulch on soil moisture and temperature. Maximum water use efficiency was observed with 90% surface cover, and maximum yield was obtained for this treatment. They believed that the increase of yield was due to the increase of soil temperature. Buried plastic mulch (7-10 inches below surface) was not efficient. They also simulated the same experiment under controlled conditions in the laboratory, and found that a surface cover of plastic mulch reduced the evaporation significantly. Furthermore, the

higher the percentage of soil cover, the less evaporation was observed.

Griffin, et al (1966), investigating the effect of soil surface cover on water retention, found that a plastic cover (100% surface cover) reduced water loss by evaporation. Willis (1962) found that when evaporation demand increases, partial cover is not effective, and full cover is required for efficient evaporation reduction.

Mbagwu (1991) tested the effect of straw mulch, black polythene, and white polythene on the temperature and water content of the soil surface. He found 60 days after rainfall the soil water content was four times greater with mulch than without mulch. Furthermore, the permanent wilting point (PWP) was reached after 15 days for bare soil, while with mulch, the soil retained enough water during 60 days after rainfall and PWP was not reached.

Jury and Bellantuoni (1976b) studied the effect of surface rocks on heat and water movement in the soil. They observed considerable amount of water retained by the soil beneath rock when compared to bare soil. The reason for this behavior is that the rocks help in retaining soil heat at night. Net heat flow is toward the rocks, which induces water movement. Also rocks act as a barrier to evaporation (Jury and Bellantuoni, 1976a).

4. SIMULATION OF ONE-DIMENSIONAL UNSATURATED WATER FLOW IN LAYERED SOIL

The general water flow equation on the basis of water content for unsaturated soil was discussed earlier in chapter 2. This chapter will focus on the modification and the solution of the equation to accommodate water flow in layered profiles. The water flow equation based on water content for unsaturated homogenous soil can be written as:

$$\frac{\partial \theta}{\partial t} = \frac{\partial}{\partial z}\left(D(\theta)\ \frac{\partial \theta}{\partial z}\right) - \frac{\partial K(\theta)}{\partial z} \qquad (14)$$

where θ is the volumetric water content ($L^3\ L^{-3}$), t is the time (T), z is the soil depth (L), $K(\theta)$ is the hydraulic conductivity as a function of water content ($L\ T^{-1}$), and $D(\theta)$ is the soil hydraulic diffusivity as a function of water content ($L\ T^{-1}$). This equation has been widely used in solving problems of unsaturated flow in homogenous soils, however, the implementation of equation 14 in water flow problems in layered soil requires some modifications.

Figure 1 shows an example of a two layer profile, soil **A** and soil **B**, with interface **a** between them. For water to leave soil **A** and enter soil **B** it has to pass through the interface controlled by the characteristics of both soils. If the water content is a continuous function of depth between two different layers, the solution would be as simple as that for homogenous soil.

Since the water content across the interface may not be a continuous function

of the depth, equation 14 is not satisfied for this type of water flow. On the other hand, soil water potential is a continuous function of depth .

Hills etal (1989) introduced a new variable to account for the jump of water content across an interface and they show that the water content-based formulation can be used to simulate water flow in layered soil with the addition of a source term to the right-hand side of equation 14. Accordingly, equation 14 was modified for the points that surround the interface to handle the jump in water content between two layers. Therefore, equation 14 near the interface becomes:

$$\frac{\partial \theta}{\partial t} = \frac{\partial}{\partial z}\left(D(\theta)\ \frac{\partial \theta}{\partial z}\right) - \frac{\partial K(\theta)}{\partial z} - S \qquad (15)$$

to evaluate water content at a point just above the interface, and

$$\frac{\partial \theta}{\partial t} = \frac{\partial}{\partial z}\left(D(\theta)\ \frac{\partial \theta}{\partial z}\right) - \frac{\partial K(\theta)}{\partial z} + S \qquad (16)$$

to evaluate water content at a point just below the interface. The variable S is the source term that accounts for the jump, its derivation and the algorithm for its evaluation are given in details by Hills etal (1989). The evaluation of S will be illustrated in the subsequent sections.

Equations 14-16 together can be used to evaluate water flow in layered soil, where equation 14 is applied for the entire length of soil layer and equation 15 and 16 are applied only at the interface between two layers.

To obtain a unique solution for the system, boundary equations must be added for the upper and lower boundaries of the system as well as an initial condition. The

initial condition will be:

$$\theta(i,t) = \theta_{initial} \; ; \quad i = 0, 1, \ldots, m \quad at \quad t = 0 \qquad (17)$$

where $\theta_{initial}$ is the initial volumetric water content ($L^3\ L^{-3}$).

4.1 Boundary equation for soil surface:

The objectives of this study as stated earlier are to simulate the effect of soil layering on water storage and the impacts on solute distribution. Commonly, this type of investigation requires a dynamic boundary that involves infiltration and evaporation, therefore, a flux boundary condition was chosen at the soil surface. Accordingly, the flux condition at the surface is:

$$q = -D(\theta)\ \frac{\partial \theta}{\partial z} + K(\theta) \qquad (18)$$

where

$$q(0,t) > 0 \quad at \quad t \geq 0\ , \qquad (19)$$

$$q(0,t) = 0 \quad at \quad t \geq 0\ , \qquad (20)$$

or

$$q(0,t) < 0 \quad at \quad t \geq 0 \qquad (21)$$

where q is the Darcian flux ($L^3\ L^{-2}\ T^{-1}$) and is equal to the rate of water introduced at the soil surface. It is either positive when the condition is infiltration, zero for the

redistribution, or negative for the evaporation condition. Since the exact rate of infiltration is subject to soil conditions, higher values of q that exceed the infiltration capacity of the soil may introduce an error in the solution, therefore, low rates of water flux at the surface are applied in this study.

4.2 Boundary equation for soil bottom:

A semi-infinite soil profile is assumed for the lower boundary, that is, water will not reach the bottom of the soil during the simulation period, and there is no influence of water table. Hence, the water gradient at the soil bottom is assumed to be zero as described by the following equation:

$$\frac{\partial \theta}{\partial z}(z,t) = 0, \quad at \quad z = z_m, \quad t \geq 0 \qquad (22)$$

where m is the maximum depth of the soil profile. Values of z at $z = z_m$ must be relatively large, especially when the period of the simulation is large and/or higher rates of infiltration are specified at the surface, to ensure that water will not reach the bottom of the soil column during the computation.

4.3 Assumptions of the model:

This model approximates one-dimensional water flow in layered soil under the following assumptions:

1. While the effect of hysteresis on water distribution is very common in soils, inclusion of hysteresis in the solution adds some complications. Therefore, it is neglected.
2. The flow of water is isothermal.
3. The contribution of water vapor transport is considered very small, thus neglected.
4. Water flow at (or more than) complete saturation (100% saturation) is not supported. The maximum saturation allowed does not exceed 0.999999 of θ_s.
5. Presence of solute has no effect on water flow.

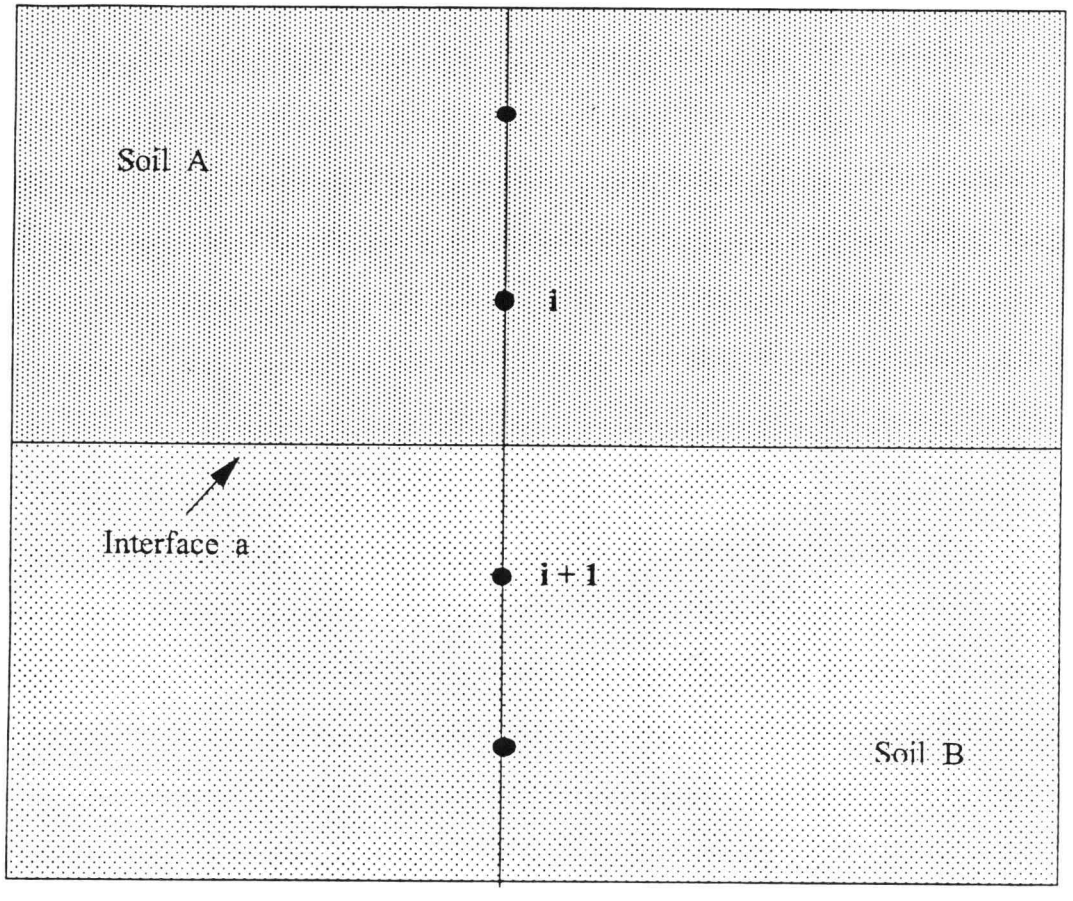

Figure 1: Sketch showing a profile of two soils (A and B) and the interface (a).

4.4 Solution to water flow equations

The Crank-Nicolson finite difference approximation for equation 14 is:

$$\frac{\theta_i^{n+1} - \theta_i^n}{\Delta t} = \frac{D(\theta)_{i+1/2}^{n+1/2}}{\Delta z_3}\left(\frac{\theta_{i+1}^{n+1} + \theta_{i+1}^n - \theta_i^{n+1} - \theta_i^n}{2\Delta z_2}\right) - \frac{D(\theta)_{i-1/2}^{n+1/2}}{\Delta z_3}\left(\frac{\theta_i^{n+1} + \theta_i^n - \theta_{i-1}^{n+1} - \theta_{i-1}^n}{2\Delta z_1}\right) - \frac{K(\theta)_{i+1/2}^{n+1/2} - K(\theta)_{i-1/2}^{n+1/2}}{\Delta z_3} \quad (23)$$

where:

$$D(\theta)_{i+1/2}^{n+1/2} = \frac{D(\theta)_{i+1}^{n+1} + D(\theta)_i^{n+1} + D(\theta)_{i+1}^n + D(\theta)_i^n}{4} \quad (24)$$

$$D(\theta)_{i-1/2}^{n+1/2} = \frac{D(\theta)_i^{n+1} + D(\theta)_{i-1}^{n+1} + D(\theta)_i^n + D(\theta)_{i-1}^n}{4} \quad (25)$$

$$K(\theta)_{i+1/2}^{n+1/2} = \frac{K(\theta)_{i+1}^{n+1} + K(\theta)_i^{n+1} + K(\theta)_{i+1}^n + K(\theta)_i^n}{4} \quad (26)$$

$$K(\theta)_{i-1/2}^{n+1/2} = \frac{K(\theta)_i^{n+1} + K(\theta)_{i-1}^{n+1} + K(\theta)_i^n + K(\theta)_{i-1}^n}{4} \quad (27)$$

$$\Delta z_1 = z_i - z_{i-1} \quad (28)$$

$$\Delta z_2 = z_{i+1} - z_i \tag{29}$$

$$\Delta z_3 = \frac{z_{i+1} - z_{i-1}}{2} \tag{30}$$

i and n are spatial node and time increments respectively, where i = 2, 3, ..., m - 1, where m is the last node in the domain.

Note that equation 14 is evaluated only at the interior nodes which are not neighboring the interface. For the two nodes that surround the interface only equations 15 and 16 are applied, therefore, the solution for the node that is just above the interface will be:

$$\begin{aligned}\frac{\theta_i^{n+1} - \theta_i^n}{\Delta t} = & \frac{D(\theta)_{i+1/2}^{n+1/2}}{\Delta z_4}\left(\frac{\theta_{i+1}^{n+1} + \theta_{i+1}^n - \theta_i^{n+1} - \theta_i^n}{2\Delta z_2}\right) \\ & - \frac{D(\theta)_{i-1/2}^{n+1/2}}{\Delta z_4}\left(\frac{\theta_i^{n+1} + \theta_i^n - \theta_{i-1}^{n+1} - \theta_{i-1}^n}{2\Delta z_1}\right) \\ & - \frac{K(\theta)_{i+1/2}^{n+1/2} - K(\theta)_{i-\frac{1}{2}}^{n+\frac{1}{2}}}{\Delta z_3} - \frac{D(\theta)_{i+1/2}^{n+1/2}}{\Delta z_4}\left(\frac{\Delta\theta^{n+\frac{1}{2}}}{\Delta z_2}\right)\end{aligned} \tag{31}$$

and for the node just below the interface will be:

$$\begin{aligned}\frac{\theta_i^{n+1} - \theta_i^n}{\Delta t} = & \frac{D(\theta)_{i+1/2}^{n+1/2}}{\Delta z_5}\left(\frac{\theta_{i+1}^{n+1} + \theta_{i+1}^n - \theta_i^{n+1} - \theta_i^n}{2\Delta z_2}\right) \\ & - \frac{D(\theta)_{i-1/2}^{n+1/2}}{\Delta z_5}\left(\frac{\theta_i^{n+1} + \theta_i^n - \theta_{i-1}^{n+1} - \theta_{i-1}^n}{2\Delta z_1}\right) \\ & - \frac{K(\theta)_{i+1/2}^{n+1/2} - K(\theta)_{i-\frac{1}{2}}^{n+\frac{1}{2}}}{\Delta z_3} + \frac{D(\theta)_{i-1/2}^{n+1/2}}{\Delta z_5}\left(\frac{\Delta\theta^{n+\frac{1}{2}}}{\Delta z_1}\right)\end{aligned} \tag{32}$$

where:

$$\Delta z_4 = \Delta z_2 + \frac{\Delta z_1}{2} \tag{33}$$

$$\Delta z_5 = \Delta z_1 + \frac{\Delta z_2}{2} \tag{34}$$

$$\Delta\theta^{n+\frac{1}{2}} = \frac{\Delta\theta^n + \Delta\theta^{n+1}}{2} \tag{35}$$

Note that the interface is required to be centered between the two surrounding nodes. The last term in the right hand side of equation 31 and 32 is the source term S which accounts for the jump of water content between soil layers, and $\Delta\theta$ is the difference in the water content between the bottom of the upper layer and the top of the lower layer at the interface. $\Delta\theta$ is evaluated according to Hills etal (1989):

$$\Delta\theta = \theta^+ - \theta^- \tag{36}$$

where θ^- is the volumetric water content ($L^3\ L^{-3}$) at the bottom of the soil layer just above the interface and θ^+ is the volumetric water content ($L^3\ L^{-3}$) at the surface of the soil layer just below the interface. The values of θ^- and θ^+ are unknown and they cannot be evaluated directly; their average is assumed to equal the value of water content at the interface θ_a (Hills etal, 1989). θ_a also cannot be evaluated directly since the water content is not continuous across the interface, whereas water potential at the interface ψ_a is continuous and can be estimated by using the conservation of mass equation for the flux entering and leaving the interface. These fluxes are required to be

equal since the thickness of the interface is zero and no storage can take place in the interface. Accordingly ψ_a will be (Hills etal, 1989):

$$\psi_a = \frac{2\{K(\theta)_i\,\psi(\theta)_i + K(\theta)_{i+1}\,\psi(\theta)_{i+1}\} + \Delta z\{K(\theta)_i - K(\theta)_{i+1}\}}{2\{K(\theta)_i + K(\theta)_{i+1}\}} \qquad (37)$$

where

$$\Delta z = z_{i+1} - z_i \qquad (38)$$

i in equation 37 and 38 represents the last node in the upper layer which is very close to the interface and ***i*+1** is the first node in the following layer which is also very close to the interface.

As soon as ψ_a is obtained, θ^- and θ^+ can be found from the corresponding $\psi(\theta)$ relationship for each soil, and accordingly $\Delta\theta$ can be calculated and substituted in the source term in equations 31 and 32 to satisfy the dynamic equation over the interface. (hereafter the notation ψ will be used to represent soil water potential, ψp).

4.5 Solution to the upper boundary equation

The upper boundary is of the flux type, therefore the finite difference formulation for the node at the soil surface will be:

$$\frac{\theta_1^{n+1} - \theta_1^n}{\Delta t} = \frac{D(\theta)_{1+1/2}^{n+1/2}}{(z_2 - z_1)^2}\left[\theta_2^{n+1} - \theta_1^{n+1}\right] - \frac{K(\theta)_{1+1/2}^{n+1/2}}{z_2 - z_1} + \frac{q^{n+1}}{z_2 - z_1} \qquad (39)$$

The last term in equation 39 represents the value of the boundary at an imaginary node at half space above the soil surface, where q is the Darcian flux ($L^3\ L^{-2}\ T^{-1}$)and equal to the rate of water introduced at the surface. It is either one of the following:

$$q(0,t) = \begin{cases} +q & \rightarrow \textit{Infiltration} \\ 0 & \rightarrow \textit{Redistribution} \\ -q & \rightarrow \textit{Evaporation} \end{cases} \quad at \quad t \geq 0 \qquad (40)$$

and

$$D(\theta)_{1+1/2}^{n+1} = \frac{D(\theta)_2^{n+1} + D(\theta)_1^{n+1}}{2} \qquad (41)$$

$$K(\theta)_{1+1/2}^{n+1} = \frac{K(\theta)_2^{n+1} + K(\theta)_1^{n+1}}{2} \qquad (42)$$

4.6 Solution to the lower boundary equation

A semi-infinite lower boundary was chosen, where no flow can take place below the lower boundary at depth $z = z_m$., therefore a fictitious node was specified below the soil profile at $z = z_{m+1}$. This node is always identical to node ***m*-1** and contains its identity. Accordingly, the solution for the lower boundary is similar to that in equation 23 with the exception of the fictitious node (which is equal to node ***m*-1**) instead of node ***m*+1** as in equation 23. Therefore, the solution will be as follows:

$$\frac{\theta_m^{n+1} - \theta_m^n}{\Delta t} = \frac{D(\theta)_{m+1/2}^{n+1/2}}{\Delta z_3}\left(\frac{\theta_f^{n+1} + \theta_f^n - \theta_m^{n+1} - \theta_m^n}{2\Delta z_2}\right) - \frac{D(\theta)_{m-1/2}^{n+1/2}}{\Delta z_3}\left(\frac{\theta_m^{n+1} + \theta_m^n - \theta_{m-1}^{n+1} - \theta_{m-1}^n}{2\Delta z_1}\right) - \frac{K(\theta)_{m+1/2}^{n+1/2} - K(\theta)_{m-1/2}^{n+1/2}}{\Delta z_3} \quad (43)$$

where θ_f is the volumetric water content ($L^3\ L^{-3}$) at the fictitious node (equal to θ_{m-1}), and

$$D(\theta)_{m+1/2}^{n+1/2} = \frac{D(\theta)_f^{n+1} + D(\theta)_m^{n+1} + D(\theta)_f^n + D(\theta)_m^n}{4} \quad (44)$$

$$D(\theta)_{m-1/2}^{n+1/2} = \frac{D(\theta)_m^{n+1} + D(\theta)_{m-1}^{n+1} + D(\theta)_m^n + D(\theta)_{m-1}^n}{4} \quad (45)$$

$$K(\theta)_{m+1/2}^{n+1/2} = \frac{K(\theta)_f^{n+1} + K(\theta)_m^{n+1} + K(\theta)_f^n + K(\theta)_m^n}{4} \quad (46)$$

$$K(\theta)_{m-1/2}^{n+1/2} = \frac{K(\theta)_m^{n+1} + K(\theta)_{m-1}^{n+1} + K(\theta)_m^n + K(\theta)_{m-1}^n}{4} \quad (47)$$

Note that the choice of the depth of final node and the final time of simulation require little attention, in other words, flowing water must not reach the bottom of the profile during the computation, otherwise an error in the mass balance will result.

4.7 Hydraulic properties of the soil

Equations 23, 31, 32, 39, and 43 require the relationships of $K(\theta)$, $\psi(\theta)$, and $D(\theta)$ in order to be satisfied. Those functions are usually introduced in tabulated form to numerical models, or, more commonly, as empirical equations. In this study the van Genuchten equations were used because of their continuity over the entire range of water content which is very useful for numerical simulations (Paniconi, 1991) . The soil characteristic equations as given by van Genuchten (1980); van Genuchten and Nielsen (1985) are:

$$K(S_e) = K_s\, S_e^{1/2} \left[1 - \left(1 - S_e^{1/m} \right)^m \right]^2 \qquad (48)$$

$$\psi(S_e) = \frac{\left(S_e^{-1/m} - 1 \right)^{1/n}}{\alpha} \qquad (49)$$

$$D(S_e) = \left(\frac{(1 - m)\, K_s}{\alpha\, m\, (\theta_s - \theta_r)} \right) S_e^{1/2 - 1/m} * \left[\left(1 - S_e^{1/m} \right)^{-m} + \left(1 - S_e^{1/m} \right)^m - 2 \right] \qquad (50)$$

$$\theta(\psi) = (\theta_s - \theta_r) \left[\frac{1}{1 + (\alpha\, \psi)^n} \right]^m + \theta_r \qquad (51)$$

where

$$S_e = \left[\frac{\theta - \theta_r}{\theta_s - \theta_r} \right] \qquad (52)$$

θ is the actual volumetric water content ($L^3\ L^{-3}$), θ_r is the residual volumetric water

content ($L^3\ L^{-3}$), θ_s is the saturated volumetric water content ($L^3\ L^{-3}$), and K_s is saturated hydraulic conductivity ($L\ T^{-1}$). α and **n** are empirical coefficients characterizing the soil and determined by experiment, and **m** is defined as:

$$m = 1 - \frac{1}{n} \tag{53}$$

Using these equations, $K(\psi)$, $\psi(\theta)$, and $D(\theta)$ can be determined for a given θ, and $\theta(\psi)$ can be found for a given ψ as well. However, when θ approaches saturation, $D(\theta)$ approaches infinity. Therefore, in this study, the saturation water content is limited during the calculation to 0.999999 θ.

4.8 Solution scheme

Since equations 23, 31, 32, 39, and 43 are non linear, because the coefficients $K(\psi)$, $\psi(\theta)$, and $D(\theta)$ are themselves functions of the dependent variable that is sought, therefore these equations are solved by iteration. Non-iterative methods are also used in such problems but they require very short time steps. In this study the Newton-Raphson iteration method was used to linearize the equations. The form of Newton-Raphson method for non linear equation is:

$$X^{r+1} - X^{r} = - \frac{f\ (\ X^{r}\ )}{f'\ (\ X^{r}\ )} \qquad (54)$$

where the superscript r donates values obtained in the r^{th} iteration. The term in the left-hand side of equation 54 is the error term, the iteration is terminated when its value is very close to zero. In this study a system of non linear equations needed to be solved, so a matrix system was used to replace the parameters in equation 54 as follows:

$$\{E\} = \frac{-\ \{\ F\ \}}{\partial\ [\ F\ ]} \qquad (55)$$

where $\{E\}$ is the error term vector, defined as:

$$\{ E \} = \begin{bmatrix} \theta_1^{r+1} - \theta_1^r \\ \theta_2^{r+1} - \theta_2^r \\ \cdots\cdots\cdots \\ \theta_i^{r+1} - \theta_i^r \\ \cdots\cdots\cdots \\ \theta_m^{r+1} - \theta_m^r \end{bmatrix} \tag{56}$$

$\{F\}$ is defined as:

$$\{ F \} = \begin{bmatrix} F_1 \\ F_2 \\ \cdot\cdot \\ F_i \\ \cdot\cdot \\ F_m \end{bmatrix} \tag{57}$$

where F_i

$$F_i = f\left(\theta_{i-1}^{n+1},\ \theta_i^{n+1},\ \theta_{i+1}^{n+1}\right) = 0 \tag{58}$$

This represents equations 23, 31, 32, 39, and 43, for corresponding nodes along the soil column. It is obtained by taking the right-hand side of these equations to the left-hand side, and equating them to zero. Accordingly F_i will be as follows:

$$\begin{aligned} F_i = &- \theta_{i-1}^{n+1} \left[\frac{D(\theta)_{i-1/2}^{n+1/2}}{2\Delta z_1 \Delta z_3} \right] \\ &+ \theta_i^{n+1} \left[\frac{1}{\Delta t} + \frac{1}{\Delta z_3} \left(\frac{D(\theta)_{i+1/2}^{n+1/2}}{2\Delta z_2} + \frac{D(\theta)_{i-1/2}^{n+1/2}}{2\Delta z_1} \right) \right] \\ &- \theta_{i+1}^{n+1} \left[\frac{D(\theta)_{i+1/2}^{n+1/2}}{2\Delta z_2 \Delta z_3} \right] - \theta_{i-1}^{n} \left[\frac{D(\theta)_{i-1/2}^{n+1/2}}{2\Delta z_1 \Delta z_3} \right] \\ &- \theta_i^n \left[\frac{1}{\Delta t} - \frac{1}{\Delta z_3} \left(\frac{D(\theta)_{i+1/2}^{n+1/2}}{2\Delta z_2} + \frac{D(\theta)_{i-1/2}^{n+1/2}}{2\Delta z_1} \right) \right] \\ &- \theta_{i+1}^{n} \left[\frac{D(\theta)_{i+1/2}^{n+1/2}}{2\Delta z_2 \Delta z_3} \right] + \left[\frac{K(\theta)_{i+1/2}^{n+1/2} - K(\theta)_{i-1/2}^{n+1/2}}{\Delta z_3} \right] = 0 \end{aligned} \tag{59}$$

for interior nodes that are not close to the interface,

$$
\begin{aligned}
F_i = & - \theta_{i-1}^{n+1} \left[\frac{D(\theta)_{i-1/2}^{n+1/2}}{2\Delta z_1 \Delta z_4} \right] \\
& + \theta_i^{n+1} \left[\frac{1}{\Delta t} + \frac{1}{\Delta z_4} \left(\frac{D(\theta)_{i+1/2}^{n+1/2}}{2\Delta z_2} + \frac{D(\theta)_{i-1/2}^{n+1/2}}{2\Delta z_1} \right) \right] \\
& - \theta_{i+1}^{n+1} \left[\frac{D(\theta)_{i+1/2}^{n+1/2}}{2\Delta z_2 \Delta z_4} \right] - \theta_{i-1}^{n} \left[\frac{D(\theta)_{i-1/2}^{n+1/2}}{2\Delta z_1 \Delta z_4} \right] \\
& - \theta_i^{n} \left[\frac{1}{\Delta t} - \frac{1}{\Delta z_4} \left(\frac{D(\theta)_{i+1/2}^{n+1/2}}{2\Delta z_2} + \frac{D(\theta)_{i-1/2}^{n+1/2}}{2\Delta z_1} \right) \right] \\
& - \theta_{i+1}^{n} \left[\frac{D(\theta)_{i+1/2}^{n+1/2}}{2\Delta z_2 \Delta z_4} \right] + \Delta\theta^{n+1/2} \left[\frac{D(\theta)_{i+1/2}^{n+1/2}}{2\Delta z_2 \Delta z_4} \right] \\
& + \left[\frac{K(\theta)_{i+1/2}^{n+1/2} - K(\theta)_{i-1/2}^{n+1/2}}{\Delta z_4} \right] = 0
\end{aligned}
\tag{60}
$$

for the node above the interface, and

$$
\begin{aligned}
F_i = & - \theta_{i-1}^{n+1} \left[\frac{D(\theta)_{i-1/2}^{n+1/2}}{2\Delta z_1 \Delta z_5} \right] \\
& + \theta_i^{n+1} \left[\frac{1}{\Delta t} + \frac{1}{\Delta z_5} \left(\frac{D(\theta)_{i+1/2}^{n+1/2}}{2\Delta z_2} + \frac{D(\theta)_{i-1/2}^{n+1/2}}{2\Delta z_1} \right) \right] \\
& - \theta_{i+1}^{n+1} \left[\frac{D(\theta)_{i+1/2}^{n+1/2}}{2\Delta z_2 \Delta z_5} \right] - \theta_{i-1}^{n} \left[\frac{D(\theta)_{i-1/2}^{n+1/2}}{2\Delta z_1 \Delta z_5} \right] \\
& - \theta_i^{n} \left[\frac{1}{\Delta t} - \frac{1}{\Delta z_5} \left(\frac{D(\theta)_{i+1/2}^{n+1/2}}{2\Delta z_2} + \frac{D(\theta)_{i-1/2}^{n+1/2}}{2\Delta z_1} \right) \right] \\
& - \theta_{i+1}^{n} \left[\frac{D(\theta)_{i+1/2}^{n+1/2}}{2\Delta z_2 \Delta z_5} \right] - \Delta\theta^{n+1/2} \left[\frac{D(\theta)_{i+1/2}^{n+1/2}}{2\Delta z_2 \Delta z_5} \right] \\
& + \left[\frac{K(\theta)_{i+1/2}^{n+1/2} - K(\theta)_{i-1/2}^{n+1/2}}{\Delta z_5} \right] = 0
\end{aligned}
\tag{61}
$$

for the node below the interface.

The boundaries also take similar form as follows:

$$F_1 = \theta_1^{n+1}\left[\frac{1}{\Delta t} + \frac{D(\theta)_{1+1/2}^{n+1/2}}{(z_2 - z_1)^2 D}\right] - \theta_2^{n+1}\left[\frac{D(\theta)_{1+1/2}^{n+1/2}}{(z_2 - z_1)^2 D}\right] - \frac{\theta_1^n}{\Delta t} + \frac{K(\theta)_{1+1/2}^{n+1/2}}{z_2 - z_1} - \frac{q^{n+1}}{z_2 - z_1} = 0 \quad (62)$$

for the boundary at the surface, and

$$F_m = -\theta_{m-1}^{n+1}\left[\frac{D(\theta)_{m-1/2}^{n+1/2}}{\Delta z_1 \Delta z_3}\right] + \theta_m^{n+1}\left[\frac{1}{\Delta t} + \frac{D(\theta)_{m-1/2}^{n+1/2}}{\Delta z_1 \Delta z_3}\right] - \theta_{m+1}^{n+1}\left[\frac{D(\theta)_{m-1/2}^{n+1/2}}{\Delta z_1 \Delta z_3}\right] - \theta_m^n\left[\frac{1}{\Delta t} - \frac{D(\theta)_{m-1/2}^{n+1/2}}{\Delta z_1 \Delta z_3}\right] = 0 \quad (63)$$

for the lower boundaries.

The term $\partial[F]$ in equation 55 is the Jacobean matrix $[J]$ and it is composed of a series of partial derivatives of F_i with respect to θ_i at future time step $n+1$ for $i = 1, 2, \ldots, m$. When $[J]$ is obtained, it resembles the following:

$$J = \begin{bmatrix} \frac{\partial F_1}{\partial \theta_1^{n+1}} & \frac{\partial F_1}{\partial \theta_2^{n+1}} & 0 & 0 & \cdots & \cdots & \cdots & \cdots & \cdots \\ \frac{\partial F_2}{\partial \theta_1^{n+1}} & \frac{\partial F_2}{\partial \theta_2^{n+1}} & \frac{\partial F_2}{\partial \theta_3^{n+1}} & 0 & 0 & \cdots & \cdots & \cdots & \cdots \\ 0 & \frac{\partial F_3}{\partial \theta_2^{n+1}} & \frac{\partial F_3}{\partial \theta_3^{n+1}} & \frac{\partial F_3}{\partial \theta_4^{n+1}} & 0 & 0 & \cdots & \cdots & \cdots \\ \cdots & \cdots & \cdots & \cdots & \cdots & \cdots & \cdots & \cdots & \cdots \\ 0 & \cdots & 0 & \frac{\partial F_i}{\partial \theta_{i-1}^{n+1}} & \frac{\partial F_i}{\partial \theta_i^{n+1}} & \frac{\partial F_i}{\partial \theta_{i+1}^{n+1}} & 0 & \cdots & 0 \\ \cdots & \cdots & \cdots & \cdots & \cdots & \cdots & \cdots & \cdots & \cdots \\ 0 & 0 & \cdots & \cdots & \cdots & \cdots & \cdots & \frac{\partial F_m}{\partial \theta_{m-1}^{n+1}} & \frac{\partial F_m}{\partial \theta_m^{n+1}} \end{bmatrix} \quad (64)$$

The partial derivatives of F_i with respect to θ_i at time $n+1$ in the Jacobean matrix are shown in appendix A. Given $\{F\}$ and $[J]$ and rearranging equation 55 to obtain:

$$[\ J\ ]\ .\ \{\ E\ \}\ =\ -\ \{F\ \} \qquad (65)$$

since $[J]$ is a tridiagonal matrix, the error term $\{E\}$ can be solved by using Thomas algorithm at the r^{th} iteration. Then the new approximated value for water content will be:

$$\{\ \theta^{n+1}\ \}\ =\ \{\theta^{n}\ \}\ +\ \{\ E\ \} \qquad (66)$$

The iteration continues until convergence. The convergence criteria that is used here depends on the balance of the function F_i according to equations 59-63 which require the right value of θ to be zero. Accordingly, the iterations stop and the solution of water content at time t is found when the following criterion is met:

$$\sum_{i=1}^{i=m} |\ F_i\ |\ \leq\ 0.00000001 \qquad (67)$$

4.9 Algorithm to solve for water content

The following steps are required to obtain the solution for water content;

1. Future value of water content is guessed for each node by using the old value of the corresponding node.
2. Evaluate function $\{F_i\}$, When F_i is evaluated for the nodes surrounding the

interface the following procedure is followed to estimate $\Delta\theta^{n+\frac{1}{2}}$ according to Hills etal (1989):

a. Soil water potential is estimated at the interface by using equation 37 for future $t = n+1$.

b. Using the corresponding $\psi(\theta)$ relation, θ^{+} and θ^{-}can be found, and accordingly, $\Delta\theta^{n+1}$ can be calculated using equation 36.

c. Repeat steps a and b for $t = n$ to obtain $\Delta\theta^{n}$.

d. From equation 35, obtain $\Delta\theta^{n+\frac{1}{2}}$.

3. During the evaluation of $\{F_i\}$, compute the sum of absolute F_i .

4. Compute the Jacobean matrix.$[J]$.

5. Solve for the error term $\{E\}$ using Thomas algorithm.

6. Check the convergence criterion (equation 67), if satisfied, terminate the iteration and go to step 7, otherwise:

$$\theta_i^{n+1} = \theta_i^n + E_i \qquad (68)$$

go to step 2.

7. If the final time is not reached, go to step 1.

8. Report the simulation results.

5. SIMULATION OF ONE-DIMENSIONAL SOLUTE TRANSPORT IN LAYERED SOIL

Solute movement in soils has received a great deal of attention due to its importance in plant nutrition, soil reclamation, pesticide movement, groundwater contamination, and environmental quality. Since this study involves modifications in soil layers, it is worthwhile to investigate the impacts of such modifications on solute distribution.

Solutes in the soil are transported by three mechanisms, namely, convection, diffusion, and hydrodynamic dispersion. In the convection process, solutes are transported by the mass flow of water in the soil, therefore, the rate at which solute is transported is a function of solute concentration in the soil water and the flux. Diffusive transport is the process of molecular diffusion, and the rate of transport depends on the solute concentration gradient and the solute diffusion coefficient, as described by Fick's Law. The third process is hydrodynamic dispersion which is caused by unequally distributed water velocity in individual pores and by the tortuous flow path; its value depends mainly on the pore water velocity.

The general equation for one-dimensional solute transport in the soil can be written in the following form (Bresler and Hanks, 1969; Warrick etal, 1971; and Bresler, 1973):

$$\frac{\partial(\theta c + A)}{\partial t} = \frac{\partial}{\partial z}\left(\theta D_s(v)\frac{\partial c}{\partial z}\right) - \frac{\partial(qc)}{\partial z} + S \qquad (69)$$

where θ is the volumetric water content ($L^3\ L^{-3}$), c is the solute concentration in soil

water (M L^{-3}), D_s is the apparent dispersion coefficient (L^2 T^{-1}), v is the flow velocity (L T^{-1}), q is the solution flux (L^3 L^{-2} T^{-1}), t is the time (T), z is the depth, positive downward, (L), A is the local concentration of solute in the adsorbed phase (M L^{-3}), and S is the source-sink rate (M L^{-3} T^{-1}).

D_s combines both terms, molecular diffusion and hydrodynamic dispersion. It is defined as:

$$D_s = D_m + D_h \qquad (70)$$

where D_m is the molecular diffusion coefficient and D_h is the hydrodynamic dispersion coefficient which can be given by:

$$D_m = D_o \tau \qquad (71)$$

where D_o is the diffusion coefficient of solute in pure water, and τ is the tortuosity factor, dimensionless. In most soils τ ranges between 0.3-0.7 (van Genuchten and Wierenga, 1986).

$$D_h = \lambda \mid V \mid \qquad (72)$$

where λ is the dispersivity factor (L), its value is $\leq$ 1 cm for disturbed soils, and about one or two orders of magnitude for undisturbed field soil (van Genuchten and Wierenga, 1986), and V is the average pore-water velocity (L T^{-1}) and given by:

$$V = \frac{q}{\theta} \qquad (73)$$

For simplicity of the model, the last two terms 'A and S ' are neglected, and the model solved for only solute concentration in the liquid phase without source-sink

terms. Accordingly equation 69 is reduced to:

$$\frac{\partial(\theta c)}{\partial t} = \frac{\partial}{\partial z}\left(\theta D_s(v)\frac{\partial c}{\partial z}\right) - \frac{\partial(qc)}{\partial z} \qquad (74)$$

The boundary conditions for the solute transport are solute flux for the surface and semi-infinite for the bottom. They can be defined by the following equations (Bresler, 1973):

$$J(0,t) = -\theta D_s(v)\frac{\partial c}{\partial z} + q_w(0,t)\, c(0,t) \qquad (75)$$

with

$$J(0,t) = \begin{cases} q(0,t)\, c(0,t) & \rightarrow \textit{Infiltration} \\ 0 & \rightarrow \textit{Redistribution} \\ 0 & \rightarrow \textit{Evaporation} \end{cases} \qquad (76)$$

$$at \quad t \geq 0$$

for the surface boundary. For the bottom boundary, the gradient of solute concentration is assumed to be zero as described by the following equation:

$$\frac{\partial c}{\partial z}(z,t) = 0, \quad at \quad z = z_m, \quad t \geq 0 \qquad (77)$$

where m is the maximum depth of the soil profile. Semi-infinite soil profile means that solute will not reach the bottom of the soil during the simulation period. Therefore, the value of z at $z = z_m$ must be relatively large, specially when the period of the simulation is large and/or higher rates of infiltration are specified at the surface. This will assure that solute will not reach the bottom of the soil column during the computation.

The initial condition for the solute problem is:

$$c(i,t) = c_o ; \quad i = 1, 2, \ldots, m \quad at \quad t = 0 \qquad (78)$$

where c_o is the initial solute concentration (M L^{-3}).

5.1 Solution to solute transport equations

The finite difference solution for equation 73 with the implementation of Crank-Nicolson scheme is:

$$\begin{aligned}\frac{\theta_i^{n+1} c_i^{n+1} - \theta_i^n c_i^n}{\Delta t} = & \left[\frac{\theta_{i+1/2}^{n+1/2} D_s(v_{i+1/2}^{n+1/2})}{2\Delta z_2 \Delta z_3}\right](c_{i+1}^{n+1} + c_{i+1}^n - c_i^{n+1} - c_i^n) \\ & - \left[\frac{\theta_{i-1/2}^{n+1/2} D_s(v_{i-1/2}^{n+1/2})}{2\Delta z_1 \Delta z_3}\right](c_i^{n+1} + c_i^n - c_{i-1}^{n+1} - c_{i-1}^n) \\ & - \left[\frac{q_{i+1/2}^{n+1/2}}{4\Delta z_3}\right](c_{i+1}^{n+1} + c_{i+1}^n + c_i^{n+1} + c_i^n) \\ & + \left[\frac{q_{i-1/2}^{n+1/2}}{4\Delta z_3}\right](c_i^{n+1} + c_i^n + c_{i-1}^{n+1} + c_{i-1}^n)\end{aligned} \qquad (79)$$

where

$$\theta_{i+1/2}^{n+1/2} = \frac{\theta_{i+1}^{n+1} + \theta_{i+1}^n + \theta_i^{n+1} + \theta_i^n}{4} \qquad (80)$$

$$\theta_{i-1/2}^{n+1/2} = \frac{\theta_i^{n+1} + \theta_i^n + \theta_{i-1}^{n+1} + \theta_{i-1}^n}{4} \qquad (81)$$

$$q_{i+1/2}^{n+1/2} = -D(\theta_{i+1/2}^{n+1/2}) \frac{\theta_{i+1}^{n+1/2} - \theta_i^{n+1/2}}{\Delta z_2} + K(\theta_{i+1/2}^{n+1/2}) \qquad (82)$$

$$q_{i-1/2}^{n+1/2} = -D(\theta_{i-1/2}^{n+1/2}) \frac{\theta_i^{n+1/2} - \theta_{i-1}^{n+1/2}}{\Delta z_2} + K(\theta_{i-1/2}^{n+1/2}) \quad (83)$$

$$\theta_i^{n+1/2} = \frac{\theta_i^{n+1} + \theta_i^n}{2} \quad (84)$$

$$v_{i+1/2}^{n+1/2} = \frac{q_{i+1/2}^{n+1/2}}{\theta_{i+1/2}^{n+1/2}} \quad (85)$$

$$v_{i-1/2}^{n+1/2} = \frac{q_{i-1/2}^{n+1/2}}{\theta_{i-1/2}^{n+1/2}} \quad (86)$$

and for the boundaries:

$$\frac{\theta_1^{n+1} c_1^{n+1} - \theta_1^n c_1^n}{\Delta t} = \left[\frac{\theta_{1+1/2}^{n+1/2} D_s(v_{1+1/2}^{n+1/2})}{2(\Delta z_2)_2}\right](c_2^{n+1} + c_2^n - c_1^{n+1} - c_1^n) - \left[\frac{q_{i+1/2}^{n+1/2}}{4\Delta z_2}\right](c_2^{n+1} + c_2^n + c_1^{n+1} + c_1^n) + J \quad (87)$$

for upper boundary, where J is the value of flux boundary as defined in equation 76. The lower boundary is the same as equation 79 but with a fictitious node.

5.2 Transport of solute in layered soils

When a water content based formulation is used with equation 74 to simulate solute transport, equation 74 can't be applied directly to heterogenous soils. In order to be implemented for layered soil, it must be modified. The adjustments which are required here are in the part where water flow has contributions to solute transport,

namely, the convection transport of the solution which depends mainly on q. In water content based models, q depends on the gradient of water content. Since water content here is not a continuous function of depth, error will result when the solute flow equation is applied. To illustrate this, consider for example the case when a coarse-textured soil overlaying fine-textured soil, both soils are not saturated, and the water content for the lower layer is greater while water potential is lower. Accordingly the lower layer will adsorb any water coming from the top layer, and the flow direction will be downward (positive direction) as stated by the Darcy equation, assuming the effect of gravity on water flow at this point is very small:

$$q = - K(\psi) \frac{\partial \psi}{\partial z} + K(\psi) \tag{88}$$

Based on water content, equation 88 will be:

$$q = - D(\theta) \frac{\partial \theta}{\partial z} + K(\theta) \tag{89}$$

the approximation of equation 82 can be given by:

$$q_{i+1/2} = - D(\theta)_{i+1/2} \frac{\theta_{i+1} - \theta_i}{\Delta z} + K(\theta)_{i+1/2} \tag{90}$$

Now, when equation 82 is used for this example q will be negative, which means, the flow is upward, when it should be downward. Therefore, because of the discontinuity of water content in such a condition, evaluation of q in equation 74 for the convective solute transport must be modified to account for solute transport over the interface. Two methods are presented here to compute the solute flux across an interface:

Method 1:

Hills etal (1989) presented a procedure to evaluate water flow across an interface between two different soil layers. The same theory also can be implemented here for solute transport in layered soils. Provided that $\Delta\theta$ and θ_a are known (as discussed in the previous chapter) and by using half space step size, solute flux in equation 79 for nodes surrounding the interface can be evaluated by:

$$q_i^{n+1/2} = -D(\theta_i^{n+1/2}) \frac{\theta_a^{n+1/2} - \left(\frac{\Delta\theta}{2}\right)^{n+1/2} - \theta_i^{n+1/2}}{\frac{\Delta z}{2}} + K(\theta_i^{n+1/2}) \qquad (91)$$

for the node just above the interface, and

$$q_{i+1}^{n+1/2} = -D(\theta_{i+1}^{n+1/2}) \frac{\theta_{i+1}^{n+1/2} - \theta_a^{n+1/2} - \left(\frac{\Delta\theta}{2}\right)^{n+1/2}}{\frac{\Delta z}{2}} + K(\theta_{i+1}^{n+1/2}) \qquad (92)$$

for the node just below the interface. Thus,

$$q_{i+1/2}^{n+1/2} = \frac{q_{i+1}^{n+1/2} + q_i^{n+1/2}}{2} \qquad (93)$$

This evaluates $q_{i+1/2}$ for node i above the interface, which also evaluates $q_{i-1/2}$ for node i+1 below the interface.

Since the interface thickness is zero and no storage can take place at the interface, the flux entering the interface is equal to the flux exiting from the interface (conservation of mass), θ_a can be evaluated from:

$$\theta_a = \frac{\theta_{i+1} + \theta_i}{2} \qquad (94)$$

Substituting equation 94 into equations 91 and 92 will provide an expression to evaluate q between the nodes that surround the interface:

$$q_{i+1/2}^{n+1/2} = -D(\theta_{i+1/2}^{n+1/2}) \frac{\theta_{i+1}^{n+1/2} - \theta_i^{n+1/2} - \Delta\theta^{n+1/2}}{\Delta z} + K(\theta_{i+1/2}^{n+1/2}) \qquad (95)$$

Note that $q_{i+1/2}$ for node i above the interface is equal to $q_{i-1/2}$ for node i+1 below the interface.

Method 2:

In this method, soil water potential replaces the water content when computing solute flow between two layers. Since the values of water content are known (by solving water flow), values of ψ_i and ψ_{i+1} for the nodes surrounding the interface can be found from the corresponding $\psi(\theta)$ relationship of each soil. Thus, for ψ_i and ψ_{i+1} substitute θ_i and θ_{i+1} in Darcy's equation as follows:

$$q_{i+1/2}^{n+1/2} = -K(\theta_{i+1/2}^{n+1/2}) \frac{\psi_{i+1}^{n+1/2} - \psi_i^{n+1/2}}{\Delta z} + K(\theta_{i+1/2}^{n+1/2}) \qquad (96)$$

Note that $q_{i+1/2}$ for node i above the interface is equal to $q_{i-1/2}$ for node i+1 below the interface.

5.3 Algorithm to solve for solute transport

By solving the water flow equation for a given time step, all the variables in equation 73 are known except solute concentration c^{n+1}, therefore, the solution is straight forward and there is no need for iteration. The following steps illustrate the algorithm for each time step after solving the water flow for the same time step:

1. Compute time-space centered θ using equations 80 and 81, q using equations 82 and 83 for any node that is not close to the interface, and equation 95 or 96 for nodes adjacent to the interface, V using equations 85 and 86, and $D_s(V)$ using equations 70, 71, and 72.
2. Now the only unknown is c_i^{n+1}. Since there are m unknowns and m equations, the system of equations can be solved for c_i^{n+1} by using the Thomas algorithm since the coefficient matrix is tridigonal.

6. APPLICATION TOWARD WATER CONSERVATION

The mathematical model developed in the previous chapter is applied here to investigate the effect of soil layering on water and solute transport in soils, and the consequences on soil water conservation in the root zone. For this purpose a program written in C language (presented in appendix B) was used to simulate the simultaneous transport of water and solute.

Effects of mulch as well as buried barrier layers, against unmodified soil were simulated in this study. Four cases were investigated. The first case was the original soil, without modification. In the second case a barrier soil layer composed of coarse-textured soil was added to the original soil at depth 70 cm below the soil surface, where roots are assumed not to be present below it. In the third case a soil mulch layer was added to the soil surface, the soil used for mulch is also coarse-grained. And in the fourth case both mulch and buried layers were added to the soil.

In the last three cases, the effects of the thickness and texture of the added layers were examined. The thickness was 2.5, 5.5, or 10.5 cm. Two soils of different texture , sand and coarse sand, were used in the modification of the original soil (loamy sand). The properties of these soils are given in table 1 as well as in figure 2 and 3.

6.1. Simulation parameters and soil properties

All of these cases were simulated under two different evaporation demands in order to investigate the validity of such modification under moderate and severe conditions of water losses. The rates of evaporation chosen were 0.5 cm day^{-1} as moderate condition and 1.5 cm day^{-1} as severe condition.

The impacts of soil modification on solute distribution were also investigated for all cases. Because of this, only one species of solute was used in this study and applied to all cases. The molecular diffusion coefficient D_m for the solute is 1.0835 cm^2 day^{-1} (Kemper, 1986) and the dispersivity factor λ assumed to be 0.4 (van Genuchten and Wierenga, 1986).

For consistency and unbiased simulation, all the cases received the same treatments of simulation parameters which include:

- Soil Depth: The length of the soil column was chosen to be 100 cm.
- Node Distribution: The node distribution along the soil column varies with length. At the first 15 cm from the soil surface, where the mulch layer is to be examined, it was every 1 cm, then followed by 5 cm increments until a depth of 65 cm, after that by 1 cm increment until depth of 85 cm, and then followed by 5 cm increments up to the end of soil column at 100 cm.
- Initial condition: The initial water content was 0.108, 0.10, and 0.03 cm^3cm^{-3} for the original soil (loamy sand), sand, and coarse sand soils respectively. The initial solute concentration was assumed to be 0.0 meq cm^{-3} for all of the cases.

- Soil surface boundary conditions: The simulation starts with continuous irrigation or rainfall at a rate of 7.0 cm day^{-1} for two consecutive days, then followed by a continuous evaporation rate of 0.5 or 1.5 cm day^{-1}, depending on the case, until the end of the simulation time (10 days). The concentration of the solute in the irrigation water or the rainfall was assumed to be 0.05 meq cm^{-3}.

- The time step was 0.005 day, and it was constant for the entire time of the simulation.

Table 1: Parameters used to describe the soil hydraulic properties.

Soil	θ_r cm^3cm^{-3}	θ_s cm^3cm^{-3}	α cm^{-1}	n	K_s cm day^{-1}
Loamy sand[1]	0.107*	0.470	0.010	1.4*	75.0
Sand[2]	0.0914	0.3434	0.0624	1.528	250.0
Coarse sand[3]	0.0286	0.28*	0.07*	2.239	541.0

* = Parameter is modified.
1 = From Taghavi etal (1985).
2 = From Wierenga etal (1991).
3 = From Hills etal (1989).

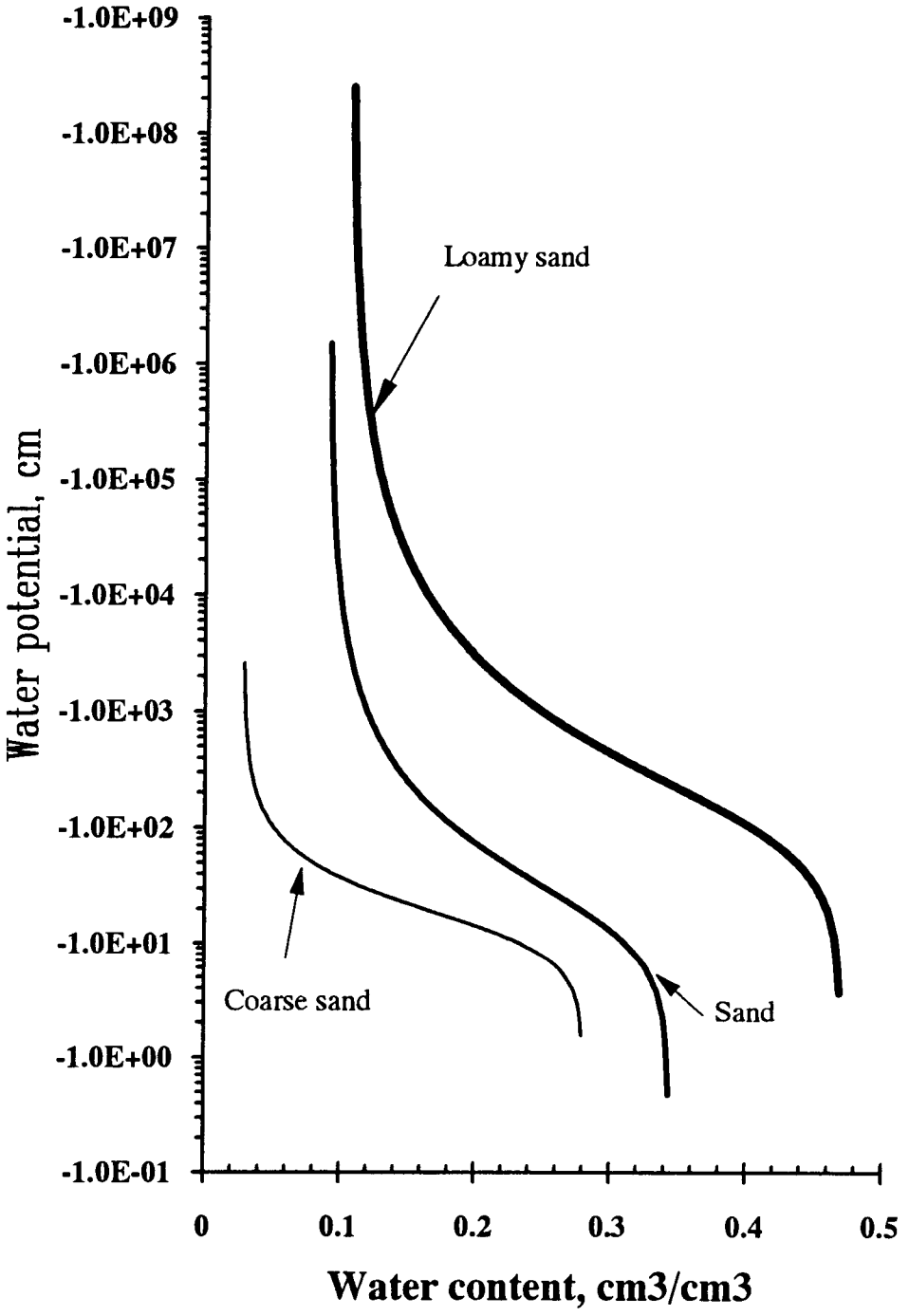

Figure 2: Soil water characteristic curves for the three soils.

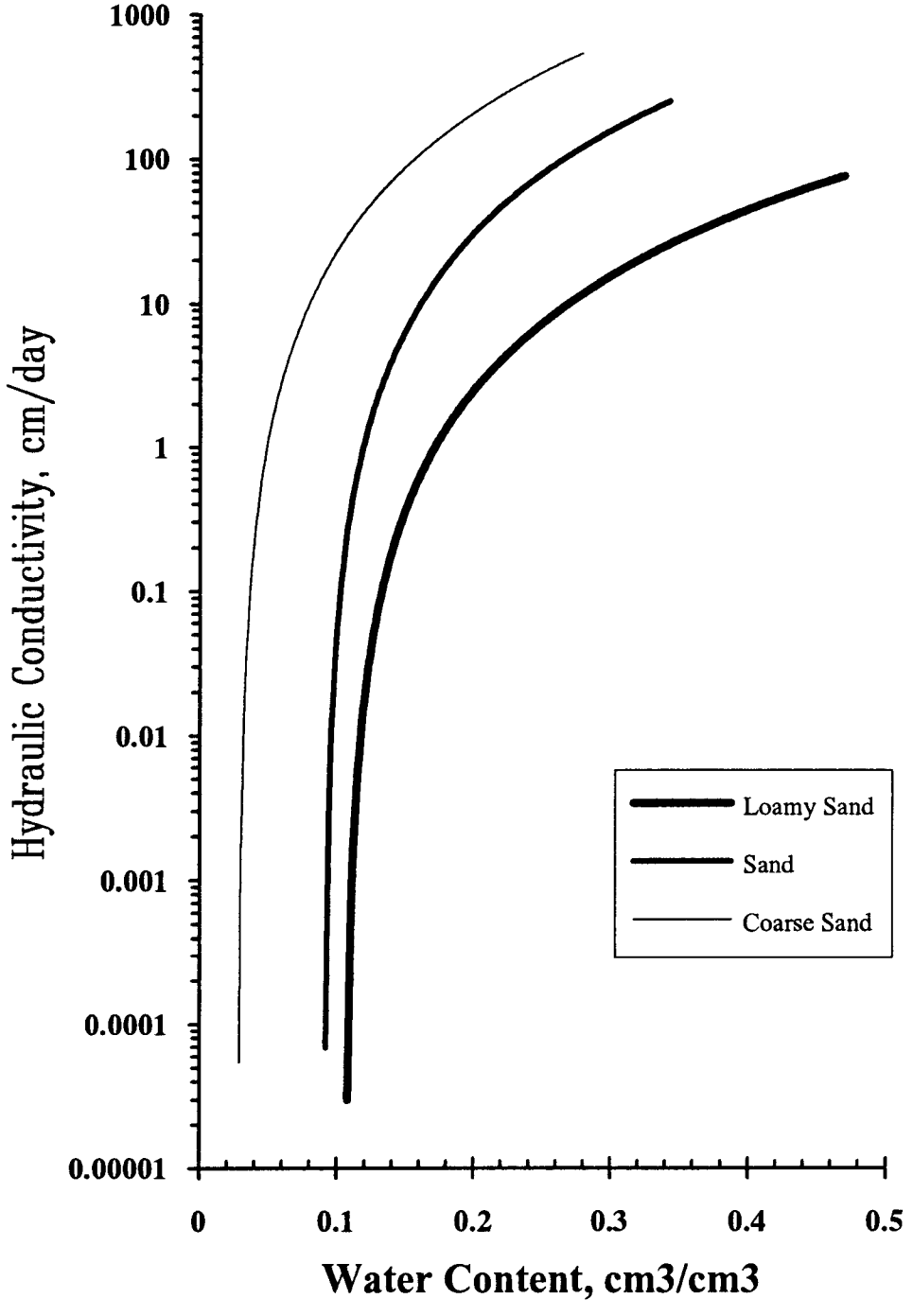

Figure 3: Hydraulic conductivity as a function of water content for the three soils.

6.2. Case 1: Water and solute transport in uniform soil

In this case a uniform soil was used without modification. Water and solute distribution was simulated for this soil under two different evaporation demands. The results of this case will be used for comparison with the other cases when modifications are applied. Table 1 shows the properties of the soil, and the conditions of the simulation.

Results and discussion

The results of the infiltration, redistribution, and evaporation as well as solute distribution are shown in figures C-1 and C-2. After 2 days of continuous irrigation (7.0 cm day^{-1}) the profile was almost saturated to a depth of about 55 cm. Then water content decreased due to evaporation and redistribution. It reached the air dry condition at the surface after the 8th day when the evaporation was 0.5 cm day^{-1}. When the evaporation rate was 1.5 cm day^{-1}, it took less than 2 days after the irrigation to bring the soil at the surface to air dry condition. Due to the redistribution, water passed the root zone (70 cm assumed in this study) just after the fourth day of the simulation, which is considered to be another loss in addition to the evaporation. See figure 4 for summary of the results.

Solute concentration increases as water content increases during the irrigation with contaminated water. When the irrigation was stopped the solute was redistributed in

the soil and reached the maximum concentration at the soil surface due to evaporation. The solute concentration reached 0.08 meq cm^{-3} in less than one day when the evaporation rate was 1.5 cm day^{-1}, while it was only 0.035 meq cm^{-3} for 0.5 cm day^{-1}. See figure 5 for summary of the results.

6.3. Case 2: Effect of buried barrier layer on soil water conservation

The texture and thickness of the buried barrier layer were examined in this case as well as the effect of the two different evaporating demands. The layer was placed at 70 cm below the soil surface in order to investigate its ability to hold the water from passing the root zone.

Results and discussion

Figures C-3 to C-14 and table 2 show the results of this case. Because of the presence of the coarse-textured soil in the middle of the profile, water was limited from being lost by internal drainage in all of the situations, regardless of the thickness, texture, or evaporation rate. The only way for water losses was through the soil surface by the evaporation process. As a result water content of the soil at the end of the simulation period was increased when compared to the unmodified soil. The increase in water content ranges from 5.7% to 7.9% depending on the condition.

By comparing the results in table 2, it is clear that the texture has a small

influence on increasing water content in the soil. This was probably due to the fact that coarse-textured soil had small water suction due to its larger pores, thus, water movement to the layer was prohibited. However, the effect would be more pronounced if the original soil was finer in texture, such as silt or clay. See figure 4 for summary of the results.

The thickness of the layer shows no significant effect on water conservation under the circumstances of this case. The results was similar whether the thickness was 2.5 cm or 10.5 cm.

The evaporation treatment does not show a difference in this case when compared with the original soil.

Solute concentration and distribution in the profile were not affected by the presence of the buried layer, since solute had not reached the layer. And since the soil surface was open, the solute distribution took a similar trend to that of the uniform soil. See figure 5 for summary of the results.

Table 2: Percentage increase in water content due to the presence of barrier layer at the end of the simulation period.

Run number	Treatment: Barrier layer			Increase in water content (%)[§]
	Texture	Thickness cm	Evap. rate cm/day	
03b	Sand	2.5	0.5	6.9
04b	Sand	2.5	1.5	5.7
05b	Sand	5.5	0.5	7.2
06d	Sand	5.5	1.5	5.8
07b	Sand	10.5	0.5	7.2
08b	Sand	10.5	1.5	5.8
09b	C. Sand	2.5	0.5	7.9
10b	C. Sand	2.5	1.5	6.3
11b	C. Sand	5.5	0.5	7.9
12b	C. Sand	5.5	1.5	6.3
13b	C. Sand	10.5	0.5	7.9
14b	C. Sand	10.5	1.5	6.3

§ = Increase of water content computed for soil above the depth of the barrier layer (70 cm), water content below that depth was not included.

6.4. Case 3: Effect of mulch layer on soil water conservation

A layer of coarse-textured soil was added at the soil surface in order to decrease the upward flow of water and hence increase the water content of the soil. To achieve the maximum possible increase in water content of the soil, the possible effects of soil texture as well as the thickness of the layer were simulated in this case. The rest of the soil profile was not modified and kept the same as the original soil.

Results and discussion

The results of the simulation for this case are shown in figures C-15 to C-26, as well as in table 3. It is obvious that the mulch layer has a great influence on water conservation for all of the treatments regardless of the texture, thickness, or the evaporation rate. The loss of water due to the evaporation process was minimal, as a result water content increased in the soil profile when compared to unmodified soil. However, because of this increase and minimal upward water redistribution, the downward redistribution was maximal in this case when compared with the other cases (one-sided redistribution of water), and water reached the bottom of the profile, which is considered to be a loss of water. Table 3 shows an increase in water content ranging from 17.9% to 29.9% depending on the condition and the treatment of the mulch layer. See figure 4 for summary of the results.

The effects of the layer texture and thickness, as well as the evaporating demand

are significant when compared to the previous case. There was about 6% greater increase in water content when the mulch layer thickness was increased from 2.5 cm to 10.5 cm. However, the effect of thickness is very small when a coarse-textured mulch layer was used; it is more pronounced in the finer-textured soils. Furthermore, the texture has more effect when the thickness of the layer is small; as the thickness increases, the effect of the texture diminishes (see table 3).

The rate of evaporation also influenced the water content in the profile. The soil retained 5-6% more water when the evaporation rate increased from 0.5 to 1.5 cm day^{-1}. This is due to the decrease in the first stage of evaporation. As a result, the surface mulch layer did not recover the lost water because of the sharp decrease in the hydraulic conductivity. Thus the water content of the soil below the mulch layer increased.

Solute distribution in the profile took the same trend as water content distribution, and was influenced by the presence of the mulch layer. Because upward water flow was limited, the solute concentration at the surface was decreased when compared with the previous cases, ranging from 0.0017 to 0.0004 meq cm^{-3}. On the other hand it was transported to the lower part of the profile and passed the target depth of 70 cm (leached). See figure 5 for summary of the results.

Table 3: Percentage increase in water content due to the presence of mulch layer at the end of the simulation period.

Run number	Treatment: Mulch layer			Increase in water content (%)[§]
	Texture	Thickness cm	Evap. rate cm/day	
15b	Sand	2.5	0.5	17.9
16b	Sand	2.5	1.5	22.6
17b	Sand	5.5	0.5	21.2
18b	Sand	5.5	1.5	26.5
19b	Sand	10.5	0.5	23.0
20b	Sand	10.5	1.5	28.6
21b	C. Sand	2.5	0.5	22.1
22b	C. Sand	2.5	1.5	27.7
23b	C. Sand	5.5	0.5	23.2
24b	C. Sand	5.5	1.5	28.9
25b	C. Sand	10.5	0.5	24.0
26b	C. Sand	10.5	1.5	29.9

§ = Increase of water content computed for soil depth below the mulch layer; water content above that depth was not included.

6.5. Case 4: Effect of barrier and mulch layers combined on soil water conservation

In this case the effect of both buried and mulch layers was simulated. The influence of texture and thickness of those layers was investigated as well. The same soil conditions and characteristics and evaporating demands were applied as before.

Results and discussion

These conditions achieved the greatest water conservation. Figures C-27 to C-38 and numerical results presented in table 4 show the water and solute distribution. From these figures, it can be seen that the water was trapped between both layers and uniformly distributed in the soil. As a result a maximum water content was achieved at the end of the simulation period. Also changes in water content between the third day and the last day of simulation were very small. Water content was increased by 25.6%- 44.4% depending on the condition of the simulation. The maximum increase was obtained with 10.5 cm thick layer of coarse sand under the severe conditions of evaporating demand, and the minimum was with 2.5 cm thick layer of sand under the moderate evaporating demand. The mulch layer has more contribution to this increase due to its ability to suppress the evaporation from the soil surface. See figure 4 for summary of the results.

The layer texture and thickness as well as the evaporating demand also have

significant influence on reducing water losses from the soil. It can be seen from the figures that when the soil layer was sand, the water infiltrated into the barrier layer, which caused about 5% reduction in water content, on the other hand, water did not infiltrate into the coarse sand layer during the simulation period.

Like the water content, solute was also trapped between the two layers, and concentrated in the middle of the profile. The presence of the barrier layer decreases leaching of solute and accumulation may result. The higher concentration of solute in a soil under such conditions may introduce salinity hazardous to plant growth. See figure 5 for summary of the results.

Table 4: Percentage increase in water content due to the presence of both buried and mulch layer at the end of the simulation period.

Run number	Treatment: Combined			Increase in water content (%)[§]
	Texture	Thickness cm	Evap. rate cm/day	
27b	Sand	2.5	0.5	25.6
28b	Sand	2.5	1.5	29.0
29b	Sand	5.5	0.5	30.7
30b	Sand	5.5	1.5	34.5
31b	Sand	10.5	0.5	34.1
32b	Sand	10.5	1.5	37.9
33b	C. Sand	2.5	0.5	34.7
34b	C. Sand	2.5	1.5	38.9
35b	C. Sand	5.5	0.5	36.6
36b	C. Sand	5.5	1.5	40.8
37b	C. Sand	10.5	0.5	40.1
38b	C. Sand	10.5	1.5	44.4

§ = Increase of water content computed for the depth of soil between the mulch layer and the barrier layer, water content above and below that was not included.

6.6 Evaluation

From the results presented above, it is clear that all of the methods which were used in this study increased water content in the soil. The degree to which this increase is significant depends on the individual method, texture and thickness of soil layer, and on the evaporating demand. Comparing individual methods, the combined layers of mulch and buried barrier ranked first in conserving water in the root zone, followed by mulch layer, which has a great influence in reducing water losses by evaporation. The least effective method was the buried barrier (see figure 4). When relating the effects of texture and thickness of the layer, it is found that both have a similar effect. Among the textures, coarse sand ranked first, and among the thicknesses, 10.5 cm ranked first then followed by 5.5 cm.

Comparing the effect of the evaporating demand, the severe condition tends to be more effective in reducing water losses. That is probably due to its ability in making the soil reach the critical point of the evaporation faster than the moderate condition, and accordingly decreasing the length of the first stage. However, the effect of heat transfer and vapor diffusion which are very significant in warm regions, were not involved in the simulation. Therefore, it is hard to tell whether the severe or moderate evaporating demand is more significant in reducing water losses from the soil surface in hot arid climates.

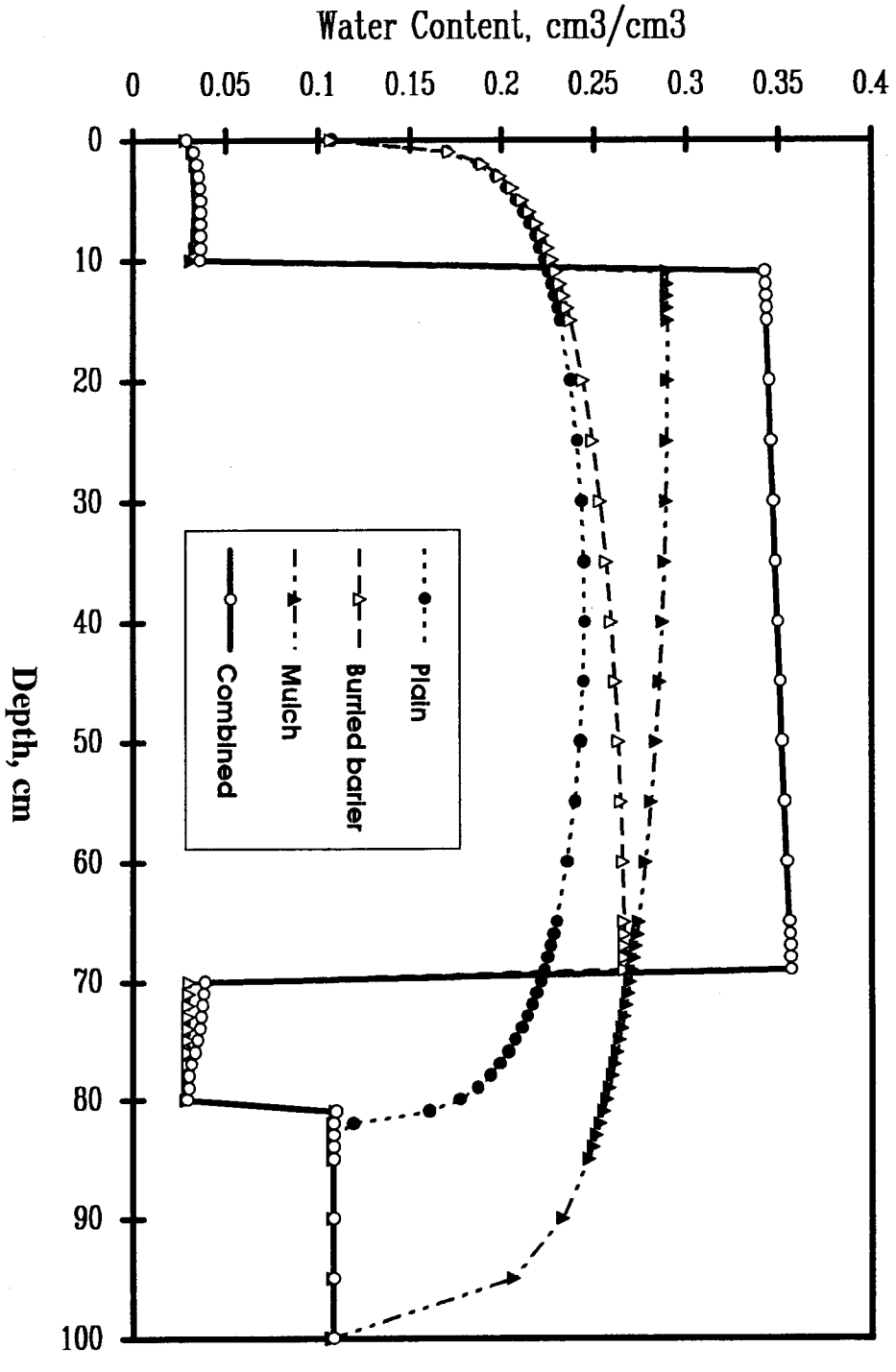

Figure 4: Summary plots for water content distribution after 10 days of simulation with 1.5 cm day^{-1} evaporation rate.

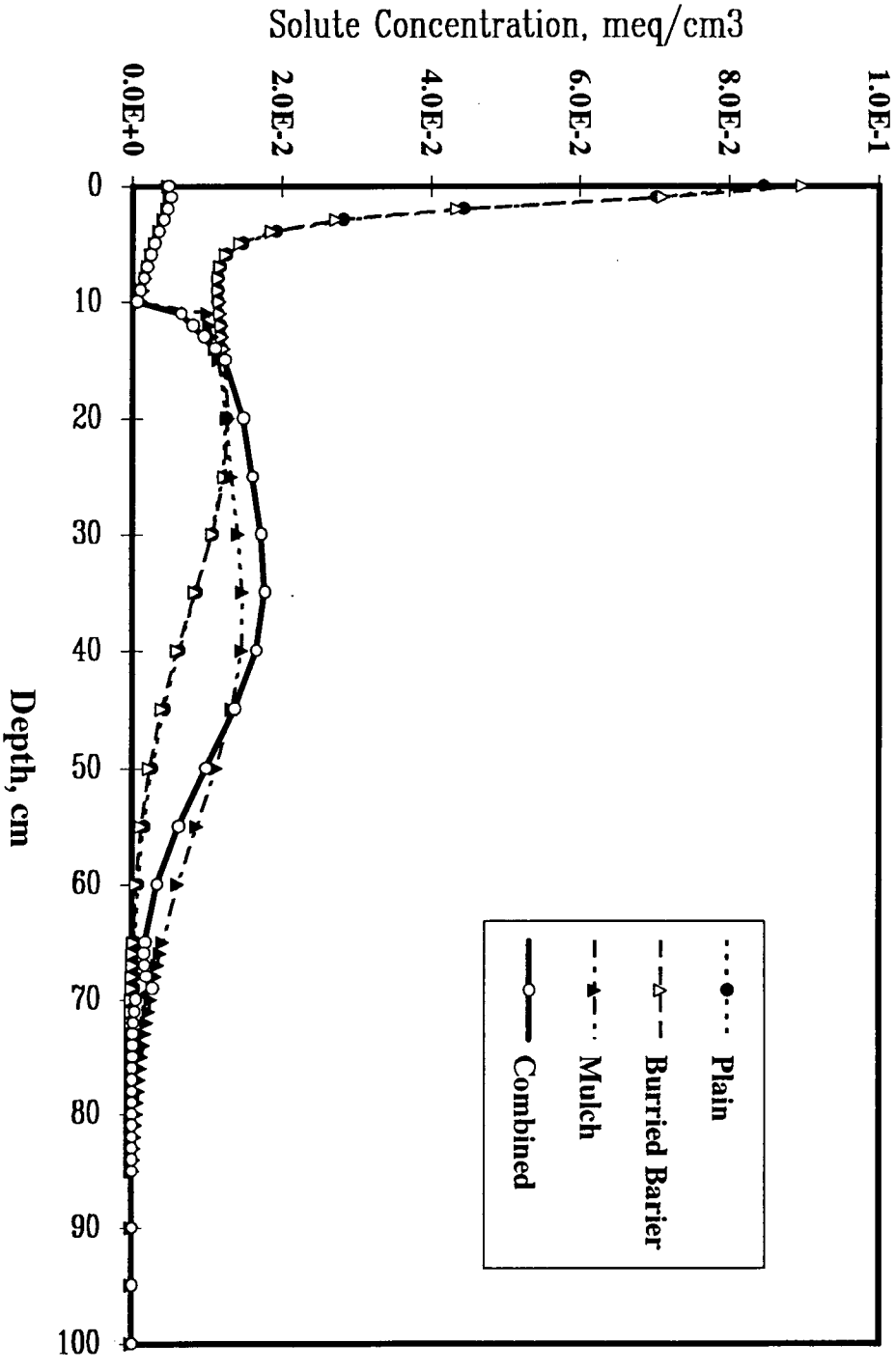

Figure 5: Summary plots for solute distribution after 10 days of simulation with 1.5 cm day^{-1} evaporation rate.

7. SUMMARY AND RECOMMENDATIONS

7.1 Summary

In order to increase the ability of sandy soils to hold more water, three methods of modification were proposed, surface mulch layer, buried barrier layer, and combination of both. The impact of these methods on solute distribution in the soil was also considered. One-dimensional water flow and solute transport in unsaturated soil was simulated for these cases. It was necessary to modify the transport equations to apply to layered soil. The approach of Hills et al, (1989) was used to handle the jump of water content between the layers.

The simulation results indicate that there is potential for enhancing water conservation in sandy soil. Up to 45% increase in water content was obtained by applying these methods. The combination method was superior, however, most of the contribution came from the surface mulch layer which suppressed evaporation from the soil surface. There is potential for solute build up in the root zone when the combination method is used.

7.2 Recommendations

During the development of the model, many assumptions were made in order to ease the task of simulation. However such assumptions rarely hold in the real soil. Thus, enhancement of the model is recommended in future studies in order to make the model more closely representative of real soils. Some recommended additions are:

1. The influence of hysteresis, specially in layered soil.
2. The influence of heat transfer and vapor diffusion, which are very common in warm climates.
3. The effect of water front instability which is very common for the conditions of this study.
4. Lateral water and solute flow should be investigated.
5. The effect of solute on water flow.

REFERENCES

Baasiri, M., Ryan,J., Mucheik,M., and Harik,S.N., 1986, Soil application of hydrophilic conditioner in relation to moisture, irrigation frequency and crop growth, Commun. in Soil Sci. Plant Anal., 17: 573-589

Bond, J.J. and Willis,W.O., 1969, Soil water evaporation: Surface residue rate placement effect, Soil Sci. Soc. Amer. Proc., 33: 445-448

Bresler, E., 1973, Simultaneous transport of solute and water under transient unsaturated flow conditions, Water Resour. Res., 9: 975-986

Bresler, E. and Hanks,R.J., 1969, Numerical method for estimating simultaneous flow of water and salt in unsaturated soils, Soil Sci. Soc. Amer. Proc., 33: 827-832

Bristow, K.L. and Abrecht,D.G., 1989, The physical environment of two semi-arid tropical soils with partial surface mulch cover, Aust. J. Soil Res., 27: 577-587

Callebaut, F., Gabriels,D., and De Boodt,M., 1979, The effect of polymer structure on soil physico-chemical properties and soil water evaporation, J. Chem. Tech. Biotechnol, 29: 723-729

Corey, A.T. and Kemper,W.D., 1968, Conservation of soil water by gravel mulches, Hydrology papers, No. 30, Colorado State University, Fort Collins, p. 23.

Daisley, L.E.A., Chong,S.K., Olsen,F.J., Singh,L., and George,C., 1988, Effect of surface-applied grass mulch on soil water content and yields of cowpea and eggplant in Antigua, Trop. Agric., 65: 300-304

Diebold, C.H., 1954, Permeability and intake rates of medium textured soils in relation to silt content and degree of compaction, Soil Sci. Soc. Amer. Proc., 18: 339-343

Diment, G.A. and Watson,K.K., 1985, Stability analysis of water movement in unsaturated porous materials: 3. Experimental studies, Water Resour. Res., 21: 979-984

Eagleman, J.R. and Jamison,V.C., 1962, Soil layering and compaction effects on unsaturated moisture movement, Soil Sci. Soc. Amer. Proc., 26: 519-522

El-Asswad, R.M. and Groenvelt,P.H., 1985, Hydrophysical modification of sandy soil and its effect on evaporation, Transactions of ASAE, 28: 1927-1932

Erickson, A.E., Hansen,C.H., and Smucker,A.J.M., 1968, The influence of subsurface asphalt barriers on the water properties and the productivity of sand soils, in Transactions of the Nineth International Congress of Soil Science, Adelaide, Australia, p. 331-337

Garber, M. and Zaslavsky,D., 1977, Flow in a soil layer underlined by an impermeable membrane, Soil Science, 123: 1-9

Greb, B.W., 1966, Effect of surface-applied wheat straw on soil water losses by solar distillation, Soil Sci. Soc. Amer. Proc., 30: 786-788

Greb, B.W., Smika,D.E., and Black,A.L., 1967, Effect of straw mulch on soil water storage during summer fallow in the great plains, Soil Sci. Soc. Amer. Proc., 31: 556-559

Greb, B.W., Smika,D.E., and Black,A.L., 1970, Water conservation with stubble mulch fallow, J. Soil and Water Cons., : 58-62

Griffin, R.H., Ott,B.J., and Stone,J.F., 1966, Effect of water management and surface applied barriers on yield and moisture utilization of grain sorghum in southern Great Plains, Agron. J., 58: 449-452

Hanks, R.J., Gardner,H.R., and Fairbourn,M.L., 1967, Evaporation of water from soils as influenced by drying with wind or radiation, Soil Sci. Soc. Amer. Proc., 31: 593-598

Hanks, R.J. and Woodruff,N.P., 1958, Influence of wind on water vapor transfer through soil, gravel, and straw mulches, Soil Science, 86: 160-164

Hanks, R.J., Bowers,S.A., and Bark,L.D., 1961, Influence of soil surface conditions on net radiation, soil temperature, and evaporation, Soil Science, 91: 233-239

Hartmann, R., Verplancke,H., and De Boodt,M., 1981, Influence of soil surface structure on infiltration and subsequent evaporation under simulated laboratory conditions, Soil & Tillage Res., 1: 351-359

Hedrick, R.M. and Mowry,D.T., 1952, Effect of synthetic polyelectrolytes on aggregation, aeration, and water relationships of soil, Soil Science, 73: 427-441

Hemyari, P. and Nofziger,D.L., 1981, Super slurper effects on crust strength, water retention, and water infiltration of soils, Soil Sci. Soc. Am. J., 45: 799-801

Hide, J.C., 1954, Observations on factors influencing the evaporation of soil moisture, Soil Sci. Soc. Amer. Proc., 18: 234-239

Hillel, D., 1982, Introduction to Soil Physics, Academic Press, Orlando, Florida,

Hillel, D. and Berliner,P., 1974, Waterproofing surface-zone soil aggregates for water conservation, Soil Science, 118: 131-135

Hillel, D. and Talpaz,H., 1977, Simulation of soil water dynamics in layerd soils, Soil Science, 123: 54-62

Hills, R.G., Porro, I., Hudson, D. B., and Wierenga, P. J., 1989, Modeling one dimensional infiltration into very dry soils: 1. Model development and evaluation, Water Resour. Res., 25: 1259-1269

Iwata, S., Tabuchi,T., and Warkentin,B.P., 1988, Soil-Water Interactions: Mechanisms and Applications, Marcel Dekker, Inc., New York,

Jamison, V.C. and Kroth,E.M., 1958, Available moisture storage capacity in relation to textural compaction and organic matter content of several Missouri soils, Soil Sci. Soc. Amer. Proc., 22: 189-192

Johnson, M.S., 1984a, The effects of gel-forming polyacrylamides on moisture storage in sandy soils, J. Sci. Food Agric., 35: 1196-1200

Johnson, M.S., 1984b, Effect of soluble salts on water absorption by gel-forming soil conditioners, J. Sci. Food Agric., 35: 1063-1066

Jury, W.A. and Bellantuoni,B., 1976, Heat and water movement under surface rocks in field soil: 1. Thermal effects, Soil Sci. Soc. Am. J., 40: 505-513

Kemper, W.D., 1986, Solute diffusivity, in Methods of Soil Analysis, part 1, Phyical and Mineralogical Methods, 2nd ed., Amer. Soc. of Agron., Inc., Madison, Wisconsin, p. 1007-1024

Kowsar, A., Boersma,L., and Jarman,G.D., 1969, Effect of petroleum mulch on soil water content and temperature, Soil Sci. Soc. Amer. Proc., 33: 783-786

Kumar, S., Malik,R.S., and Dahiya,I.S., 1984, Water retention, transmission and contact characteristics of Ludas sand as infiuenced by farmyard manure, Aust. J. Soil Res., 22: 253-259

Lemon, E.R., 1956, The potentialities for decreasing soil moisture evaporation loss, Soil Sci. Soc. Amer. Proc., 20: 120-125

Mbagwu, J.S.C., 1991, Influence of different mulch materials on soil temprature, soil water content and yield of three cassava cultivars, J. Sci. Food Agric., 54: 569-577

Miller, D.E. and Bunger,W.C., 1963, Moisture retention by soil with coarse layers in the profile, Soil Sci. Soc. Amer. Proc., 27: 586-589

Miller, D.E. and Gardner,W.H., 1962, Water infiltration into stratified soil, Soil Sci. Soc. Amer. Proc., 26: 115-119

Miller, D.E., 1979, Effect of H-Span on water retained by soils after irrigation, Soil Sci. Soc. Am. J., 43: 628-629

Modaihsh, A.S., Horton,R., and Kirkham,D., 1985, Soil water evaporation suppression by sand mulch, Soil Science, 139: 357-361

Moore, I.D. and Eigel,J.D., 1981, Infiltration into two-layered soil profiles, Transactions of ASAE, 24: 1496-1503

Mualem, Y., 1978, Hydraulic conductivity of unsaturated porous media: Generalized macroscopic approach, Water Resour. Res., 14: 325-334

Nielsen, D.R., van Genuchten,M.T., and Biggar,J.W., 1986, Water flow and solute transport processes in the unsaturated zone, Water Resour. Res., 22: 89s-108s

Nofziger, D.L., Ahuja,L.R., and Swartzendruber,D., 1974, Flux-gradient relationships and soil-water diffusivity from curves of water content versus time, Soil Sci. Soc. Amer. Proc., 38: 17-23

Paniconi, C., Aldama,A.A., and Wood,E.F., 1991, Numerical evaluation of iterative and noniterative methods for the solution of the nonlinear Richards equation, Water Resour. Res., 27: 1147-1163

Reichardt, K., Nielsen,D.R., and Biggar,J.W., 1972, Horizontal infiltration into layered soil, Soil Sci. Soc. Amer. Proc., 36: 858-863

Penman, H. L., 1941, Laboratory experiments on evaporation from fallow soil, J. Agric. Sci., 31:454-465

Richards, L.A., Gardner,W.R., and Ogata,A.G., 1956, Physical processes determining water loss from soil, Soil Sci. Soc. Amer. Proc., 20: 310-314

Richards, L.A., 1931, Capillary conduction of lquids through porous mediums, Physics, 1: 318-333

Stroosnijder, L., van Keulen,H., and Vachaud,G., 1972, Water movement in layered soils. 2. Experimental confirmation of a simulation model, Neth. J. Agric. Sci., 20: 67-72

Taghavi, S.A., Marino,M.A., and Rolston,D.E., 1985, Infiltration from a trickle source in a heterogeneous soil medium, J. Hydrol., 78: 107-121

Tayel, M.Y. and El-Hady,O.A., 1981, Super gel as soil conditioner: 1. Its effect on some soil-water relations, Acta Horti., 119: 247-255

Tayel, M.Y., Abed,F.M., and El-Hady,O.A., 1981, Effect of soil conditioners on water retention, Acta Horti., 119: 199-209

Unger, P.W. and Stewart,B.A., 1974, Feedlot waste effect on soil conditions and water evaporation, Soil Sci. Soc. Amer. Proc., 38: 954-957

Unger, P.W., 1971, Soil profile gravel layers: I. Effect on water storage, distribution, and evaporation, Soil Sci. Soc. Amer. Proc., 35: 631-634

van Genuchten, M.T. and Wierenga,P.J., 1986, Solute dispersion coefficients and retardation factors, in Methods of Soil Analysis, part 1, Phyical and Mineralogical Methods, 2nd ed., Amer. Soc. of Agron., Inc., Madison, Wisconsin, p. 1025-1054

van Genuchten, M.T. and Nielsen,D.R., 1985, On describing and predicting the hydraulic properties of unsaturated soils, Annals Geophysicae, 3: 615-628

Van De Pol, R.M., Wierenga,P.J., and Nielsen,D.R., 1977, Solute movement in a field soil, Soil Sci. Soc. Am. J., 41: 10-13

van Genuchten, M.T., 1980, A closed-form equation for predicting the hydraulic conductivity of unsaturated soils, Soil Sci. Soc. Am. J., 44: 892-898

Wallace, A., Wallace,G.A., and Abouzamzam,A.M., 1986, Effects of soil conditioners on water relationships in soils, Soil Science, 141: 346-352

Warrick, A.W., Biggar,J.W., and Nielsen,D.R., 1971, Simultaneous solute and water transfer for unsaturated soil, Water Resour. Res., 7: 1216-1225

Watson, K.K. and Whisler,F.D., 1972, Numerical analysis of drainage of heterogeneous porous medium, Soil Sci. Soc. Amer. Proc., 36: 251-256

Wierenga, P.J., Hills,R.G., and Hudson,D.B., 1991, The Las Cruces trench site: Characterization, experimental results, and one-dimensional flow predictions, Water Resour. Res., 27: 2695-2705

Willis, W.O., Haas,H.J., and Robins,J.S., 1963, Moisture conservation by surface or subsurface barriers and soil configuration under semiarid conditions, Soil Sci. Soc. Amer. Proc., 27: 577-580

Wills, W.O., 1962, Effect of partial surface covers on evaporation from soil, Soil Sci. Soc. Amer. Proc., 26: 598-601

Yong, R.N. and Warkentin,B.P., 1975, Soil Properties and Behaviour, Elsevier Scientific Publishing Company, Amsterdam.

APPENDICES

APPENDIX A

The partial derivatives of function [F_i] with respect to θ_i that are used to perform the Jacobian matrix are:

1. For the interior nodes which are not adjacent to the interface:

$$\frac{\partial F_i(\theta)}{\partial \theta_{i-1}^{n+1}} = \left(\frac{-D(\theta)_{i-1/2}^{n+1/2}}{2\Delta z_1 \Delta z_3} \right) + \frac{\partial D(\theta)_{i-1}^{n+1/2}}{\partial \theta_{i-1}^{n+1}} \left(\frac{-\theta_{i-1}^{n+1} + \theta_i^{n+1} - \theta_{i-1}^{n} + \theta_i^{n}}{8\ \Delta z_1 \Delta z_3} \right) - \frac{\partial K(\theta)_{i-1}^{n+1/2}}{\partial \theta_{i-1}^{n+1}} \left(\frac{1}{4\ \Delta z_3} \right) \tag{A-1}$$

$$\frac{\partial F_i(\theta)}{\partial \theta_i^{n+1}} = \left(\frac{1}{\Delta t} + \frac{D(\theta)_{i+1/2}^{n+1/2}}{2\Delta z_2 \Delta z_3} + \frac{D(\theta)_{i-1/2}^{n+1}}{2\Delta z_1 \Delta z_3} \right) + \frac{\partial D(\theta)_i^{n+1/2}}{\partial \theta_i^{n+1}} \left(\frac{\theta_i^{n+1} - \theta_{i+1}^{n+1} + \theta_i^{n} - \theta_{i+1}^{n}}{8\ \Delta z_2 \Delta z_3} \right) + \frac{\partial D(\theta)_i^{n+1/2}}{\partial \theta_i^{n+1}} \left(\frac{-\theta_{i-1}^{n+1} + \theta_i^{n+1} - \theta_{i-1}^{n} + \theta_i^{n}}{8\ \Delta z_1 \Delta z_3} \right) \tag{A-2}$$

$$\frac{\partial F_i(\theta)}{\partial \theta_{i+1}^{n+1}} = \left(\frac{-D(\theta)_{i+1/2}^{n+1/2}}{2\Delta z_2 \Delta z_3} \right) + \frac{\partial D(\theta)_{i+1}^{n+1/2}}{\partial \theta_{i+1}^{n+1}} \left(\frac{\theta_i^{n+1} - \theta_{i+1}^{n+1} + \theta_i^{n} - \theta_{i+1}^{n}}{8\ \Delta z_2 \Delta z_3} \right) - \frac{\partial K(\theta)_{i+1}^{n+1/2}}{\partial \theta_{i+1}^{n+1}} \left(\frac{1}{4\ \Delta z_3} \right) \tag{A-3}$$

2. For the node just above an interface:

$$\frac{\partial F_i(\theta)}{\partial \theta_{i-1}^{n+1}} = \left(\frac{-\, D(\theta)_{i-1/2}^{n+1/2}}{2\Delta z_1 \Delta z_4} \right) + \frac{\partial D(\theta)_{i-1}^{n+1/2}}{\partial \theta_{i-1}^{n+1}} \left(\frac{-\, \theta_{i-1}^{n+1} + \theta_i^{n+1} - \theta_{i-1}^{n} + \theta_i^{n}}{8\ \Delta z_1 \Delta z_4} \right) - \frac{\partial K(\theta)_{i-1}^{n+1/2}}{\partial \theta_{i-1}^{n+1}} \left(\frac{1}{4\ \Delta z_4} \right) \tag{A-4}$$

$$\frac{\partial F_i(\theta)}{\partial \theta_i^{n+1}} = \left(\frac{1}{\Delta t} + \frac{D(\theta)_{i+1/2}^{n+1/2}}{2\Delta z_2 \Delta z_4} \left[1 + 2\, \frac{\partial \Delta \theta^{n+1}}{\partial \theta_i^{n+1}} \right] + \frac{D(\theta)_{i-1/2}^{n+1}}{2\Delta z_1 \Delta z_4} \right) + \frac{\partial D(\theta)_i^{n+1/2}}{\partial \theta_i^{n+1}} \left(\frac{\theta_i^{n+1} - \theta_{i+1}^{n+1} + \theta_i^{n} - \theta_{i+1}^{n} + 8\Delta\theta^{n+1}}{8\ \Delta z_2 \Delta z_4} \right) + \frac{\partial D(\theta)_i^{n+1/2}}{\partial \theta_i^{n+1}} \left(\frac{-\, \theta_{i-1}^{n+1} + \theta_i^{n+1} - \theta_{i-1}^{n} + \theta_i^{n}}{8\ \Delta z_1 \Delta z_4} \right) \tag{A-5}$$

$$\frac{\partial F_i(\theta)}{\partial \theta_{i+1}^{n+1}} = \left(\frac{-\, D(\theta)_{i+1/2}^{n+1/2}}{2\Delta z_2 \Delta z_4} \right) \left[1 - 2\, \frac{\partial \Delta \theta^{n+1}}{\partial \theta_{i+1}^{n+1}} \right] + \frac{\partial D(\theta)_{i+1}^{n+1/2}}{\partial \theta_{i+1}^{n+1}} \left(\frac{\theta_i^{n+1} - \theta_{i+1}^{n+1} + \theta_i^{n} - \theta_{i+1}^{n} + 2\Delta\theta^{n+1}}{8\ \Delta z_2 \Delta z_4} \right) - \frac{\partial K(\theta)_{i+1}^{n+1/2}}{\partial \theta_{i+1}^{n+1}} \left(\frac{1}{4\ \Delta z_4} \right) \tag{A-6}$$

3. For the node just below an interface:

$$\frac{\partial F_i(\theta)}{\partial \theta_{i-1}^{n+1}} = \left(\frac{-\, D(\theta)_{i-1/2}^{n+1/2}}{2\Delta z_1 \Delta z_5} \right) \left[1 + 2 \frac{\partial \Delta\theta^{n+1}}{\partial \theta_{i-1}^{n+1}} \right] + \frac{\partial D(\theta)_{i-1}^{n+1/2}}{\partial \theta_{i-1}^{n+1}} \left(\frac{-\, \theta_{i-1}^{n+1} + \theta_i^{n+1} - \theta_{i-1}^{n} + \theta_i^{n} - 8\Delta\theta^{n+1}}{8\ \Delta z_1 \Delta z_5} \right) - \frac{\partial K(\theta)_{i-1}^{n+1/2}}{\partial \theta_{i-1}^{n+1}} \left(\frac{1}{4\ \Delta z_5} \right) \tag{A-7}$$

$$\frac{\partial F_i(\theta)}{\partial \theta_i^{n+1}} = \left(\frac{1}{\Delta t} + \frac{D(\theta)_{i+1/2}^{n+1/2}}{2\Delta z_2 \Delta z_5} + \frac{D(\theta)_{i-1/2}^{n+1}}{2\Delta z_1 \Delta z_5} \left[1 - 2 \frac{\partial \Delta\Theta^{n+1}}{\partial \theta_i^{n+1}} \right] \right) + \frac{\partial D(\theta)_i^{n+1/2}}{\partial \theta_i^{n+1}} \left(\frac{\theta_i^{n+1} - \theta_{i+1}^{n+1} + \theta_i^{n} - \theta_{i+1}^{n}}{8\ \Delta z_2 \Delta z_5} \right) + \frac{\partial D(\theta)_i^{n+1/2}}{\partial \theta_i^{n+1}} \left(\frac{-\, \theta_{i-1}^{n+1} + \theta_i^{n+1} - \theta_{i-1}^{n} + \theta_i^{n} - 8\Delta\Theta^{n+1}}{8\ \Delta z_1 \Delta z_5} \right) \tag{A-8}$$

$$\frac{\partial F_i(\theta)}{\partial \theta_{i+1}^{n+1}} = \left(\frac{-\, D(\theta)_{i+1/2}^{n+1/2}}{2\Delta z_2 \Delta z_5} \right) + \frac{\partial D(\theta)_{i+1}^{n+1/2}}{\partial \theta_{i+1}^{n+1}} \left(\frac{\theta_i^{n+1} - \theta_{i+1}^{n+1} + \theta_i^{n} - \theta_{i+1}^{n}}{8\ \Delta z_2 \Delta z_5} \right) - \frac{\partial K(\theta)_{i+1}^{n+1/2}}{\partial \theta_{i+1}^{n+1}} \left(\frac{1}{4\ \Delta z_5} \right) \tag{A-9}$$

4. For the upper boundary:

$$\frac{\partial F_i(\theta)}{\partial \theta_1^{n+1}} = \frac{1}{\Delta t} + \frac{D(\theta)_{1+1/2}^{n+1/2}}{(z_2 - z_1)^2} + \frac{\partial D(\theta)_1^{n+1/2}}{\partial \theta_1^{n+1}} \left(\frac{\theta_1^{n+1} - \theta_2^{n+1}}{2\,(z_2 - z_1)^2} \right) + \frac{\partial K(\theta)_1^{n+1/2}}{\partial \theta_1^{n+1}} \left(\frac{1}{2\,z_2 - z_1} \right) \tag{A-10}$$

$$\frac{\partial F_1(\theta)}{\partial \theta_2^{n+1}} = \frac{-\,D(\theta)_{1+1/2}^{n+1/2}}{(z_2 - z_1)^2} + \frac{\partial D(\theta)_2^{n+1/2}}{\partial \theta_2^{n+1}} \left(\frac{\theta_1^{n+1} - \theta_2^{n+1}}{2\,(z_2 - z_1)^2} \right) + \frac{\partial K(\theta)_2^{n+1/2}}{\partial \theta_2^{n+1}} \left(\frac{1}{2\,z_2 - z_1} \right) \tag{A-11}$$

5. For the lower boundary:

$$\frac{\partial F_m(\theta)}{\partial \theta_{m-1}^{n+1}} = \left(\frac{-\,D(\theta)_{m-1/2}^{n+1/2}}{\Delta z_1 \Delta z_3} \right) + \frac{\partial D(\theta)_{m-1}^{n+1/2}}{\partial \theta_{m-1}^{n+1}} \left(\frac{-\,\theta_{m-1}^{n+1} + \theta_m^{n+1} - \theta_{m-1}^{n} + \theta_m^{n}}{4\,\Delta z_1 \Delta z_3} \right) \tag{A-12}$$

$$\frac{\partial F_m(\theta)}{\partial \theta_m^{n+1}} = \left(\frac{1}{\Delta t} + \frac{D(\theta)_{m-1/2}^{n+1}}{\Delta z_1 \Delta z_3} \right) + \frac{\partial D(\theta)_m^{n+1/2}}{\partial \theta_m^{n+1}} \left(\frac{-\,\theta_{m-1}^{n+1} + \theta_m^{n+1} - \theta_{m-1}^{n} + \theta_m^{n}}{4\,\Delta z_1 \Delta z_3} \right) \tag{A-13}$$

Where:

$$\frac{\partial D(\theta)_i^{n+1/2}}{\partial \theta_i} = \frac{d\,D(Se)}{d\,Se} \cdot \frac{d\,Se}{d\,\theta} \tag{A-14}$$

$$\frac{d\,D(Se)}{d\,Se} = \frac{(1-m)\,K_s}{\alpha\, m(\theta_s - \theta_r)} \left[(1-Se^{1/m})^{-m} + (1-Se^{1/m})^{m} - 2\right] + \frac{(1-m)\,K_s}{\alpha\, m(\theta_s - \theta_r)}\, Se^{-1/2} \left[1-Se^{1/m}\right]^{-m-1} - \left[1-Se^{1/m}\right]^{m-1} \tag{A-15}$$

$$\frac{d\,Se(\theta)}{d\,\theta} = \frac{1}{\theta_s - \theta_r} \tag{A-16}$$

$$\frac{\partial K(\theta)_i^{n+1/2}}{\partial \theta_i} = \frac{d\,K(Se)}{d\,Se} \cdot \frac{d\,Se}{d\,\theta} \tag{A-17}$$

$$\frac{d\,K(Se)}{d\,Se} = K_s \left[\frac{Se^{-1/2}}{2} \left[1 - \left(1 - Se^{1/m} \right)^{m} \right]^2 + 2\, Se^{1/2} \left(1 - Se^{1/m} \right)^{m-1} \left(Se^{\frac{1-m}{m}} \right) \left[1 - \left(1 - Se1/m \right)^{m} \right] \right] \tag{A-18}$$

$$\frac{\partial \Delta\theta}{\partial \theta_i} = -\frac{1}{2} \frac{\partial \theta^{-}}{\partial \psi} \frac{\partial \psi\downarrow}{\partial \theta_i} \tag{A-19}$$

for the node just above the interface, and

$$\frac{\partial \Delta\theta}{\partial \theta_i} = \frac{1}{2} \frac{\partial \theta^{+}}{\partial \psi} \frac{\partial \psi\uparrow}{\partial \theta_i} \tag{A-20}$$

for the node just below the interface.

$$\frac{\partial \theta}{\partial \psi} = m\,(\theta_s - \theta_r)\left[\frac{1}{1 + (\alpha\ \psi)^n}\right]^{m-1}\left[\frac{-\alpha\ n\ (\alpha\ \psi)^{n-1}}{(\ 1 + (\alpha\ \psi)^n\ )^2}\right] \qquad \text{(A-21)}$$

$$\frac{\partial \psi\downarrow}{\partial \theta_i} = \frac{1}{2}\left(2\left[\frac{\partial K(\theta_i)}{\partial \theta_i}\ \psi(\theta_i) + K(\theta_i)\frac{\partial \psi(\theta_i)}{\partial \theta_i}\right] + \Delta z\ \frac{\partial K(\theta_i)}{\partial \theta_i}\right)(\ K(\theta_i) + K(\theta_{i+1})\ )^{-1}$$
$$- \frac{1}{2}\left[(\ K(\theta_i) + K(\theta_{i+1})\ )^{-2}\ \frac{\partial K(\theta_i)}{\partial \theta_i}\right] \qquad \text{(A-22)}$$
$$* \left(\frac{1}{2}(\ 2\ [\ K(\theta_i)\ h(\theta_i) + K(\theta_{i+1})\ h(\theta_{i+1})\ ] + \Delta z\ [\ k(\theta_i) - K(\theta_{i+1})\ ]\ )\right)$$

$$\frac{\partial \psi\uparrow}{\partial \theta_i} = \frac{1}{2}\left(2\left[\frac{\partial K(\theta_i)}{\partial \theta_i}\ \psi(\theta_i) + K(\theta_i)\frac{\partial \psi(\theta_i)}{\partial \theta_i}\right] - \Delta z\ \frac{\partial K(\theta_i)}{\partial \theta_i}\right)(\ K(\theta_i) + K(\theta_{i-1})\ )^{-1}$$
$$- \frac{1}{2}\left[(\ K(\theta_i) + K(\theta_{i-1})\ )^{-2}\ \frac{\partial K(\theta_i)}{\partial \theta_i}\right] \qquad \text{(A-23)}$$
$$* \left(\frac{1}{2}(\ 2\ [\ K(\theta_i)\ h(\theta_i) + K(\theta_{i+1})\ h(\theta_{i+1})\ ] + \Delta z\ [\ k(\theta_i) - K(\theta_{i+1})\ ]\ )\right)$$

APPENDIX B

Computer program codes in C language were written to simulate the water and solute transport in layered soil.

```
#include <stdio.h>
#include <conio.h>
#include <math.h>
#include <float.h>
void water();
void solute();
void newton();
void soil_hydraulics();
void K_and_D(int);
void jump(int, int);
void initialize();
void vector_F_theta();
void matrix_jacob();
double Deriv_THETA(double,int);
double THETA(double,int);
double Deriv_conduc(int);
double conduc(int,int);
double Deriv_diffu(int);
double diffu(int,int);
double Deriv_potential(int);
double potential(int,int);
double Deriv_Dtheta1(double,int);
double Deriv_Dtheta2(double,int);
double potential(int, int);
void water_balance();
void solute_balance();
void Read_input();
void Write_output_1();
void Write_output_2();
// Global variables
double theta_sat[6], theta_dry[6], initial_theta[6];
double m, n[6], alpha[6];
```

```
double K_sat[6], Dtheta, mass_balance, balance;
double HC1, HC2, HD1, HD2, DZ4, DZ5;
double Wbound1, Wbound2, Sbound1, Sbound2, W_q,  start_B2;
    double sum_flux = 0.0, balance_ratio, initial_water_vol = 0.0;
    double sum_C = 0.0, balance_C, initial_solute = 0.0, balance_ratio_C;
    double S_j, S_Diffusion, initial_C[6], lambda[6];
    double thetaA[2], D_theta[6][2], Gama[210], Beta[210];
    double Dt, time_end, Printout[8];
    int num_nodes, num_layers, layer[6], L, max_itir;
typedef struct {
    double theta[3], K_sat, theta_sat, theta_dry, alpha, n, depth;
    double DZ1, DZ2, DZ3;
    double F_theta, residual, Deriv_HC, Deriv_HD;
    double Diff[2], HC[2], jacob_A, jacob_B, jacob_C;
    double C[2], S_A, S_B, S_C, S_Known, lambda;
} soil;
soil node[210];
FILE *input, *output;
main()
    {   int i, P = 0;
        ouble Time = 0.0, dz;
        clrscr();
        input = fopen("DATA.IN", "r");
        output = fopen("DATA.OUT", "w");
        Read_input();
        initialize();
        Write_output_1();
        W_q = Wbound1;
         node[0].theta[1] = (W_q * Dt / (node[1].depth - node[0].depth))
                          + node[0].theta[0];
        if (node[0].theta[1] >= node[0].theta_sat)
                    node[0].theta[1] = node[0].theta_sat *   0.99999;
        if (node[0].theta[1] <= node[0].theta_dry)
                    node[0].theta[1] =  node[0].theta_dry
                                      + (node[0].theta_dry * 0.00001);
    // calculation of the volume of initial water content an solute concentration
    // in the soil
        L = 0;
        for (i=0; i < num_nodes-1; i++)
             {  dz = node[i+1].depth - node[i].depth;
             if (i+1 == layer[L+1]) jump(i,L);
                {   initial_water_vol += node[i].theta[2] * dz/2;
                    initial_water_vol += node[i+1].theta[2] * dz/2;
                    L++;
```

```
                }
            initial_water_vol += node[i].theta[0] * dz;
            initial_solute += node[i].theta[0] * node[i].C[0] * dz;
             }
    for (i=1; i < num_nodes; i++) node[i].theta[1] = node[i].theta[0];
    do {
        Time += Dt;
        W_q = Wbound1;
        S_j = Sbound1 * W_q;
        if (Time >= start_B2) { W_q = Wbound2; S_j = Sbound2 * W_q; }
        water();
        solute();
        solute_balance();
        for (i=0; i < num_nodes; i++)
           {
              node[i].theta[0] = node[i].theta[2];
              node[i].C[0] = node[i].C[1];
                node[i].theta[1] = node[i].theta[0];
             }
        if (Time >= Printout[P]) { Write_output_2(); P++; }
        } while (Time < time_end);
    return;
}
void water (void)
    {
        newton();
         water_balance();
         return;
    }
void newton(void)
    {
        int i, j, flag, itir= 0;
        double max;
        do {
             itir += 1;
             node[num_nodes].theta[0] = node[num_nodes-2].theta[0];
             node[num_nodes].theta[1] = node[num_nodes-2].theta[1];
             soil_hydraulics();
             matrix_jacob();
             vector_F_theta();
    //
    // Solve for residual vector using Thomas method for Tri-diagonal matrix.
    //
             node[0].jacob_A = node[num_nodes - 1].jacob_C = 0;
```

```
            Beta[0] = node[0].jacob_B;
            Gama[0] = (-1 * node[0].F_theta) / node[0].jacob_B;
            for (i=1; i < num_nodes; i++)
              {
                  Beta[i] = node[i].jacob_B - (node[i].jacob_A
                          * node[i-1].jacob_C / Beta[i-1]);
                   Gama[i] = ((-1 * node[i].F_theta) - (node[i].jacob_A
                           * Gama[i-1])) / Beta[i];
              }
            node[num_nodes - 1].residual = Gama[num_nodes - 1];
            for (i = num_nodes - 2; i >= 0; i--)
                 node[i].residual = Gama[i] - ( node[i].jacob_C
                          * node[i+1].residual / Beta[i]);
            for (i=0; i < num_nodes; i++)
                  node[i].theta[2] = node[i].theta[1] + node[i].residual;
            max = fabs(node[0].residual);
            for (i=1; i < num_nodes; i++)
                  if (fabs(node[i].residual) > max)  max = fabs(node[i].residual);
            for (i = 0; i < num_nodes; i++)
              {
                    if (node[i].theta[2] >= node[i].theta_sat)
                         node[i].theta[2] = node[i].theta_sat * 0.99999;
                    if (node[i].theta[2] <= node[i].theta_dry)
                         node[i].theta[2] = node[i].theta_dry
                                          + (node[i].theta_dry * 0.00001);
              }
            for (i=0; i < num_nodes; i++) node[i].theta[1] = node[i].theta[2];
             if(mass_balance <= 0.0000001) return;
         } while (itir < max_itir);
          return;
}
void vector_F_theta()
{ int i, L = 0;
  double DZ1;
  mass_balance = 0.0;
  HD1 = (node[1].Diff[1] + node[0].Diff[1]) / 2;
  HC1 = (node[1].HC[1] + node[0].HC[1]) / 2;
  node[0].F_theta =  (node[0].theta[1] * ((1/Dt)
                  + (HD1 / pow(node[1].depth-node[0].depth,2))))
                  - (node[1].theta[1] *  (HD1 / pow(node[1].depth-node[0].depth,2)))
                  - (node[0].theta[0] / Dt) + (HC1 / (node[1].depth-node[0].depth))
                  - (W_q / (node[1].depth - node[0].depth));
  mass_balance += fabs(node[i].F_theta);
  for (i=1; i < num_nodes; i++)
```

```
    {
        K_and_D(i);
        if (i+1 == layer[L+1]) jump(i,L);
        else if (i == layer[L+1]) L++;
        else
            {
                node[i].F_theta =  (-node[i-1].theta[1] * (1/node[i].DZ3)
                                   * (HD2/(2*node[i].DZ1))) + (node[i].theta[1] * ((1/Dt)
                                   + ((1 / node[i].DZ3) * ((HD1/(2 * node[i].DZ2))
                                   + (HD2 / (2 * node[i].DZ1))))))
                                   - (node[i+1].theta[1] * (1 / node[i].DZ3)
                                   * (HD1 / (2 * node[i].DZ2)))
                                   - (node[i-1].theta[0] * (1/node[i].DZ3)
                                   * (HD2/(2*node[i].DZ1)))
                                    - (node[i].theta[0] * ((1/Dt)- ((1/node[i].DZ3)
                                    *  ((HD1/(2*node[i].DZ2))
                                   + (HD2/(2*node[i].DZ1))))))
                                    - (node[i+1].theta[0] * ((1/node[i].DZ3)
                                    * (HD1/(2*node[i].DZ2))))
                                    + ((HC1 - HC2)/node[i].DZ3);
                mass_balance += fabs(node[i].F_theta);
            }
    }
}
void matrix_jacob()
{ int i;
  double DZ1;
  HD1 = (node[1].Diff[1] + node[0].Diff[1]) / 2;
  node[0].jacob_B =  ((1/Dt) + (HD1 / pow(node[1].depth-node[0].depth,2))) +
                      (((node[0].theta[1] - node[1].theta[1]) /
                      pow(node[1].depth-node[0].depth,2)) * node[0].Deriv_HD)
                     + ((node[0].Deriv_HC/2) / (node[1].depth-node[0].depth));
  node[0].jacob_C =   (-HD1 / pow(node[1].depth-node[0].depth,2))
                    + (((node[0].theta[1] - node[1].theta[1]) /
pow(node[1].depth-node[0].depth,2)) * node[1].Deriv_HD)
                    + ((node[1].Deriv_HC/4) / (node[1].depth-node[0].depth));
  i = num_nodes - 1;
  K_and_D(i);
  node[i].jacob_A =  ((-1/node[i].DZ3) * (HD2/(2*node[i].DZ1)))
                     + (((-node[i-1].theta[1] + node[i].theta[1] - node[i-1].theta[0]
                             + node[i].theta[0]) / (2 * node[i].DZ3 * node[i].DZ1))
                             * node[i-1].Deriv_HD)
                     - ((node[i-1].Deriv_HC/4) / (node[i].DZ3));
```

```
  node[i].jacob_B =  (1/Dt + ((1/node[i].DZ3) * ((HD1/(2*node[i].DZ2))
                          + (HD2/(2*node[i].DZ1)))))
                     + (((-node[i-1].theta[1] + node[i].theta[1] - node[i-1].theta[0]
                          + node[i].theta[0]) / (2 * node[i].DZ3 * node[i].DZ1))
                          * node[i].Deriv_HD)
                     + (((node[i].theta[1] - node[i+1].theta[1] + node[i].theta[0]
                           - node[i+1].theta[0]) / (2 * node[i].DZ3 * node[i].DZ2))
                           * node[i].Deriv_HD);
  for (i=1; i < num_nodes-1; i++)
   {    K_and_D(i);
    node[i].jacob_A =  ((-1/node[i].DZ3) * (HD2/(2*node[i].DZ1)))
                       + (((-node[i-1].theta[1] + node[i].theta[1] - node[i-1].theta[0]
                            + node[i].theta[0]) / (2 * node[i].DZ3
                            * node[i].DZ1)) * node[i-1].Deriv_HD)
                         - ((node[i-1].Deriv_HC/4) / (node[i].DZ3));
    node[i].jacob_B =  (1/Dt + ((1/node[i].DZ3) * ((HD1/(2*node[i].DZ2))
                            + (HD2/(2*node[i].DZ1)))))
                       + (((-node[i-1].theta[1] + node[i].theta[1] - node[i-1].theta[0]
                            + node[i].theta[0]) / (2 * node[i].DZ3
                            * node[i].DZ1)) * node[i].Deriv_HD)
                       + (((node[i].theta[1] - node[i+1].theta[1] + node[i].theta[0]
                            - node[i+1].theta[0]) / (2 * node[i].DZ3
                            * node[i].DZ2)) * node[i].Deriv_HD);
    node[i].jacob_C =  ((-1/node[i].DZ3) * (HD1/(2*node[i].DZ2)))
                            + (((node[i].theta[1] - node[i+1].theta[1]
                            + node[i].theta[0] - node[i+1].theta[0]) / (2
                            * node[i].DZ3 * node[i].DZ2))
                            * node[i+1].Deriv_HD)
                            - ((node[i+1].Deriv_HC/4) / (node[i].DZ3));
   }
}
void jump(i,L)
{ int k;
  double Dtheta_last, Dtheta_next, theta_up[2], theta_dn[2], DZ;
  double last_pot_int, next_pot_int, Wpot[2], Se_par[2];
/*
   Calculation of the jump in the water content at the interface
*/
   DZ = (node[i+1].depth - node[i].depth)/2;
   Wpot[0] = potential(i,0);
   Wpot[1] = potential(i+1,0);
   last_pot_int = ((2 * ((node[i].HC[0] * Wpot[0]) + (node[i+1].HC[0] * Wpot[1])))
                  + (DZ * (node[i].HC[0] - node[i+1].HC[0]))) / (2*(node[i].HC[0]
                        + node[i+1].HC[0]));
```

```
   Wpot[0] = potential(i,1);
   Wpot[1] = potential(i+1,1);
   next_pot_int = ((2 * ((node[i].HC[1] * Wpot[0]) + (node[i+1].HC[1] * Wpot[1])))
                  + (DZ * (node[i].HC[1] - node[i+1].HC[1]))) / (2*(node[i].HC[1]
                       + node[i+1].HC[1]));
   theta_up[0] = THETA(fabs(last_pot_int),i);
   theta_up[1] = THETA(fabs(next_pot_int),i);
   theta_dn[0] = THETA(fabs(last_pot_int),i+1);
   theta_dn[1] = THETA(fabs(next_pot_int),i+1);
   Dtheta_last = theta_dn[0] - theta_up[0];
   Dtheta_next = theta_dn[1] - theta_up[1];
   Dtheta = (Dtheta_next + Dtheta_last) / 2;
   D_theta[L][0] = Dtheta_last;
   D_theta[L][1] = Dtheta_next;
/*
   Calculation of the mass balance equation to F(theta) vector for
   flow equation at the interface
*/
   K_and_D(i);
   DZ4 = ((node[i].DZ2/2) + node[i].DZ1)/2;
   node[i].F_theta =  (-node[i-1].theta[1] * (1/DZ4) * (HD2/(2*node[i].DZ1)))
                              + (node[i].theta[1] * ((1/Dt) + ((1/DZ4)
                              * ((HD1/(2*node[i].DZ2)) + (HD2/(2*node[i].DZ1))))))
                              - (node[i+1].theta[1] * ((1/DZ4)
                              * (HD1/(2*node[i].DZ2))))
                              - (node[i-1].theta[0] * (1/DZ4) * (HD2/(2*node[i].DZ1)))
                              + (node[i].theta[0] * (((1/DZ4) * ((HD1/(2*node[i].DZ2))
                              + (HD2/(2*node[i].DZ1)))) - (1/Dt)))
                              - (node[i+1].theta[0] * ((1/DZ4)
                              * (HD1/(2*node[i].DZ2))))
                              + (Dtheta * (1/DZ4) * (HD1/node[i].DZ2))
                               + ((HC1 - HC2)/node[i].DZ3);
   mass_balance += fabs(node[i].F_theta);
   k = i+1;
   K_and_D(k);
   DZ5 = ((node[k].DZ1/2) + node[k].DZ2)/2;
   node[k].F_theta = (-node[k-1].theta[1] * (1/DZ5) * (HD2/(2*node[k].DZ1)))+
                     (node[k].theta[1] * ((1/Dt) + ((1/DZ5) * ((HD1/(2*node[k].DZ2))
                     +(HD2/(2*node[k].DZ1))))))- (node[k+1].theta[1] * ((1/DZ5) *
                     (HD1/(2*node[k].DZ2))))- (node[k-1].theta[0] * (1/DZ5) *
                     (HD2/(2*node[k].DZ1)))- (node[k].theta[0] * ((1/Dt) - ((1/DZ5) *
                     ((HD1/(2*node[k].DZ2)) + (HD2/(2*node[k].DZ1))))))-
                     (node[k+1].theta[0] * ((1/DZ5) * (HD1/(2*node[k].DZ2))))-
                     (Dtheta * (1/DZ5) * (HD2/node[k].DZ1)) + ((HC1
```

```
                    -HC2)/node[k].DZ3);
  mass_balance += fabs(node[k].F_theta);
/*
  Calculation of the coefficients for the Jacobian matrix for the two
  nodes that bounding the interface.
*/
  K_and_D(i);
  node[i].jacob_A =  (-(1/DZ4) * (HD2/(2*node[i].DZ1)))
                   - (((node[i-1].theta[1] - node[i].theta[1] + node[i-1].theta[0]
                   - node[i].theta[0]) /( 2 * DZ4 * node[i].DZ1))
                   * node[i-1].Deriv_HD) - ((1/node[i].DZ3)
                   * (node[i-1].Deriv_HC/4));
  node[i].jacob_B =  (((-node[i-1].theta[1] + node[i].theta[1] - node[i-1].theta[0]
                  + node[i].theta[0]) /( 2 * DZ4 * node[i].DZ1)) * node[i].Deriv_HD)
                  + (((node[i].theta[1] - node[i+1].theta[1] + node[i].theta[0]
                  - node[i+1].theta[0]) /( 2 * DZ4 * node[i].DZ2))
                  * node[i].Deriv_HD) + ((1/Dt) + ((1/DZ4)
                  * ((HD1/(2*node[i].DZ2)) + (HD2/(2*node[i].DZ1)))))
                  + (Deriv_Dtheta1(fabs(next_pot_int),i) * (1/DZ4)
                  * (HD1/node[i].DZ2)) + ((Dtheta / (DZ4 * node[i].DZ2))
                  * node[i].Deriv_HD);
  node[i].jacob_C =  (((node[i].theta[1] - node[i+1].theta[1] + node[i].theta[0]
                  - node[i+1].theta[0] + (2*Dtheta)) /( 2 * DZ4 * node[i].DZ2))
                  * node[i+1].Deriv_HD) - ((1/DZ4) * (HD1/(2*node[i].DZ2)))
                  + (Deriv_Dtheta2(fabs(next_pot_int),i+1) * (1/DZ4)
                  * (HD1/node[i].DZ2));
  K_and_D(k);
  node[k].jacob_A =  (-(1/DZ5) * (HD2/(2*node[k].DZ1))) + (((-node[k-1].theta[1]
                   + node[k].theta[1] - node[k-1].theta[0] + node[k].theta[0]
                   - (2*Dtheta)) /( 2 * DZ5 * node[k].DZ1)) * node[k-1].Deriv_HD)
                   - (Deriv_Dtheta1(fabs(next_pot_int),k-1) * (1/DZ5)
                   * (HD2/node[k].DZ1)) - ((1/node[k].DZ3)
                   * (node[k-1].Deriv_HC/4));
  node[k].jacob_B =  (((-node[k-1].theta[1] + node[k].theta[1] - node[k-1].theta[0]
                  + node[k].theta[0] - (2*Dtheta)) /( 2 * DZ5 * node[k].DZ1))
                  * node[k].Deriv_HD) + (((node[k].theta[1] - node[k+1].theta[1]
                  + node[k].theta[0] - node[k+1].theta[0]) / (2 * DZ5
                            * node[k].DZ2)) * node[k].Deriv_HD) + ((1/Dt)
                  + ((1/DZ5) * ((HD1/(2*node[k].DZ2)) + (HD2/(2*node[k].DZ1)))))
                   - (Deriv_Dtheta2(fabs(next_pot_int),k) * (1/DZ5)
                            * (HD2/node[k].DZ1));
```

```
node[k].jacob_C =  (((node[k].theta[1] - node[k+1].theta[1] + node[k].theta[0]
                              - node[k+1].theta[0]) / (2 * DZ5 * node[k].DZ2))
                             * node[k+1].Deriv_HD) - ((1/DZ5)
                             * (HD1/(2*node[k].DZ2))) + ((1/node[k].DZ3)
                             * (node[k+1].Deriv_HC/4));
  return;
}
void solute(void)
{
 int i, L = 0;
 double th0, th1, th2, th3, th4, flux0, flux1, veloc0, veloc1, dz, DZ3;
 double solute_Dis0, solute_Dis1;
 double th0a, th0b, th2a, th2b, flux0a, flux0b, flux1a, flux1b;
 soil_hydraulics();
 dz = node[1].depth - node[0].depth;
 HD1 = (node[1].Diff[1] + node[0].Diff[1] + node[1].Diff[0] + node[0].Diff[0]) / 4;
 HC1 = (node[1].HC[1] + node[0].HC[1] + node[1].HC[0] + node[0].HC[0]) / 4;
 th1 = (node[0].theta[1] + node[0].theta[0]) / 2;
 th2 = (node[1].theta[1] + node[1].theta[0]) / 2;
 th4 = (node[1].theta[1] + node[0].theta[1] + node[1].theta[0] + node[0].theta[0]) / 4;
 flux1 = (-HD1 * (th2 - th1) / dz) + HC1;
 veloc1 = fabs(flux1 / th4);
 solute_Dis1 = S_Diffusion + (node[0].lambda * veloc1);
 node[0].S_B =  (node[0].theta[1]/Dt) + (th4 * solute_Dis1 / (2 * dz * dz))
                        + (flux1 / (4 * dz));
 node[0].S_C =  ((th4 * solute_Dis1 / (2 * dz * dz)) - (flux1 / (4 * dz))) * -1;
 node[0].S_Known =  (node[0].C[0] * ((node[0].theta[0]/Dt)
                              - (th4 * solute_Dis1 / (2 * dz * dz))
                              - (flux1 / (4 * dz))))
                             + (node[1].C[0] * ((th4 * solute_Dis1 / (2 * dz * dz))
                              - (flux1 / (4 * dz))))  + (S_j / dz);
 node[num_nodes].theta[0] = node[num_nodes-2].theta[0];
 node[num_nodes].theta[1] = node[num_nodes-2].theta[1];
 node[num_nodes].C[0] = node[num_nodes-2].C[0];
 i = num_nodes-1;
 K_and_D(i);
 th0 = (node[i-1].theta[1] + node[i-1].theta[0]) / 2;
 th1 = (node[i].theta[1] + node[i].theta[0]) / 2;
 th2 = (node[i+1].theta[1] + node[i+1].theta[0]) /2;
 th3 = (node[i].theta[1] + node[i-1].theta[1] + node[i].theta[0] + node[i-1].theta[0]) / 4;
 th4 = (node[i+1].theta[1] + node[i].theta[1] + node[i+1].theta[0] + node[i].theta[0]) /4;
 flux0 = (-HD2 * (th1 - th0) / node[i].DZ1) + HC2;
 flux1 = (-HD1 * (th2 - th1) / node[i].DZ2) + HC1;
 veloc0 = fabs(flux0 / th3);
```

```
 veloc1 = fabs(flux1 / th4);
 solute_Dis0 = S_Diffusion + (node[i].lambda * veloc0);
 solute_Dis1 = S_Diffusion + (node[i].lambda * veloc1);
 node[i].S_A =  ((th3 * solute_Dis0 / (2 * node[i].DZ1 * node[i].DZ3))
                    + (flux0 / (4 * node[i].DZ3)) + (th4 * solute_Dis1 / (2
                        * node[i].DZ2 * node[i].DZ3))-(flux1 / (4 * node[i].DZ3))) *-1;
 node[i].S_B =  (node[i].theta[1]/Dt)
           + (th4 * solute_Dis1 / (2 * node[i].DZ2 * node[i].DZ3))
           + (th3 * solute_Dis0 / (2 * node[i].DZ1 * node[i].DZ3))
           + (flux1 / (4 * node[i].DZ3))
           - (flux0 / (4 * node[i].DZ3));
 node[i].S_Known =  (node[i-1].C[0] * ((th3 * solute_Dis0 / (2 * node[i].DZ1 *
node[i].DZ3)) + (flux0 / (4 * node[i].DZ3))))
              + (node[i].C[0] *  ((node[i].theta[0]/Dt)
              - (th4 * solute_Dis1 / (2 * node[i].DZ2 * node[i].DZ3))
              - (th3 * solute_Dis0 / (2 * node[i].DZ1 * node[i].DZ3))
              - (flux1 / (4 * node[i].DZ3)) + (flux0 / (4 * node[i].DZ3))))
              + (node[i+1].C[0] * ((th4 * solute_Dis1 / (2 * node[i].DZ2 *
node[i].DZ3))
              - (flux1 / (4 * node[i].DZ3))));
 for (i=1; i < num_nodes-1; i++)
 {
 K_and_D(i);
 th0 = (node[i-1].theta[1] + node[i-1].theta[0]) / 2;
 th1 = (node[i].theta[1] + node[i].theta[0]) / 2;
 th2 = (node[i+1].theta[1] + node[i+1].theta[0]) / 2;
 th3 = (node[i].theta[1] + node[i-1].theta[1] + node[i].theta[0] + node[i-1].theta[0]) / 4;
 th4 = (node[i+1].theta[1] + node[i].theta[1] + node[i+1].theta[0] + node[i].theta[0]) /
4;
 if (i+1 == layer[L+1])
 {
  thetaA[1] = (node[i].theta[1] + node[i+1].theta[1])/2;
  thetaA[0] = (node[i].theta[0] + node[i+1].theta[0])/2;
  th2a = ((thetaA[1] - (D_theta[L][1] / 2)) +  (thetaA[0] - (D_theta[L][0] / 2))) / 2;
  th2b = ((thetaA[1] + (D_theta[L][1] / 2)) + (thetaA[0] + (D_theta[L][0] / 2))) / 2;
  th4 = ((thetaA[1] - (D_theta[L][1] / 2)) + node[i].theta[1] + (thetaA[0] -
(D_theta[L][0] / 2)) + node[i].theta[0]) / 4;
  flux0 = (-HD2 * (th1 - th0) / node[i].DZ1) + HC2;
  flux1a = (-HD1 * (th2a - th1) / (node[i].DZ2 / 2)) + HC1;
  flux1b = (-HD1 * (th2 - th2b) / (node[i].DZ2 / 2)) + HC1;
  flux1 = (flux1a + flux1b) / 2;
  DZ3 = node[i].DZ3;
  DZ4 = node[i].DZ3;
//  DZ4 = ((node[i].DZ2/2) + node[i].DZ1)/2;
```

```
 }
 else if (i == layer[L+1])
 {
  thetaA[1] = (node[i].theta[1] + node[i-1].theta[1])/2;
  thetaA[0] = (node[i].theta[0] + node[i-1].theta[0])/2;
     th0a = ((thetaA[1] - (D_theta[L][1] / 2)) +  (thetaA[0] - (D_theta[L][0] / 2))) / 2;
     th0b = ((thetaA[1] + (D_theta[L][1] / 2)) + (thetaA[0] + (D_theta[L][0] / 2))) / 2;
     th3 = (node[i].theta[1] + (thetaA[1] + (D_theta[L][1] / 2)) + node[i].theta[0] +
(thetaA[0] + (D_theta[L][0] / 2))) / 4;
     flux0a = (-HD2 * (th0a - th0) / (node[i].DZ1 / 2)) + HC2;
     flux0b = (-HD2 * (th1 - th0b) / (node[i].DZ1 / 2)) + HC2;
     flux0 = (flux0a + flux0b) / 2;
     flux1 = (-HD1 * (th2 - th1) / node[i].DZ2) + HC1;
//     DZ3 = ((node[i].DZ1/2) + node[i].DZ2)/2;
     DZ3 = node[i].DZ3;
     DZ4 = node[i].DZ3;
     L++;
 }
 else
 {
     flux0 = (-HD2 * (th1 - th0) / node[i].DZ1) + HC2;
     flux1 = (-HD1 * (th2 - th1) / node[i].DZ2) + HC1;
     DZ3 = node[i].DZ3;
     DZ4 = node[i].DZ3;
 }
 veloc0 = fabs(flux0 / th3);
 veloc1 = fabs(flux1 / th4);
 solute_Dis0 = S_Diffusion + (node[i].lambda * veloc0);
 solute_Dis1 = S_Diffusion + (node[i].lambda * veloc1);
 node[i].S_A =  ((th3 * solute_Dis0 / (2 * node[i].DZ1 * node[i].DZ3))
           + (flux0 / (4 * DZ3))) * -1;
 node[i].S_B =  (node[i].theta[1]/Dt)
           + (th4 * solute_Dis1 / (2 * node[i].DZ2 * node[i].DZ3))
           + (th3 * solute_Dis0 / (2 * node[i].DZ1 * node[i].DZ3))
           + (flux1 / (4 * DZ4))
           - (flux0 / (4 * DZ3));
 node[i].S_C =  ((th4 * solute_Dis1 / (2 * node[i].DZ2 * node[i].DZ3))
           - (flux1 / (4 * DZ4))) * -1;
 node[i].S_Known =  (node[i-1].C[0] * ((th3 * solute_Dis0 / (2 * node[i].DZ1 *
node[i].DZ3)) + (flux0 / (4 * DZ3))))
              + (node[i].C[0] *  ((node[i].theta[0]/Dt)
              - (th4 * solute_Dis1 / (2 * node[i].DZ2 * node[i].DZ3))
              - (th3 * solute_Dis0 / (2 * node[i].DZ1 * node[i].DZ3))
              - (flux1 / (4 * DZ4)) + (flux0 / (4 * DZ3))))
```

```
            + (node[i+1].C[0] * ((th4 * solute_Dis1 / (2 * node[i].DZ2 *
node[i].DZ3))
            - (flux1 / (4 * DZ4))));
 }
//
// Solve for solute Ci vector using Thomas method for Tri-diagonal matrix.
//
  node[0].S_A = node[num_nodes - 1].S_C = 0;
  Beta[0] = node[0].S_B;
  Gama[0] = (node[0].S_Known) / node[0].S_B;
  for (i=1; i < num_nodes; i++)
    { Beta[i] = node[i].S_B - (node[i].S_A * node[i-1].S_C / Beta[i-1]);
     Gama[i] = (node[i].S_Known - (node[i].S_A * Gama[i-1])) / Beta[i];
    }
  node[num_nodes - 1].C[1] = Gama[num_nodes - 1];
  for (i = num_nodes - 2; i >= 0; i--)
     node[i].C[1] = Gama[i] - (node[i].S_C * node[i+1].C[1] / Beta[i]);
  for (i=0; i < num_nodes; i++) if (node[i].C[1] < 0) node[i].C[1] = 0;
}
void K_and_D(i)
{
   HD1 = (node[i+1].Diff[0] + node[i+1].Diff[1] + node[i].Diff[0] + node[i].Diff[1]) /
4;
   HC1 = (node[i+1].HC[0] + node[i+1].HC[1] + node[i].HC[0] + node[i].HC[1]) / 4;
   HD2 = (node[i].Diff[0] + node[i].Diff[1] + node[i-1].Diff[0] + node[i-1].Diff[1]) /
4;
   HC2 = (node[i].HC[0] + node[i].HC[1] + node[i-1].HC[0] + node[i-1].HC[1]) / 4;
}

void initialize(void)
{ int i,j=0;
  for (i = 0; i < num_nodes+1; i++)
   { if (layer[j+1] == i) j++;
    node[i].n = n[j];
    node[i].alpha = alpha[j];
    node[i].K_sat = K_sat[j];
    node[i].theta_sat = theta_sat[j];
    node[i].theta_dry = theta_dry[j];
    node[i].theta[0] = initial_theta[j];
    node[i].lambda = lambda[j];
    node[i].C[0] = initial_C[j];
    if (node[i].theta[0] > node[i].theta_sat) node[i].theta[0] = node[i].theta_sat *
0.99999;
    if (node[i].theta[0] < node[i].theta_dry) node[i].theta[0] = node[i].theta_dry +
```

```
(node[i].theta_dry * 0.00001);
    node[i].theta[1] = node[i].theta[0];
   }
  for (i = 1; i < num_nodes; i++)
   {
    node[i].DZ1 = node[i].depth - node[i-1].depth;
    node[i].DZ2 = node[i+1].depth - node[i].depth;
    node[i].DZ3 = (node[i+1].depth - node[i-1].depth) / 2;
   }
 return;
}

void soil_hydraulics()
{
 int i;
 for (i=0;i < num_nodes+1; i++)
 {
  node[i].HC[0] = conduc(i,0);
  node[i].HC[1] = conduc(i,1);
  node[i].Diff[0] = diffu(i,0);
  node[i].Diff[1] = diffu(i,1);
  node[i].Deriv_HC = Deriv_conduc(i);
  node[i].Deriv_HD = Deriv_diffu(i);
 }
return;
}
//
// this function computes water potential as a function of water content
//
double potential(int i, int j)
{
  double Wp, Se, m;
      Se = (node[i].theta[j] - node[i].theta_dry) / (node[i].theta_sat - node[i].theta_dry);
      m = 1 - (1 / node[i].n);
      Wp = (pow((pow(Se,-1 / m) - 1), (1/node[i].n))) / node[i].alpha;
      return Wp;
}
//
// this function computes the derivative of water potential with respect
// to water content
//
double Deriv_potential(int i)
{
  double Deriv_wp_theta, Deriv_Wp, Deriv_Se, Se, m;
```

```
  Se = (node[i].theta[1] - node[i].theta_dry) / (node[i].theta_sat - node[i].theta_dry);
  Deriv_Se = 1 / (node[i].theta_sat - node[i].theta_dry);
  m = 1 - (1 / node[i].n);
  Deriv_Wp = (1 / node[i].alpha) * (1/node[i].n)
          * pow((pow(Se,-1 / m) - 1), ((1/node[i].n) - 1))
          * (-1/m) * pow(Se,((-1 / m) - 1));
  Deriv_wp_theta = Deriv_Wp * Deriv_Se;
  return Deriv_wp_theta;
}
//
// this function computes the diffusivity as a function of water content
//
double diffu(int i, int j)
{
  double Diffu, Se, m;
  m = 1-(1/node[i].n);
  Se = (node[i].theta[j] - node[i].theta_dry) / (node[i].theta_sat - node[i].theta_dry);
  Diffu = (((1-m) * node[i].K_sat) / (node[i].alpha * m * (node[i].theta_sat -
node[i].theta_dry)))
        * pow(Se, (0.5 - (1/m)))
        * (pow((1-pow(Se,(1/m))),-m) + pow((1-pow(Se,(1/m))),m) - 2);
  return Diffu;
}
//
// this function computes the derivative of the diffusivity with respect
// to water content
//
double Deriv_diffu(int i)
{
  double Deriv_Diffu_theta, Deriv_Se, Deriv_Diffu, Diffu, Se, m;
  m = 1-(1/node[i].n);
  Se = (node[i].theta[1] - node[i].theta_dry) / (node[i].theta_sat - node[i].theta_dry);
  Deriv_Se = 1 / (node[i].theta_sat - node[i].theta_dry);
  Deriv_Diffu = ((((1-m) * node[i].K_sat) / (node[i].alpha * m * (node[i].theta_sat -
node[i].theta_dry)))
            * (pow((1-pow(Se,(1/m))),-m) + pow((1-pow(Se,(1/m))),m) - 2)
            * ((0.5 - (1/m)) * pow(Se, -((1/m) + 0.5))))
            + ((((1-m) * node[i].K_sat) / (node[i].alpha * m * (node[i].theta_sat -
node[i].theta_dry)))
            * (pow(Se,-0.5)) * (pow((1-pow(Se,(1/m))),-m-1) -
pow((1-pow(Se,(1/m))),m-1)));
  if (i == 0) Deriv_Diffu_theta = (Deriv_Diffu * Deriv_Se)/2;
  else Deriv_Diffu_theta = (Deriv_Diffu * Deriv_Se)/4;
  return Deriv_Diffu_theta;
```

```
}
//
// this function computes the hydraulic conductivity as a function of
// water content
//
double conduc(int i,int j)
{
  double Cond, Se, m;
  m = 1-(1/node[i].n);
  Se = (node[i].theta[j] - node[i].theta_dry) / (node[i].theta_sat - node[i].theta_dry);
  Cond = node[i].K_sat * sqrt(Se) * pow(1-pow(1-pow(Se,(1/m)),m),2);
  return Cond;
}
//
// this function computes the derivative of the hydraulic conductivity
// with respect to water content
//
double Deriv_conduc(int i)
{
  double Deriv_Cond_theta, Deriv_Cond, Deriv_Se, Se, m;
  m = 1-(1/node[i].n);
  Se = (node[i].theta[1] - node[i].theta_dry) / (node[i].theta_sat - node[i].theta_dry);
  Deriv_Se = 1 / (node[i].theta_sat - node[i].theta_dry);
  Deriv_Cond = node[i].K_sat * ((0.5 * pow(Se, -0.5) *
pow(1-pow(1-pow(Se,(1/m)),m),2))
          + (2 * sqrt(Se) * pow(1-pow(Se,(1/m)),m-1) * pow(Se,(1-m)/m) * (1-
pow(1-pow(Se,(1/m)),m))));
  Deriv_Cond_theta = Deriv_Cond * Deriv_Se;
  return Deriv_Cond_theta;
}
//
// this function computes water content as a function of water potential
//
double THETA(double Wp,int i)
{ double that, m;
  m = 1-(1/node[i].n);
  that = ((node[i].theta_sat - node[i].theta_dry)
       * pow((1 / (1 + pow(node[i].alpha * Wp,node[i].n))), m)) + node[i].theta_dry;
  return that;
}
//
// this function computes the derivative of water content with respect
// to water potential
//
```

```
double Deriv_THETA(double Wp,int i)
{ double Deriv_that, m;
  m = 1-(1/node[i].n);
  Deriv_that = m * (node[i].theta_sat - node[i].theta_dry)
       * pow(1/(1+ pow( node[i].alpha * Wp, node[i].n)) ,m-1)
       *((-node[i].alpha * node[i].n * pow(node[i].alpha * Wp, node[i].n-1))
       / pow(1+pow(node[i].alpha * Wp, node[i].n),2));
  return Deriv_that;
}
//
// this function computes the derivative of delta theta with respect
// to water content for the jump at the interface for the "upper" node
//
double Deriv_Dtheta1(double Wp,int i)
{ double Deriv_pot_int, D_theta, D_wp, DZ, p, p2, k, k2, dp, dk;
 DZ = (node[i+1].depth - node[i].depth)/2;
  p = potential(i,1);
  p2= potential(i+1,1);
  k = conduc(i,1);
  k2= conduc(i+1,1);
 dp = Deriv_potential(i);
 dk = node[i].Deriv_HC/4;
 D_wp = Deriv_THETA(Wp,i);
 Deriv_pot_int = (((1/2) * ((2 * ((dk * p) + (k * dp))) + (DZ * dk))) * pow(k+k2,-1))
            - ((1/2) * pow(k+k2,-2) * dk * ((2*((k*p) + (k2*p2))) + (DZ * (k-k2))));
 D_theta = (-1/2)* D_wp * Deriv_pot_int;
 return D_theta;
}
//
// this function computes the derivative of delta theta with respect
// to water content for the jump at the interface for the "lower" node
//
double Deriv_Dtheta2(double Wp, int i)
{ double Deriv_pot_int, D_theta, D_wp, DZ, p1, p2, k1, k2, dp, dk;
 DZ = (node[i].depth - node[i-1].depth)/2;
  p1 = potential(i-1,1);
  p2= potential(i,1);
  k1 = conduc(i-1,1);
  k2= conduc(i,1);
 dp = Deriv_potential(i);
 dk = node[i].Deriv_HC/4;
 D_wp = Deriv_THETA(Wp,i);
 Deriv_pot_int = (((1/2) * ((2 * ((dk * p2) + (k2 * dp))) - (DZ * dk))) *
pow(k1+k2,-1))
```

```
            - ((1/2) * pow(k1+k2,-2) * dk * ((2*((k1*p1) + (k2*p2))) + (DZ *
(k1-k2))));
 D_theta = (1/2)* D_wp * Deriv_pot_int;
 return D_theta;
}
void water_balance()
{ int i;
  double current_water_vol = 0.0, dz;
  L = 0;
  for (i=0; i < num_nodes-1; i++)
    { dz = node[i+1].depth - node[i].depth;
      if (i+1 == layer[L+1]) jump(i,L);
         { current_water_vol += node[i].theta[2] * dz/2;
           current_water_vol += node[i+1].theta[2] * dz/2;
           L++;
          }
      current_water_vol += node[i].theta[2] * dz;
    }
  sum_flux += W_q * Dt;
  balance = current_water_vol - sum_flux - initial_water_vol;
  balance_ratio = fabs(balance) / current_water_vol;
  return;
}
void solute_balance()
{ int i;
  double current_C = 0.0, dz;
  for (i=0; i < num_nodes-1; i++)
    { dz = node[i+1].depth - node[i].depth;
      current_C += node[i].theta[2] * node[i].C[1] * dz;
    }
  sum_C += S_j * Dt;
  balance_C = current_C - sum_C - initial_solute;
  balance_ratio_C = fabs(balance_C) / current_C;
  return;
}
void Read_input()
{
 int i;
 fscanf(input,"%d %d", &num_nodes, &num_layers);
 for(i=0; i < num_layers; i++)
 {
   fscanf(input,"%lf %lf %lf %lf %lf %lf %lf %lf %d", &K_sat[i], &theta_sat[i],
&theta_dry[i],
        &alpha[i], &n[i], &initial_theta[i], &lambda[i], &initial_C[i], &layer[i]);
```

```
 }
 fscanf(input,"%lf ", &S_Diffusion);
 for(i=0; i < num_nodes; i++)  fscanf(input,"%lf ", &node[i].depth);
 fscanf(input,"%lf %lf %lf ", &start_B2, &Wbound1, &Wbound2);
 fscanf(input,"%lf %lf ",  &Sbound1, &Sbound2);
 fscanf(input,"%lf %lf %d", &time_end, &Dt, &max_itir);
 fscanf(input,"%lf %lf %lf %lf %lf %lf %lf %lf ", &Printout[0], &Printout[1],
    &Printout[2], &Printout[3], &Printout[4], &Printout[5], &Printout[6],
&Printout[7]);
}
void Write_output_1()
{
 int i;
 for (i=0; i < num_nodes; i++) fprintf(output,"%10.5f %10.4f %10.4E\n",
         node[i].depth, node[i].theta[0], node[i].C[0] * node[i].theta[0]);
}
void Write_output_2()
{
 int i;
 fprintf(output,"\n");
 for (i=0; i < num_nodes; i++) fprintf(output,"%10.4f %10.4E\n",
          node[i].theta[0], node[i].C[0] * node[i].theta[0]);
}
```

APPENDIX C

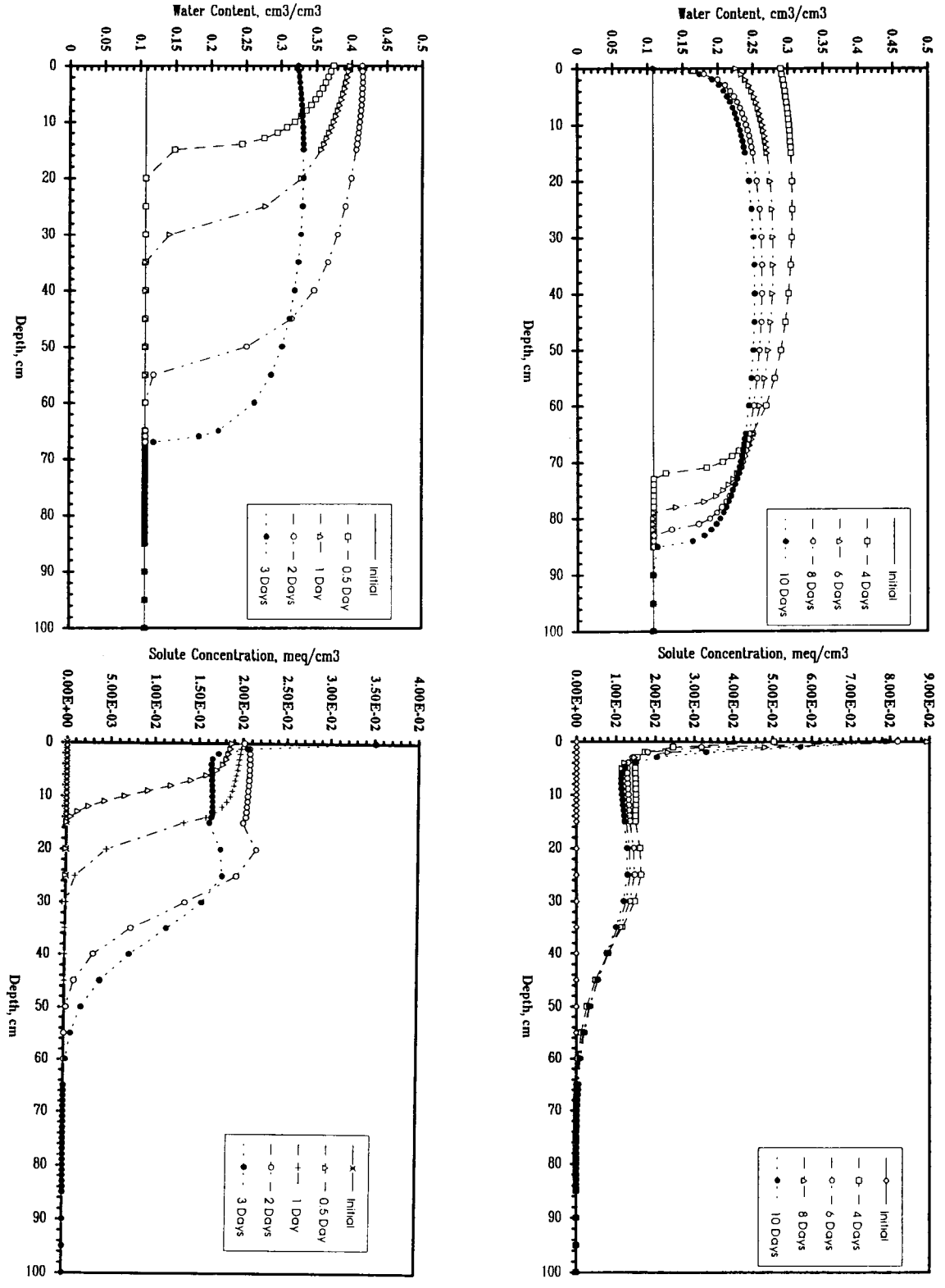

Figure C-1: Water and solute distribution in unmodified soil.
(evaporation rate = 0.5 cm/day).

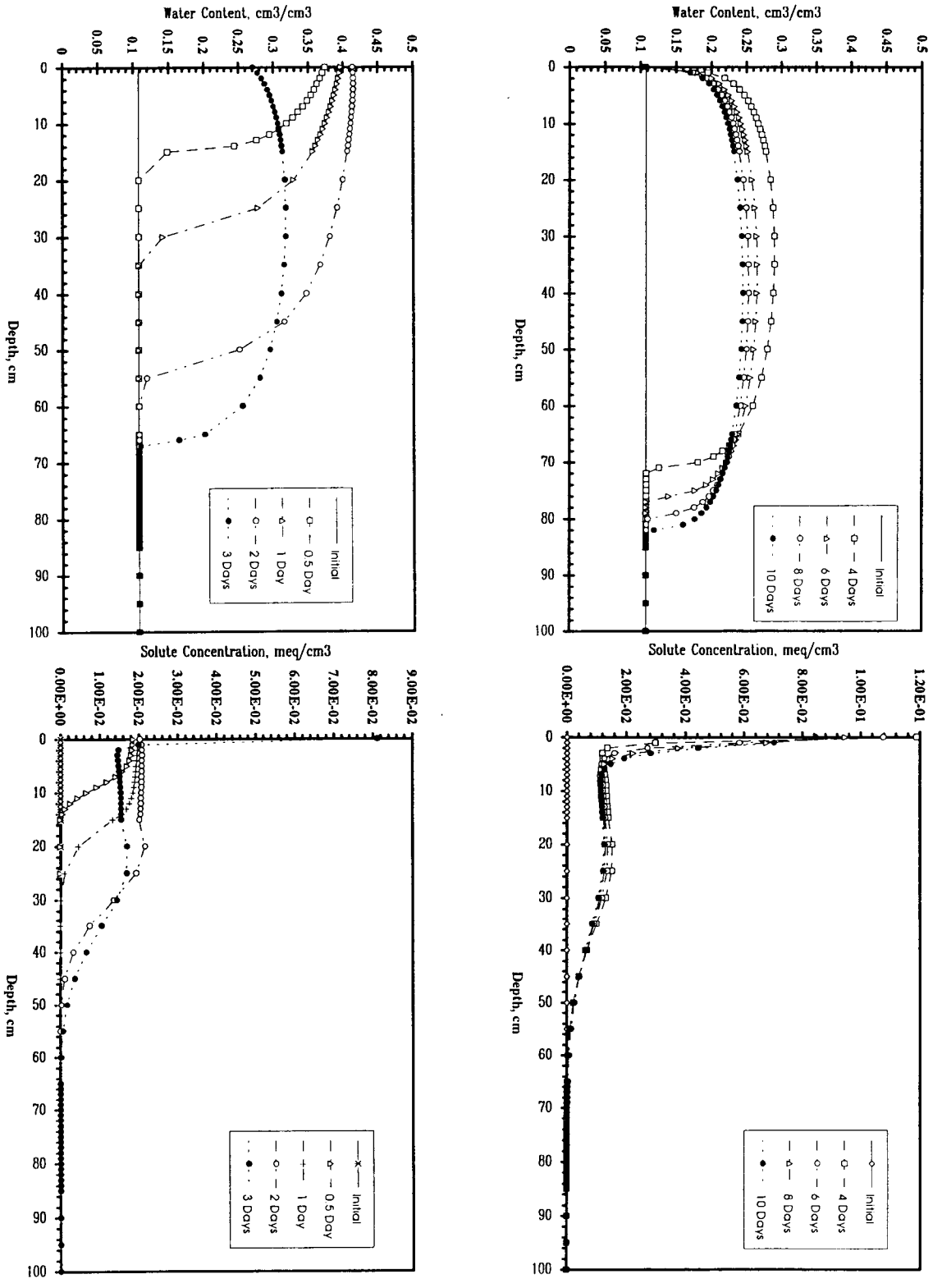

Figure C-2: Water and solute distribution in unmodified soil.
(evaporation rate = 1.5 cm/day).

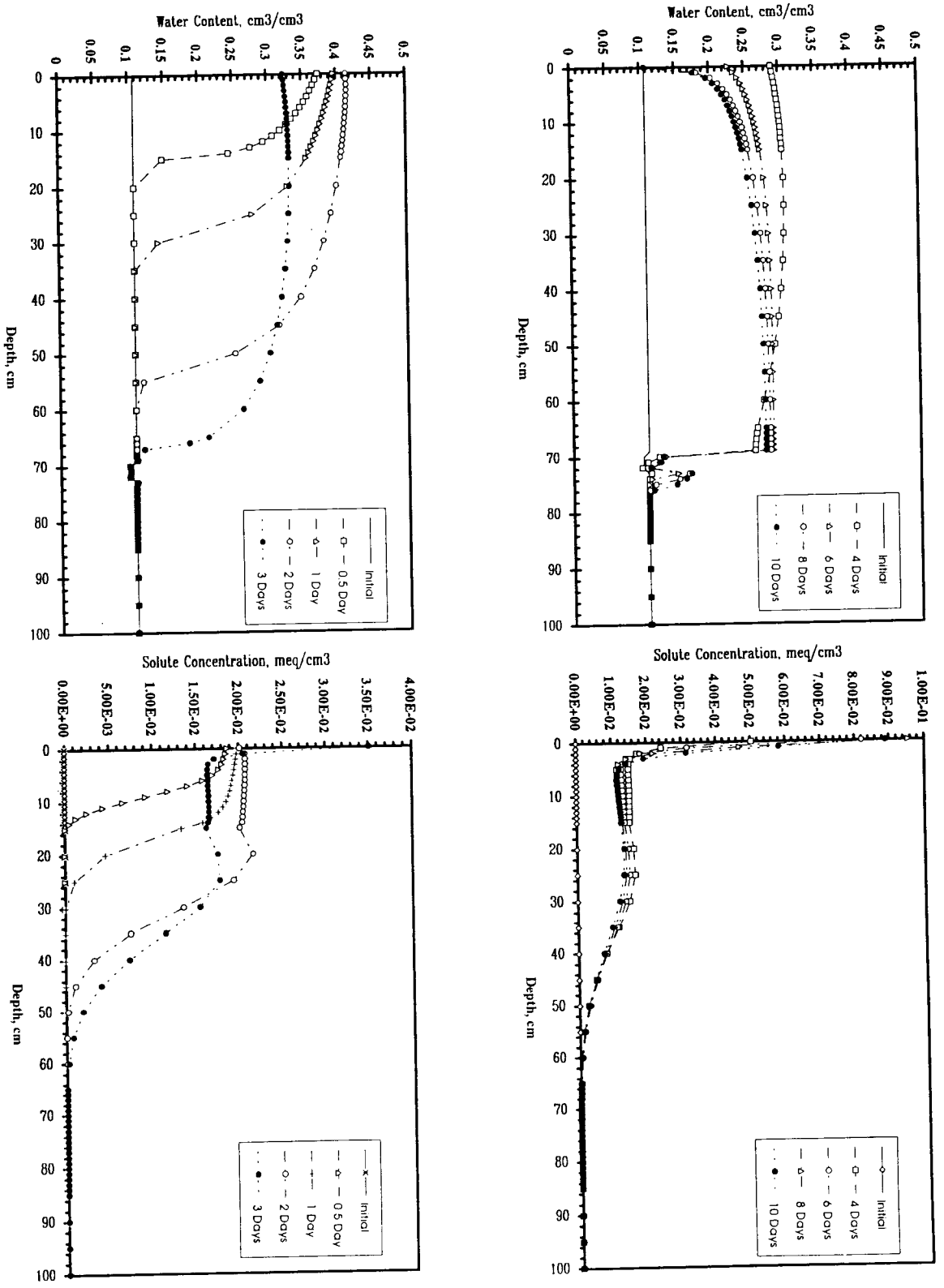

Figure C-3: Water and solute distribution.
(Treatment: 2.5 cm sand barrier layer - evaporation rate = 0.5 cm/day).

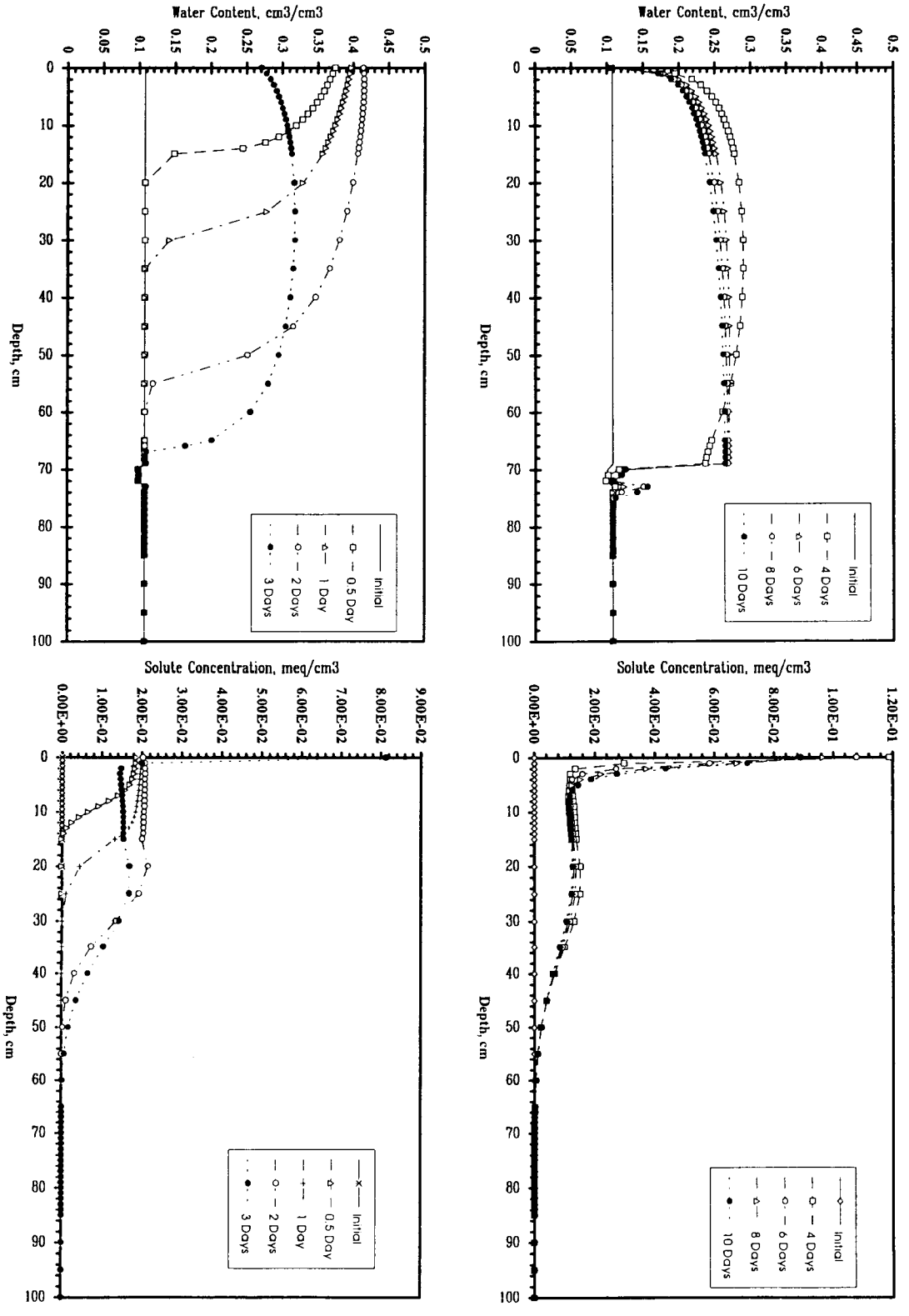

Figure C-4: Water and solute distribution.
(Treatment: 2.5 cm sand barrier layer - evaporation rate = 1.5 cm/day).

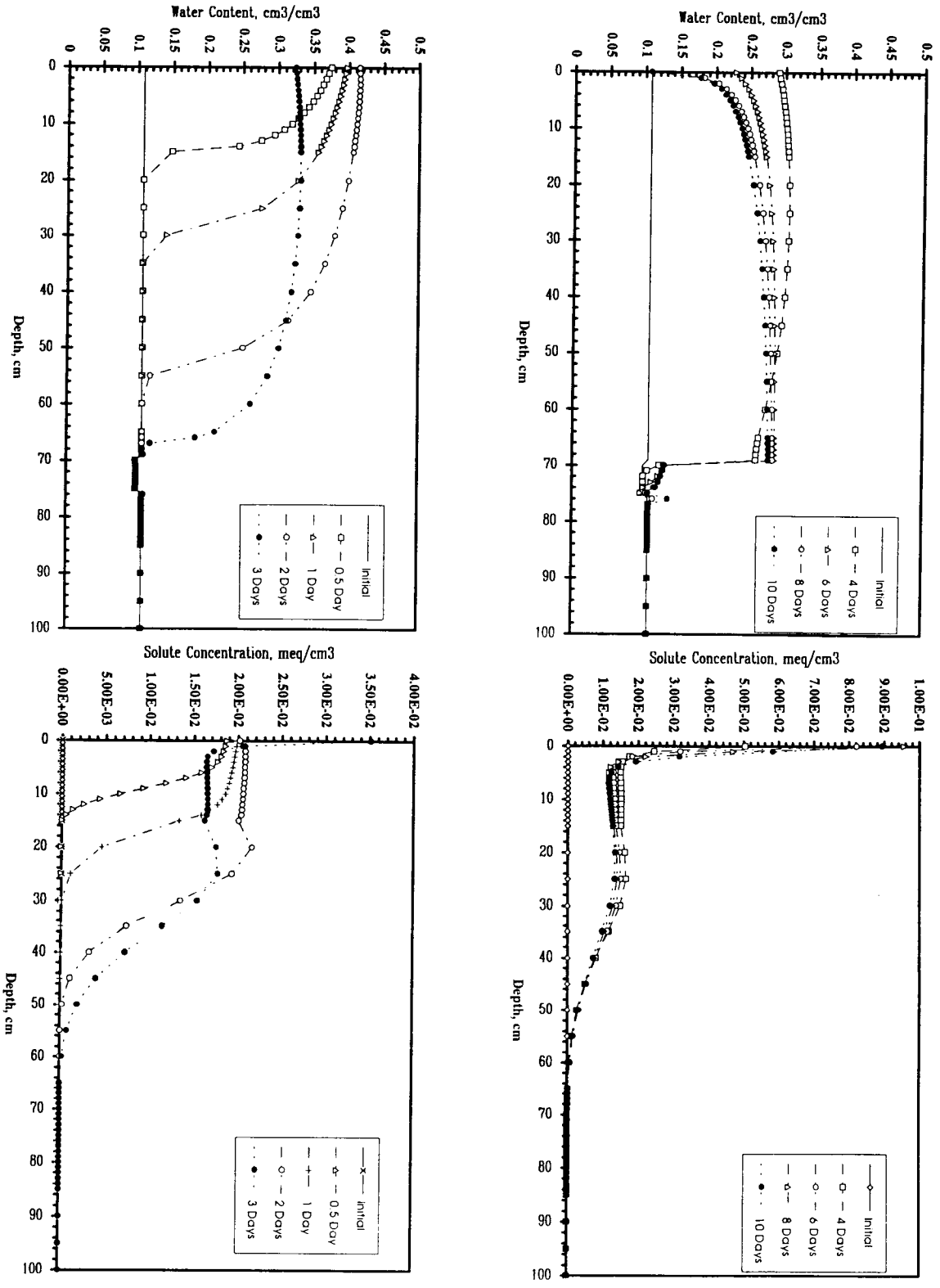

Figure C-5: Water and solute distribution.
(Treatment: 5.5 cm sand barrier layer - evaporation rate = 0.5 cm/day).

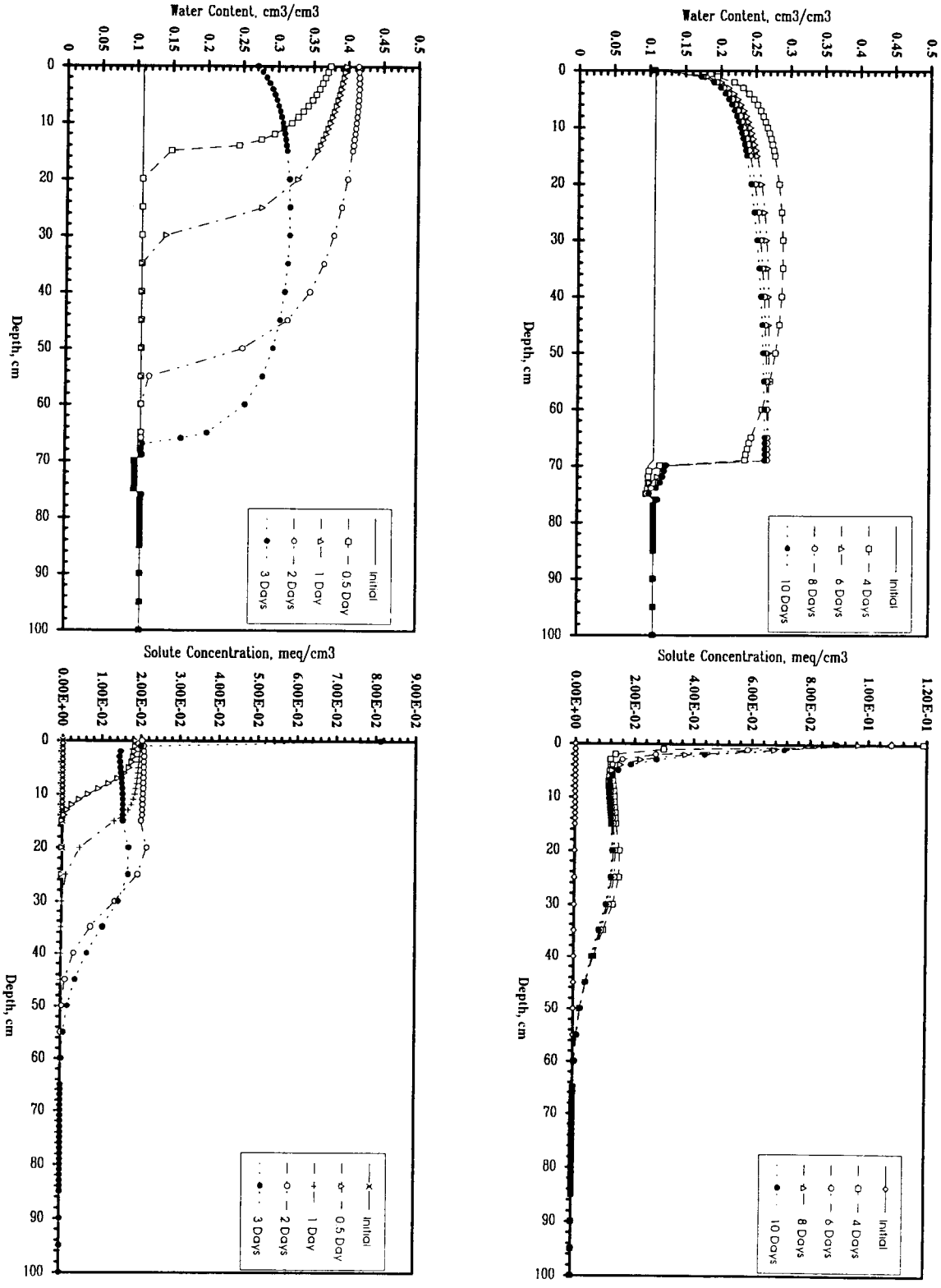

Figure C-6: Water and solute distribution.
(Treatment: 5.5 cm sand barrier layer - evaporation rate = 1.5 cm/day).

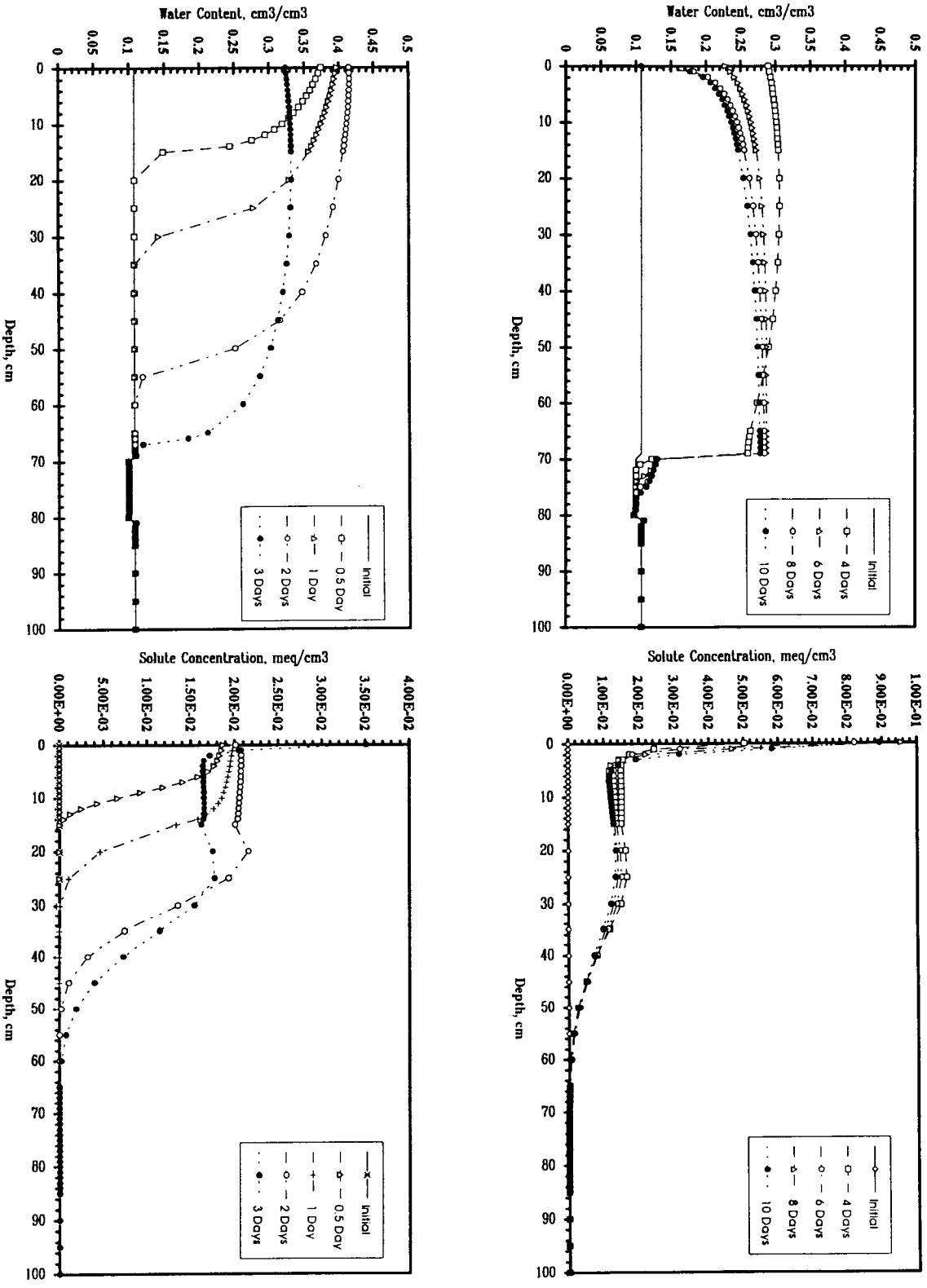

Figure C-7: Water and solute distribution.
(Treatment: 10.5 cm sand barrier layer - evaporation rate = 0.5 cm/day).

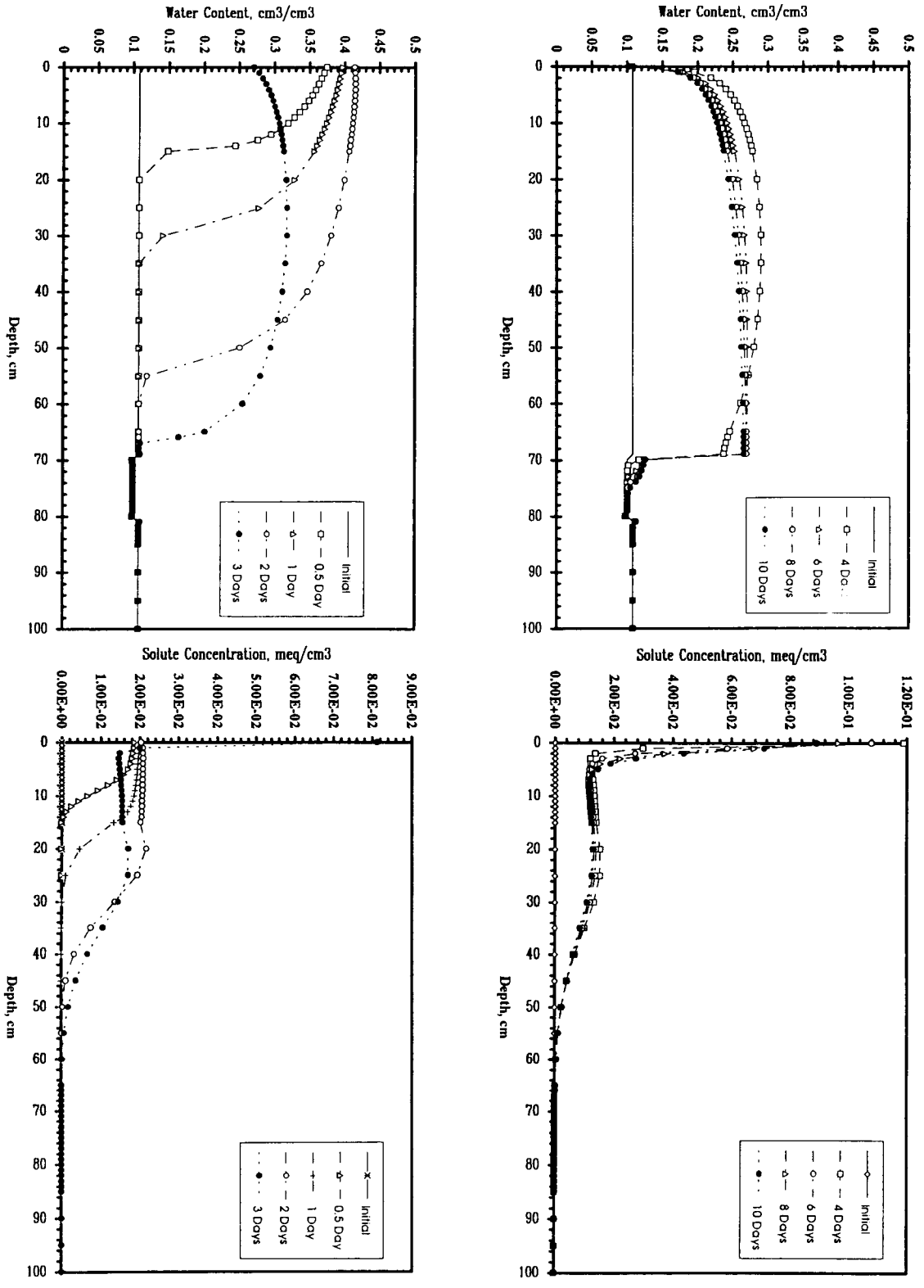

Figure C-8: Water and solute distribution.
(Treatment: 10.5 cm sand barrier layer - evaporation rate = 1.5 cm/day).

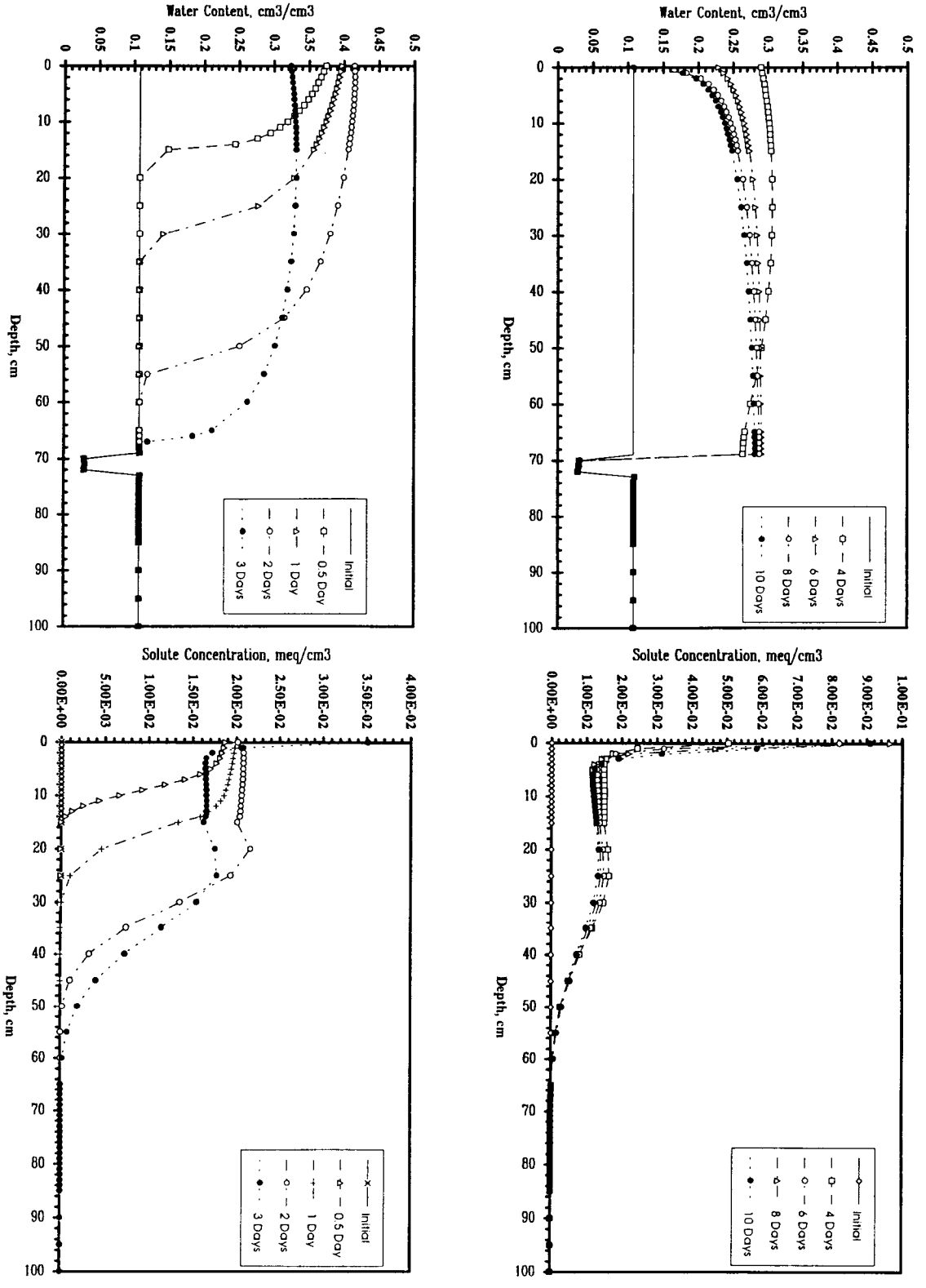

Figure C-9: Water and solute distribution.
(Treatment: 2.5 cm coarse sand barrier layer - evaporation rate = 0.5 cm/day).

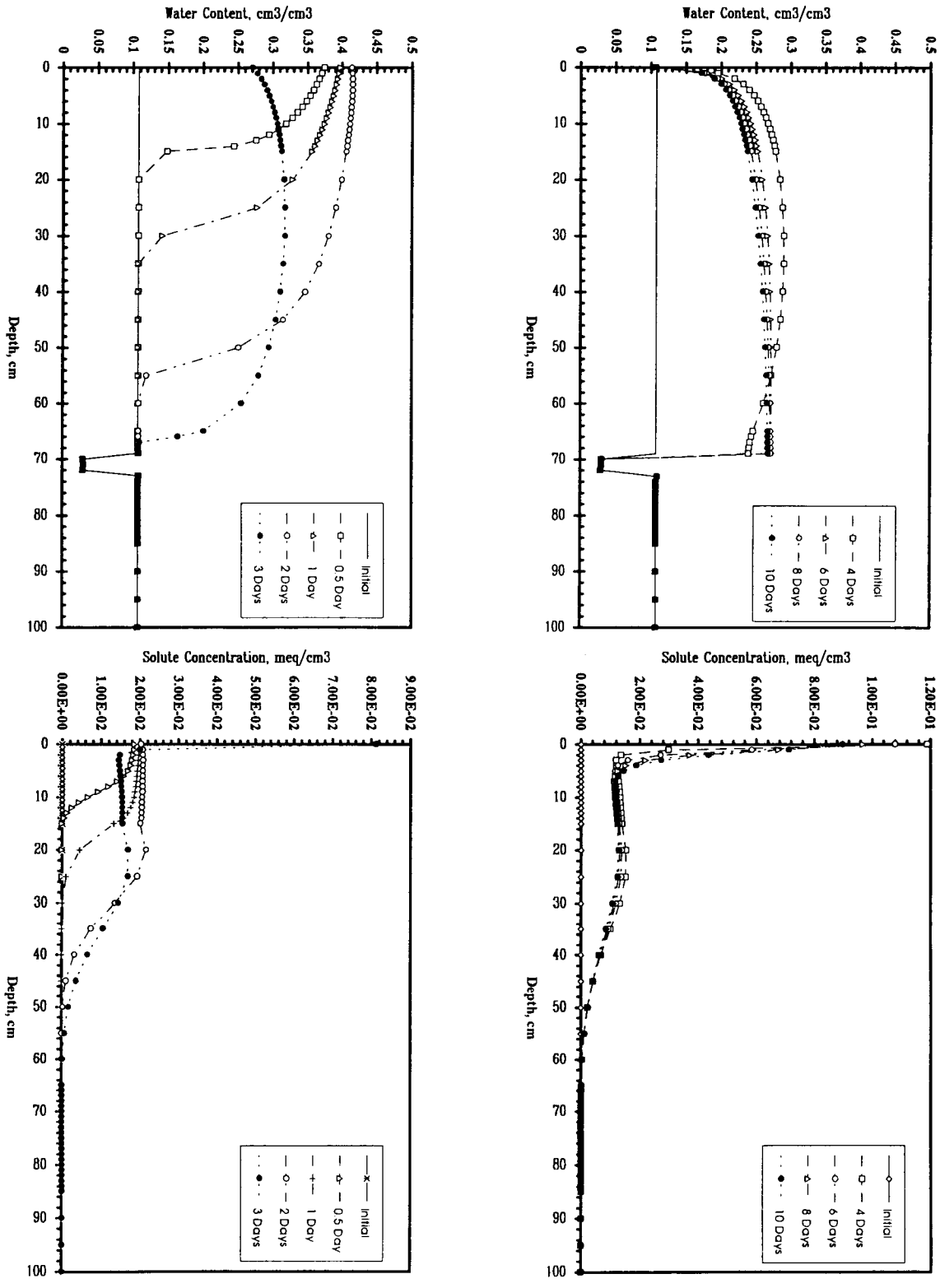

Figure C-10: Water and solute distribution.
(Treatment: 2.5 cm coarse sand barrier layer - evaporation rate = 1.5 cm/day).

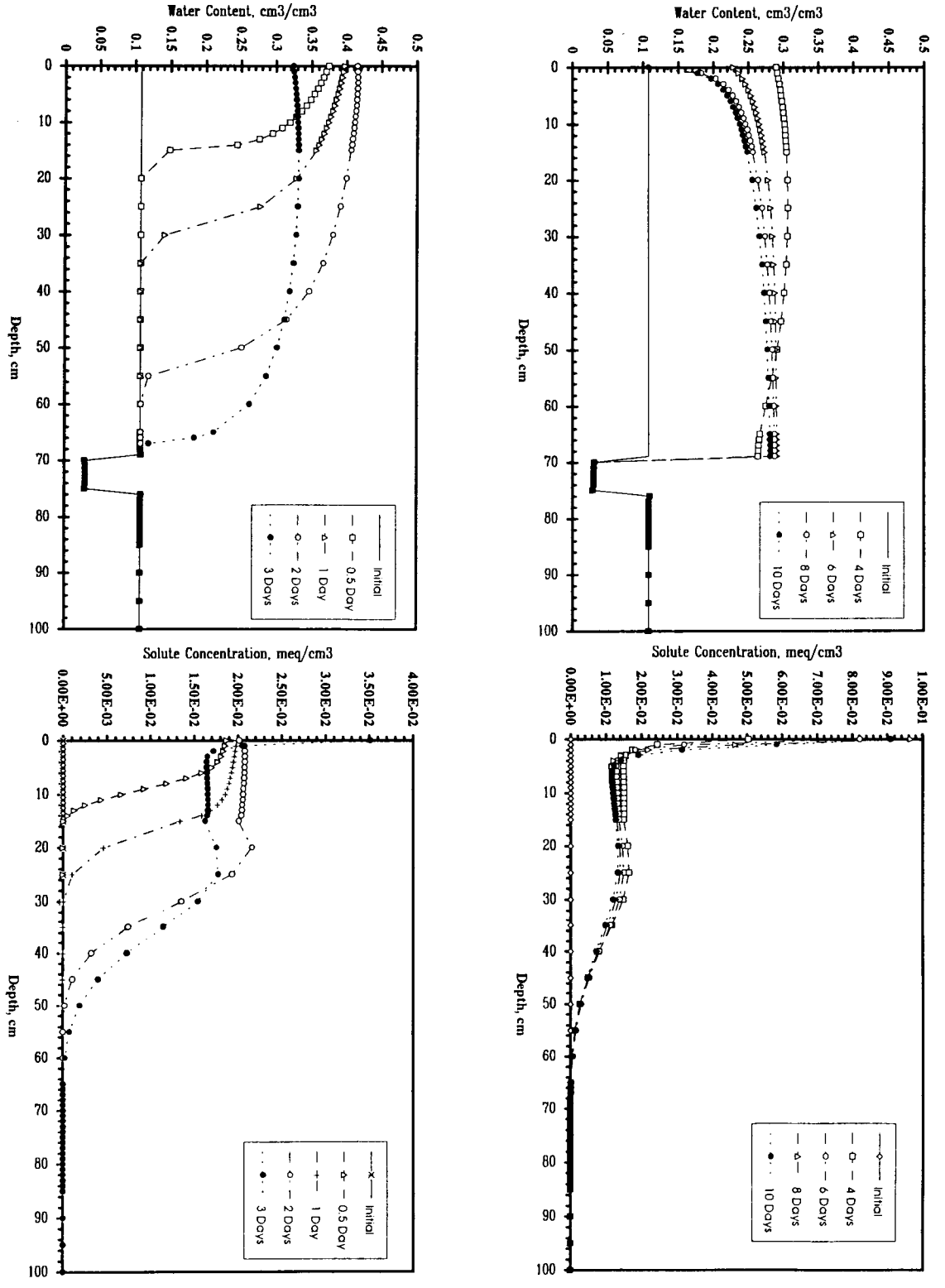

Figure C-11: Water and solute distribution.
(Treatment: 5.5 cm coarse sand barrier layer - evaporation rate = 0.5 cm/day).

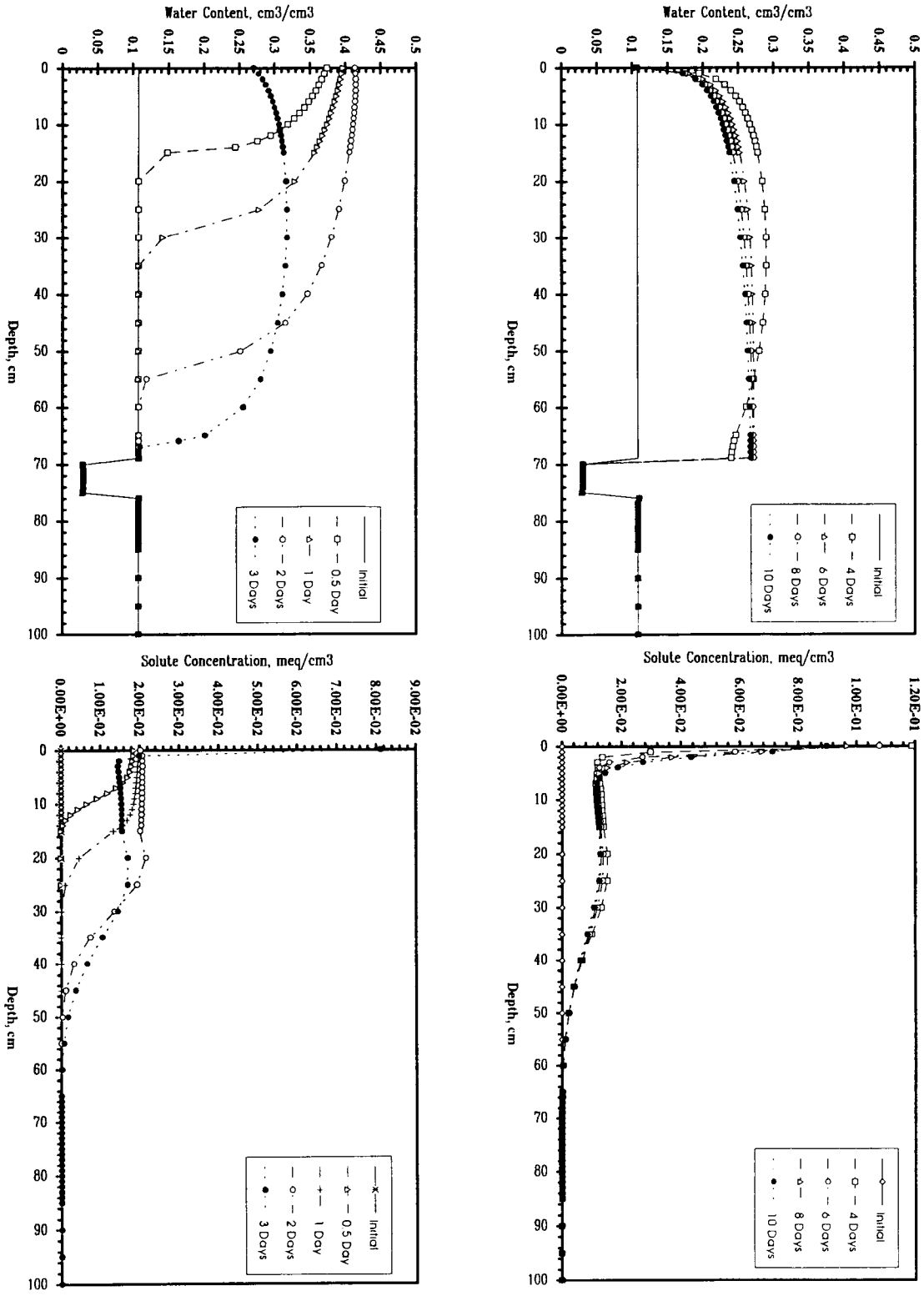

Figure C-12: Water and solute distribution.
(Treatment: 5.5 cm coarse sand barrier layer - evaporation rate = 1.5 cm/day).

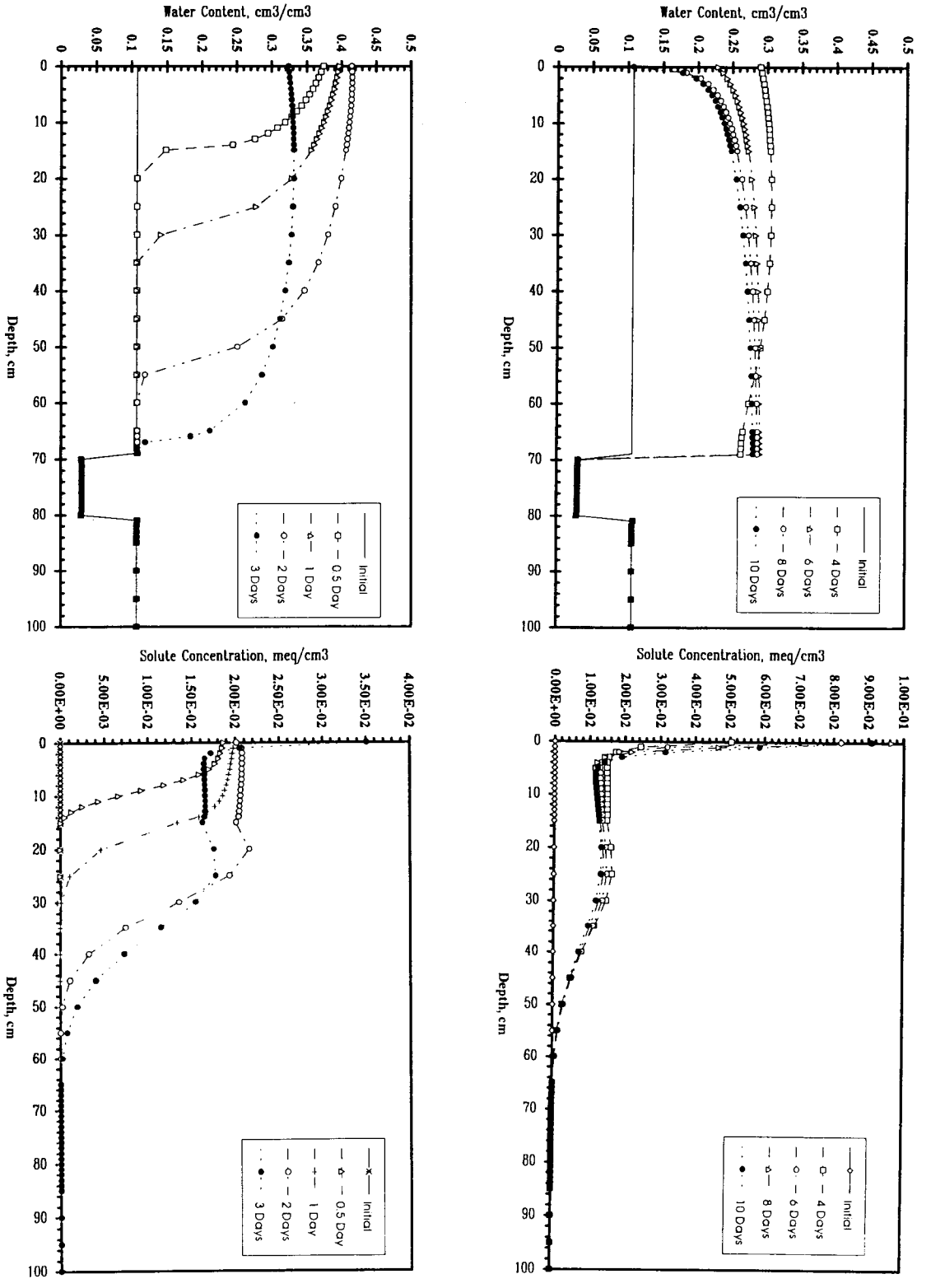

Figure C-13: Water and solute distribution.
(Treatment: 10.5 cm coarse sand barrier layer - evaporation rate = 0.5 cm/day).

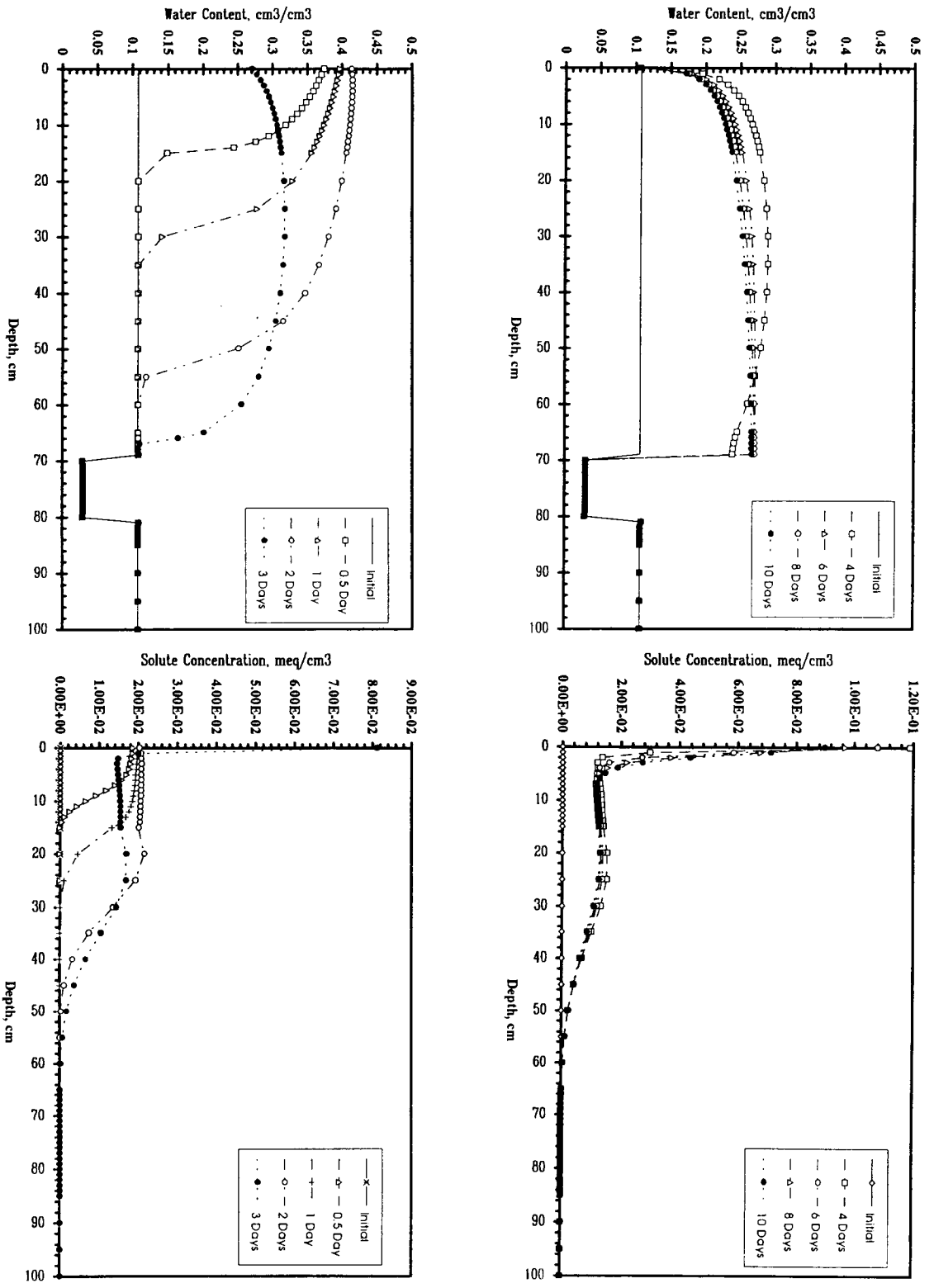

Figure C-14: Water and solute distribution.
(Treatment: 10.5 cm coarse sand barrier layer - evaporation rate = 1.5 cm/day).

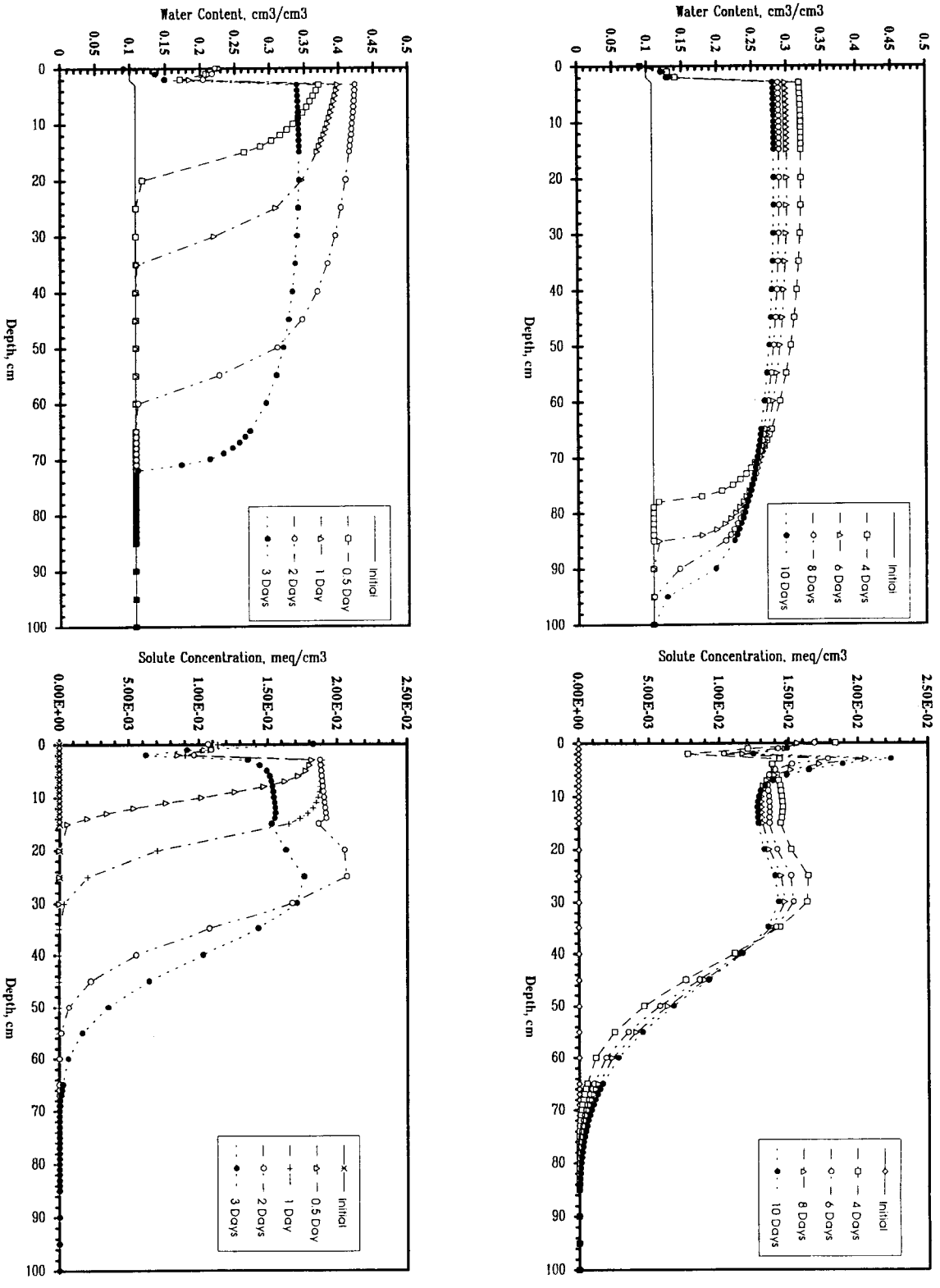

Figure C-15: Water and solute distribution.
(Treatment: 2.5 cm sand mulch layer - evaporation rate = 0.5 cm/day).

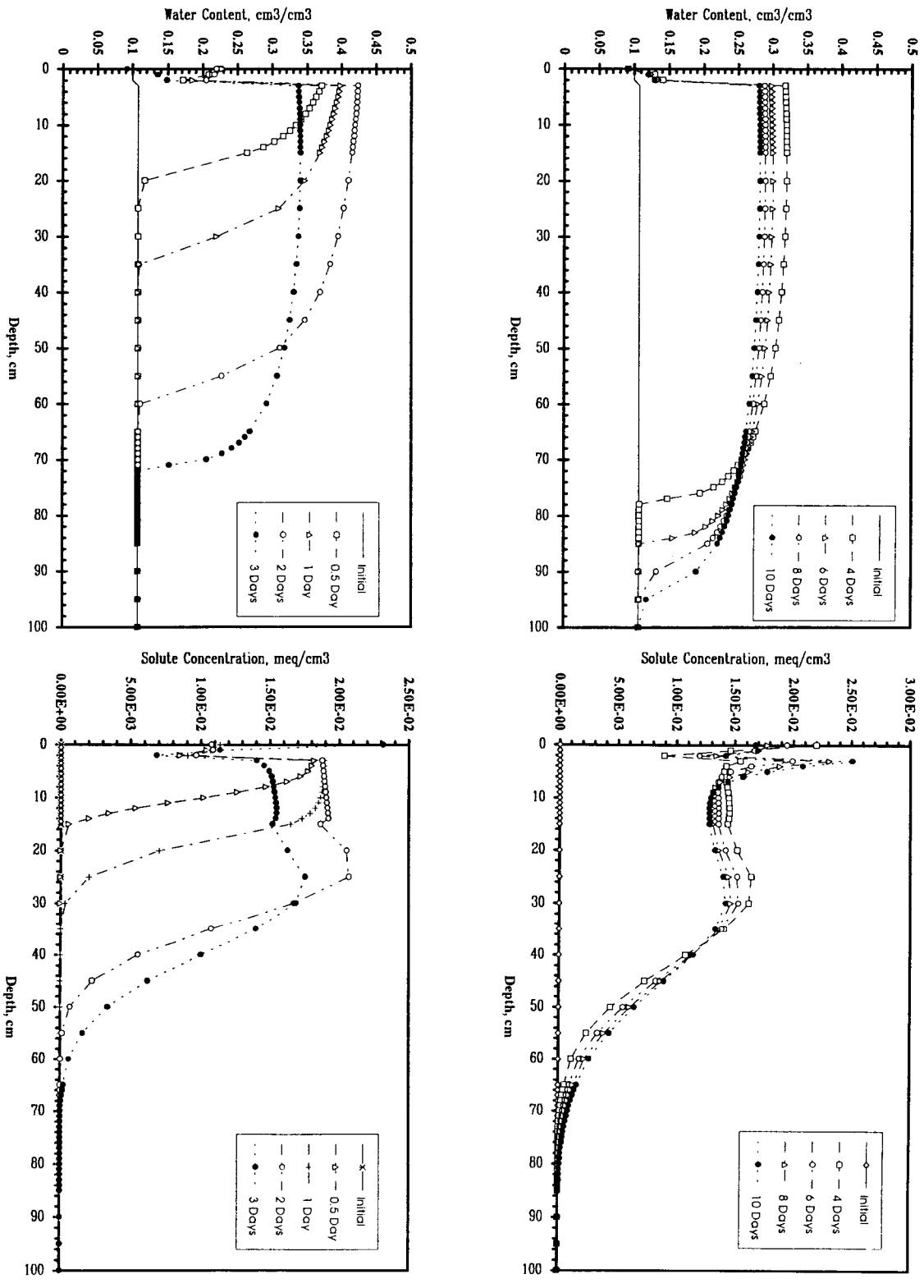

Figure C-16: Water and solute distribution.
(Treatment: 2.5 cm sand mulch layer - evaporation rate = 1.5 cm/day).

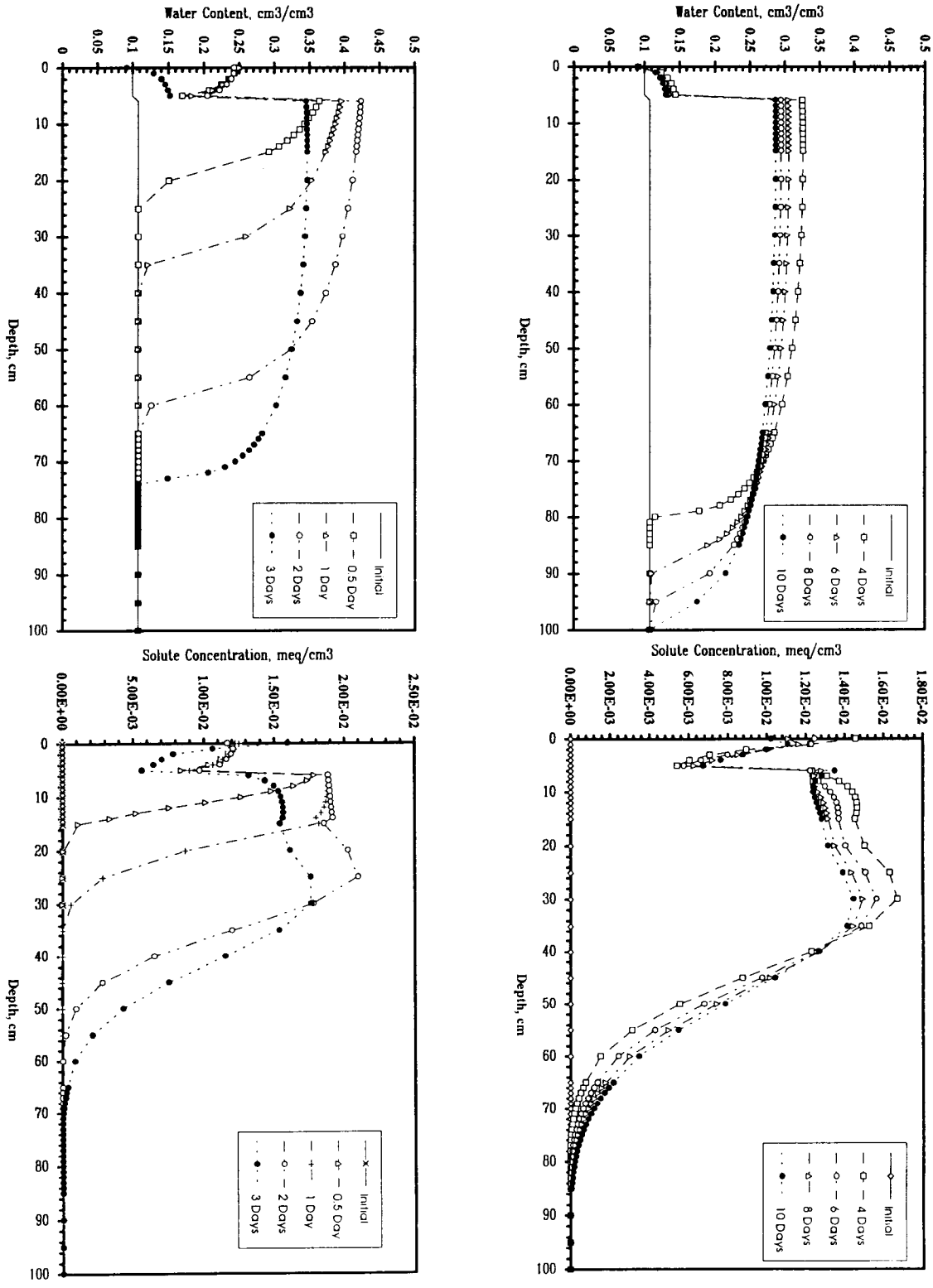

Figure C-17: Water and solute distribution.
(Treatment: 5.5 cm sand mulch layer - evaporation rate = 0.5 cm/day).

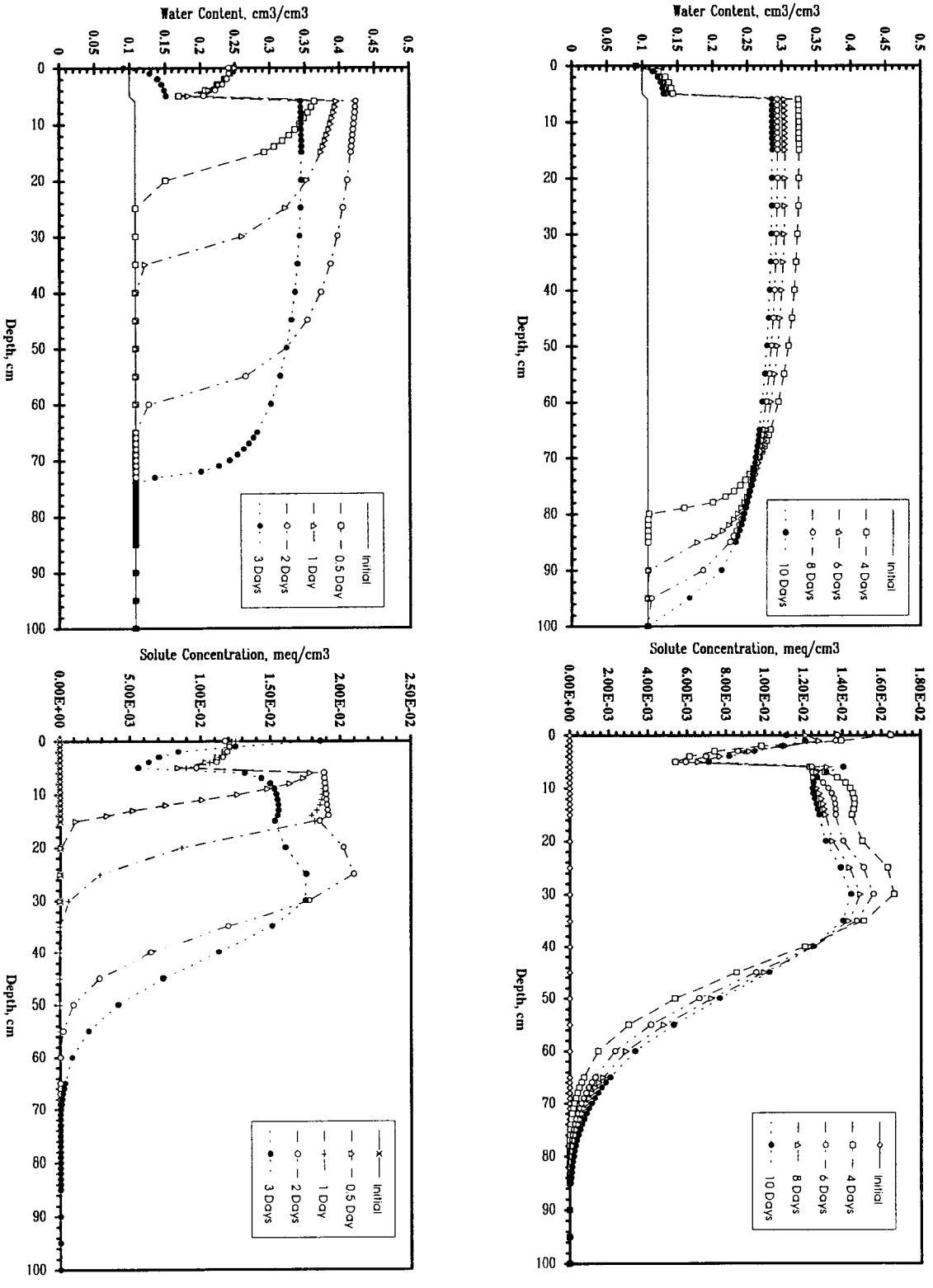

Figure C-18: Water and solute distribution.
(Treatment: 5.5 cm sand mulch layer - evaporation rate = 1.5 cm/day).

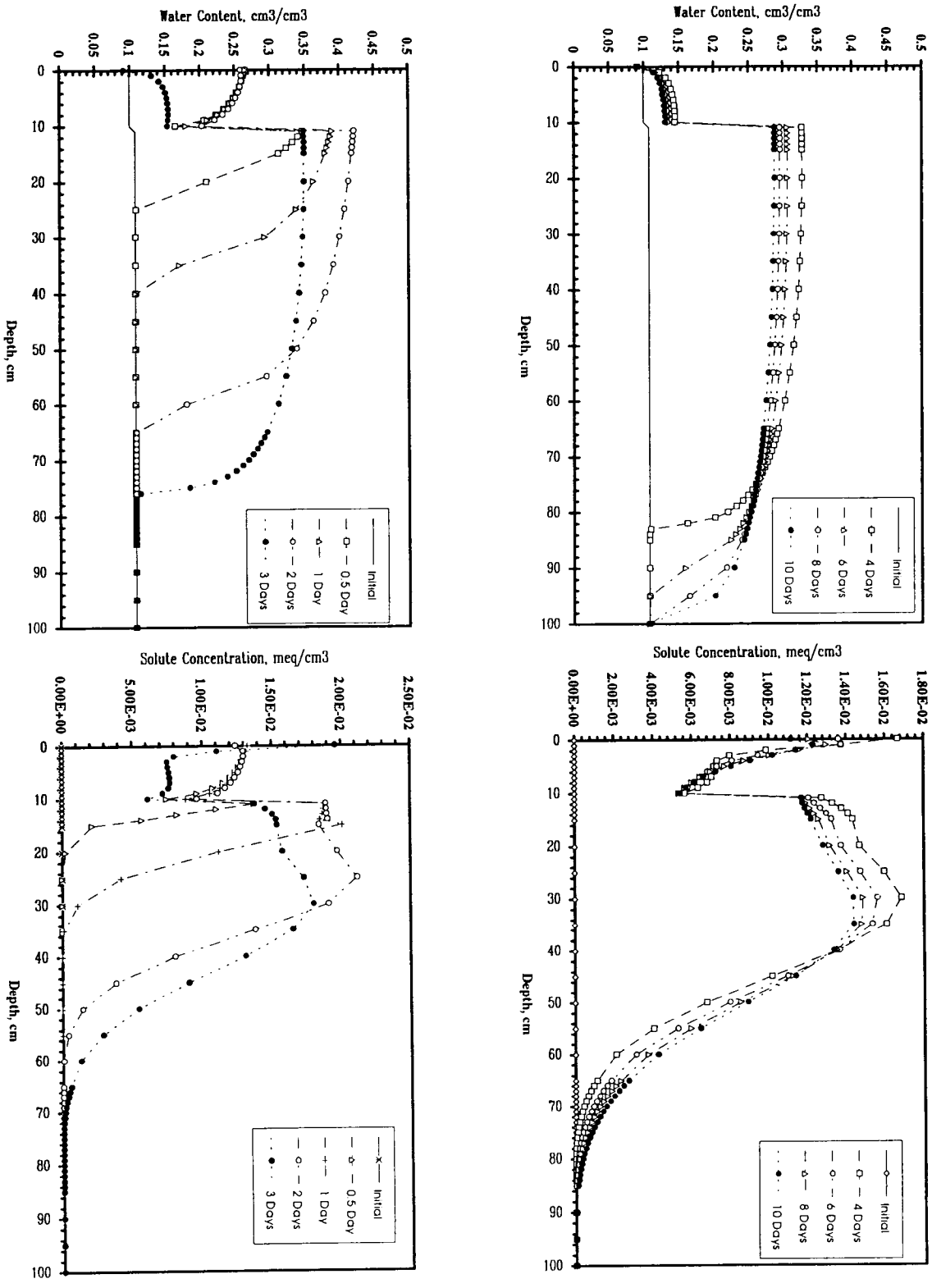

Figure C-19: Water and solute distribution.
(Treatment: 10.5 cm sand mulch layer - evaporation rate = 0.5 cm/day).

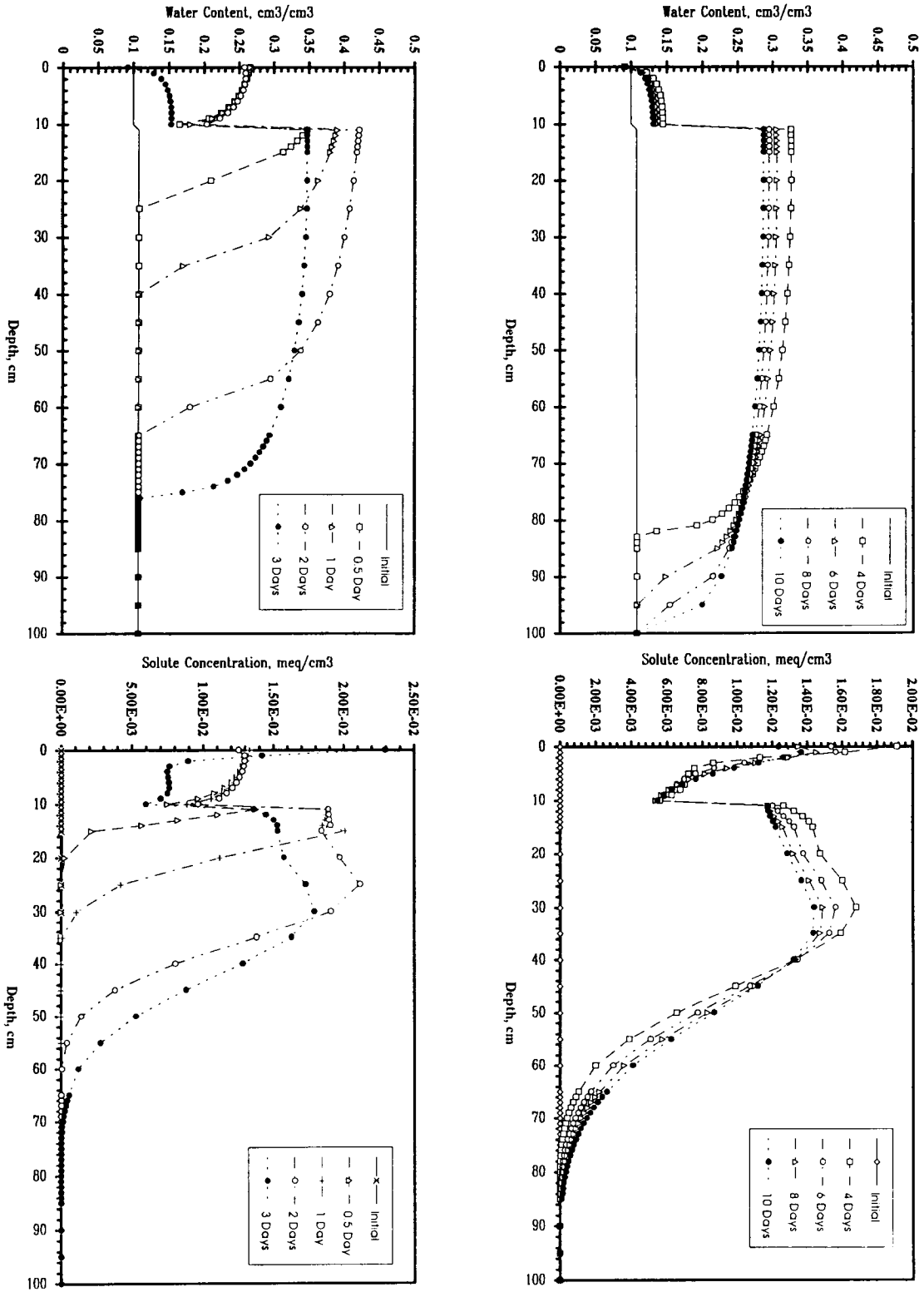

Figure C-20: Water and solute distribution.
(Treatment: 10.5 cm sand mulch layer - evaporation rate = 1.5 cm/day).

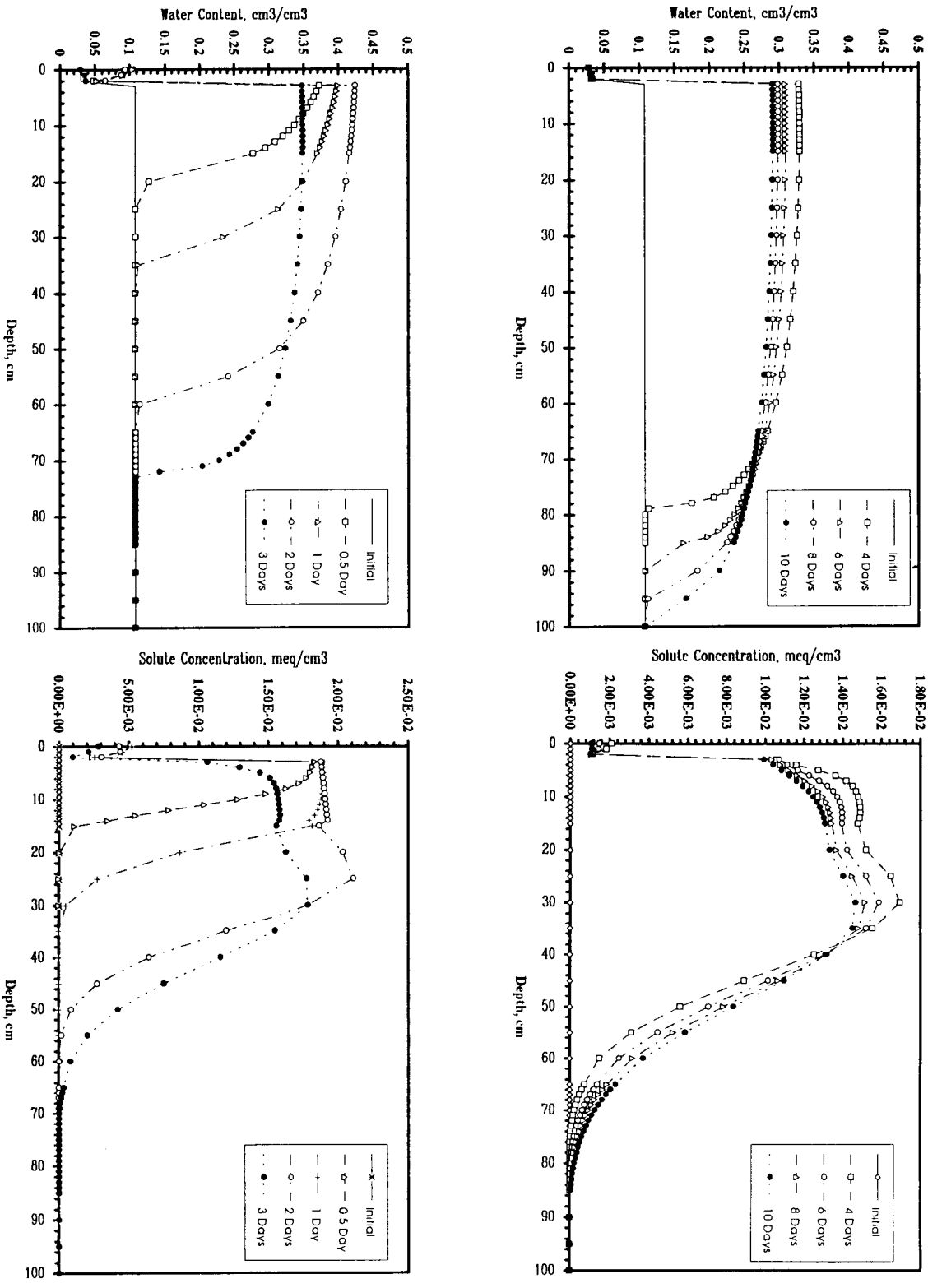

Figure C-21: Water and solute distribution.
(Treatment: 2.5 cm coarse sand mulch layer - evaporation rate = 0.5 cm/day).

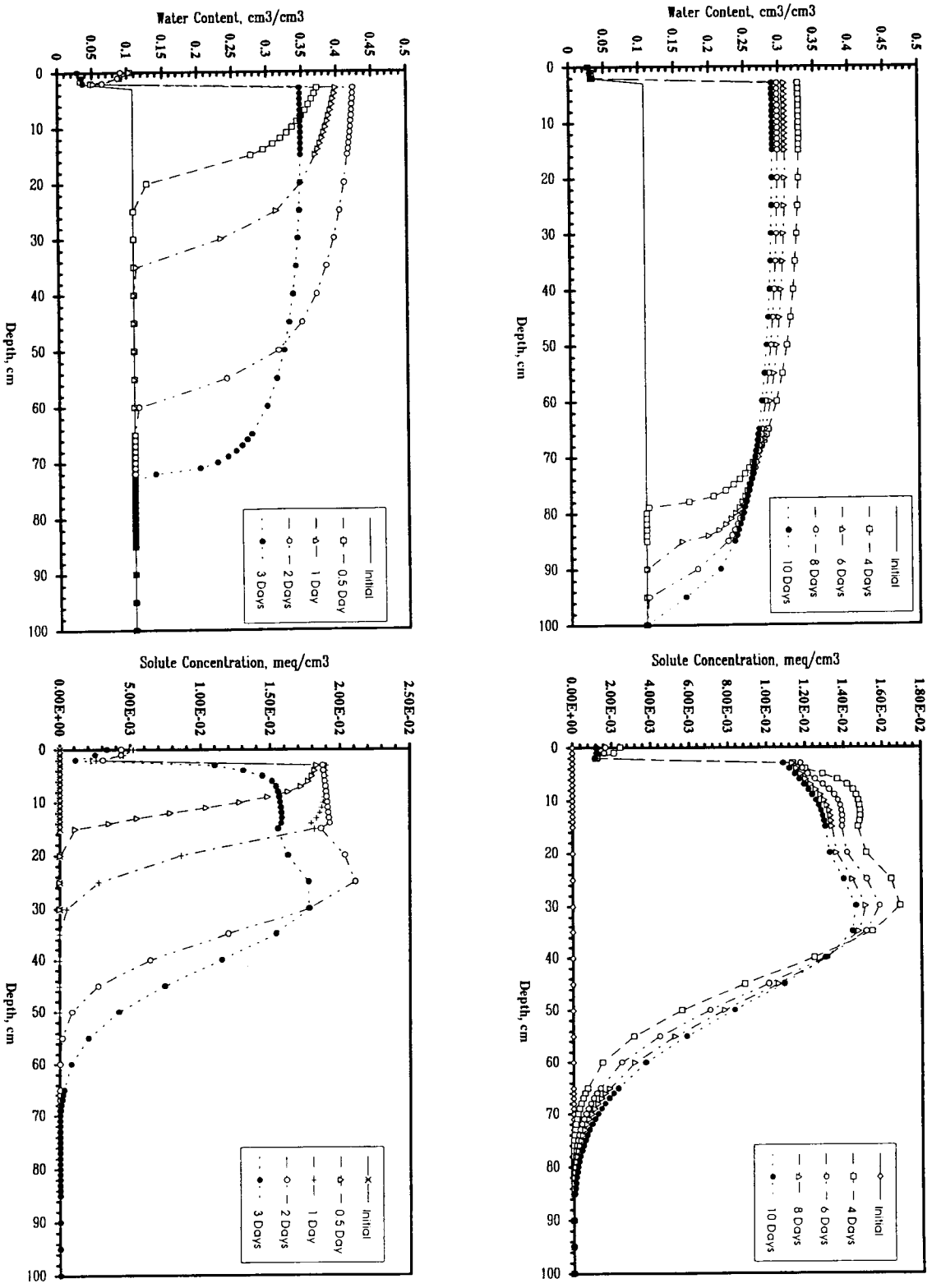

Figure C-22: Water and solute distribution.
(Treatment: 2.5 cm coarse sand mulch layer - evaporation rate = 1.5 cm/day).

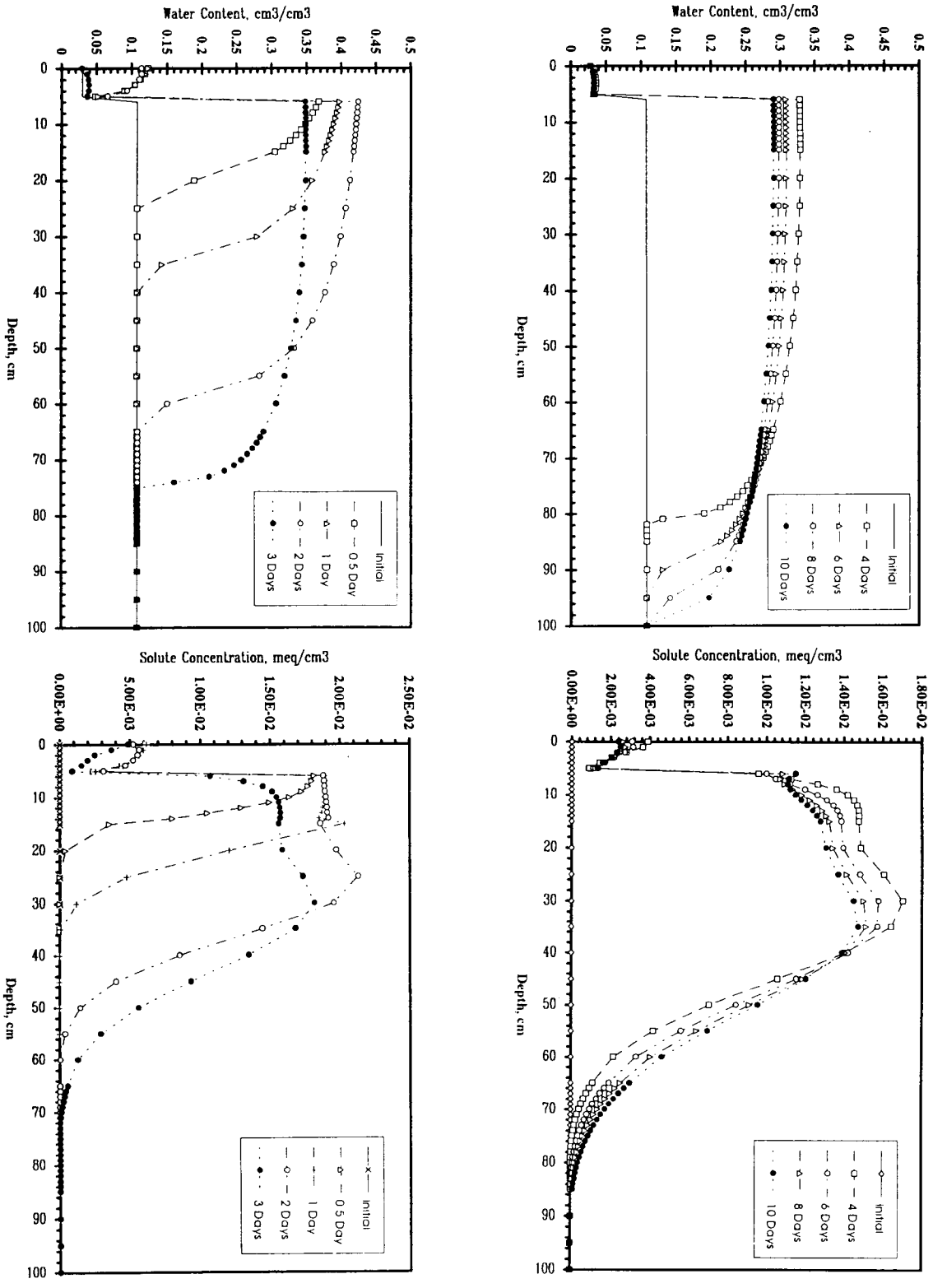

Figure C-23: Water and solute distribution.
(Treatment: 5.5 cm coarse sand mulch layer - evaporation rate = 0.5 cm/day).

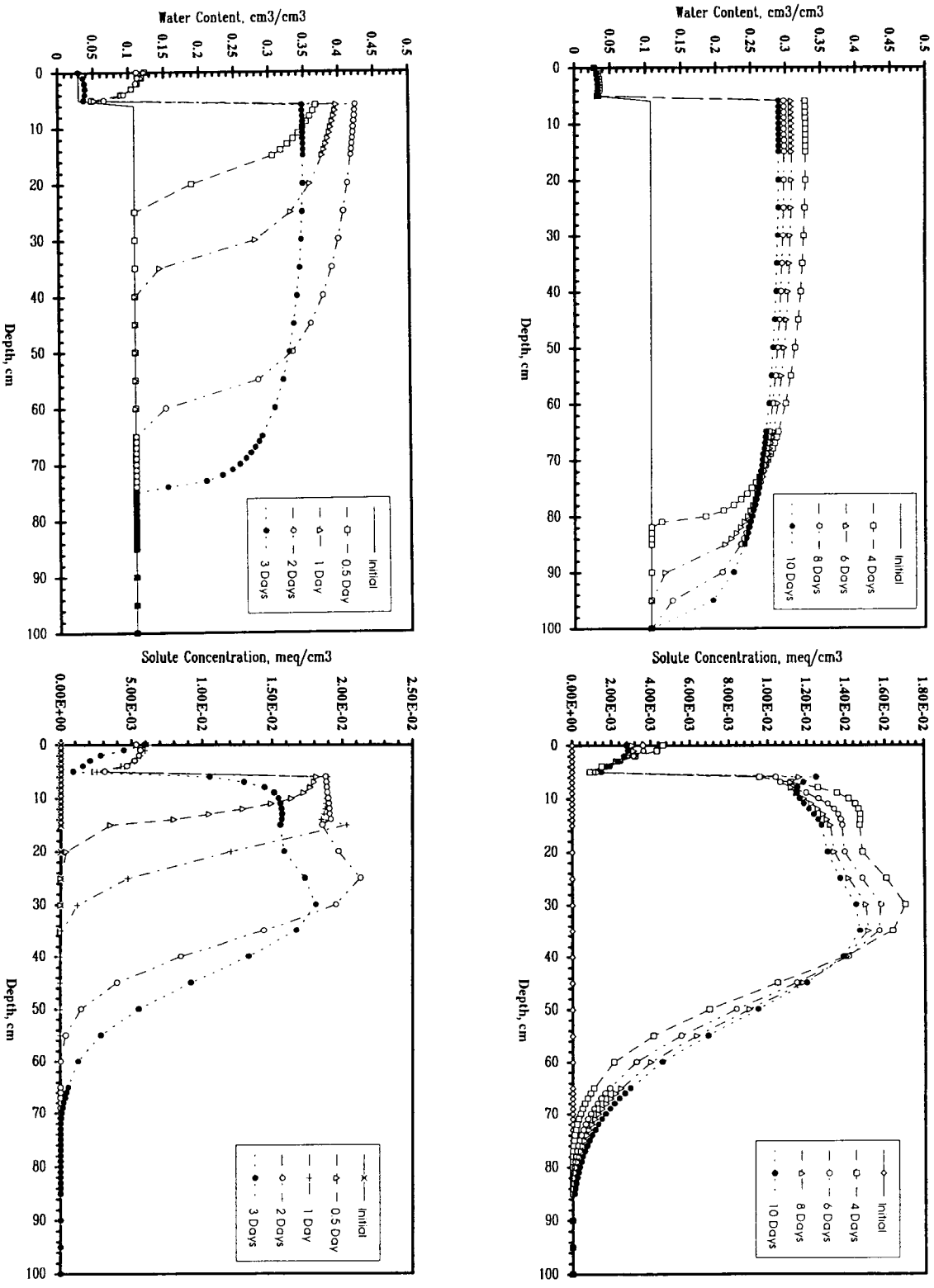

Figure C-24: Water and solute distribution.
(Treatment: 5.5 cm coarse sand mulch layer - evaporation rate = 1.5 cm/day).

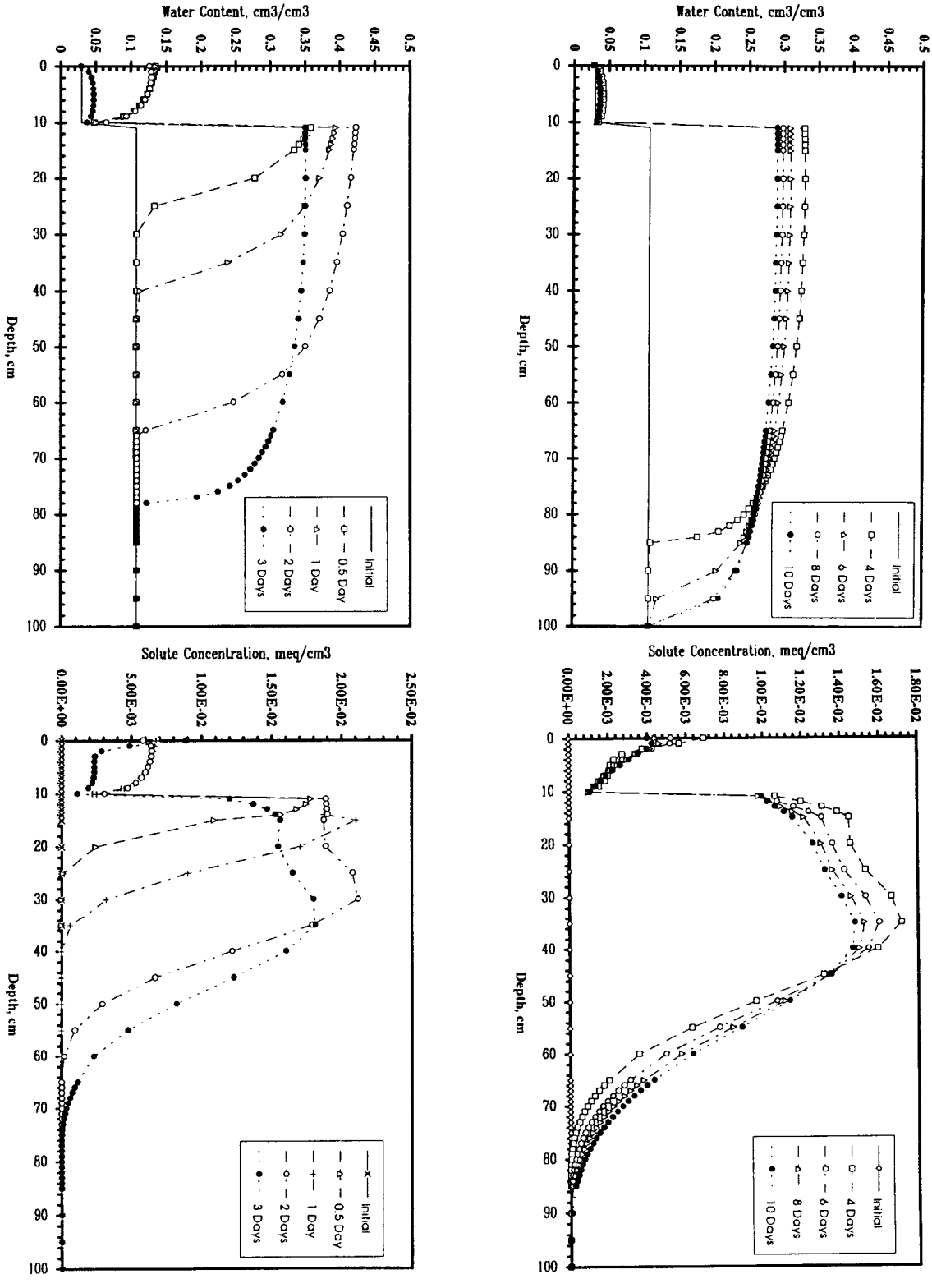

Figure C-25: Water and solute distribution.
(Treatment: 10.5 cm coarse sand mulch layer - evaporation rate = 0.5 cm/day).

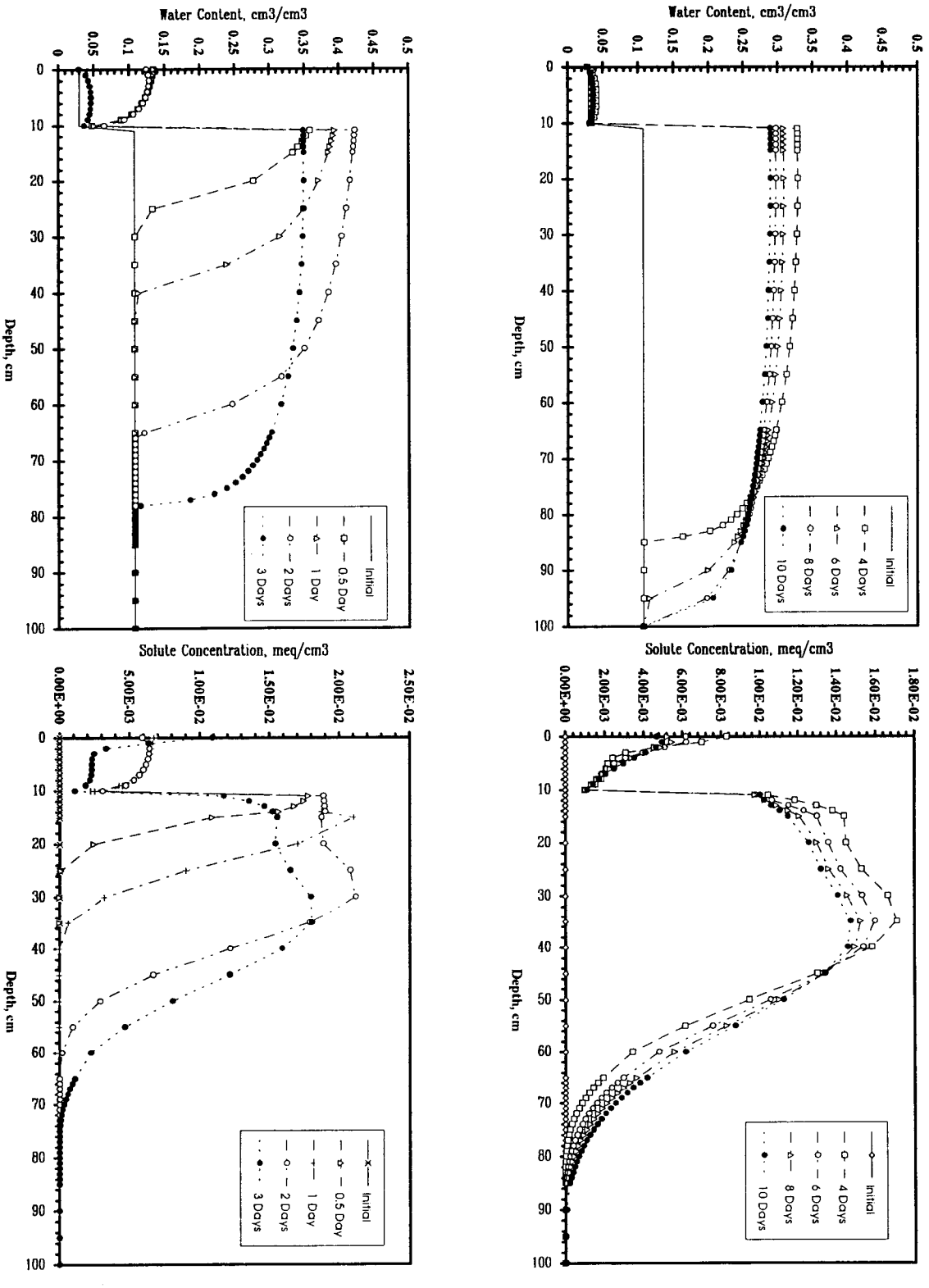

Figure C-26: Water and solute distribution.
(Treatment: 10.5 cm coarse sand mulch layer - evaporation rate = 1.5 cm/day).

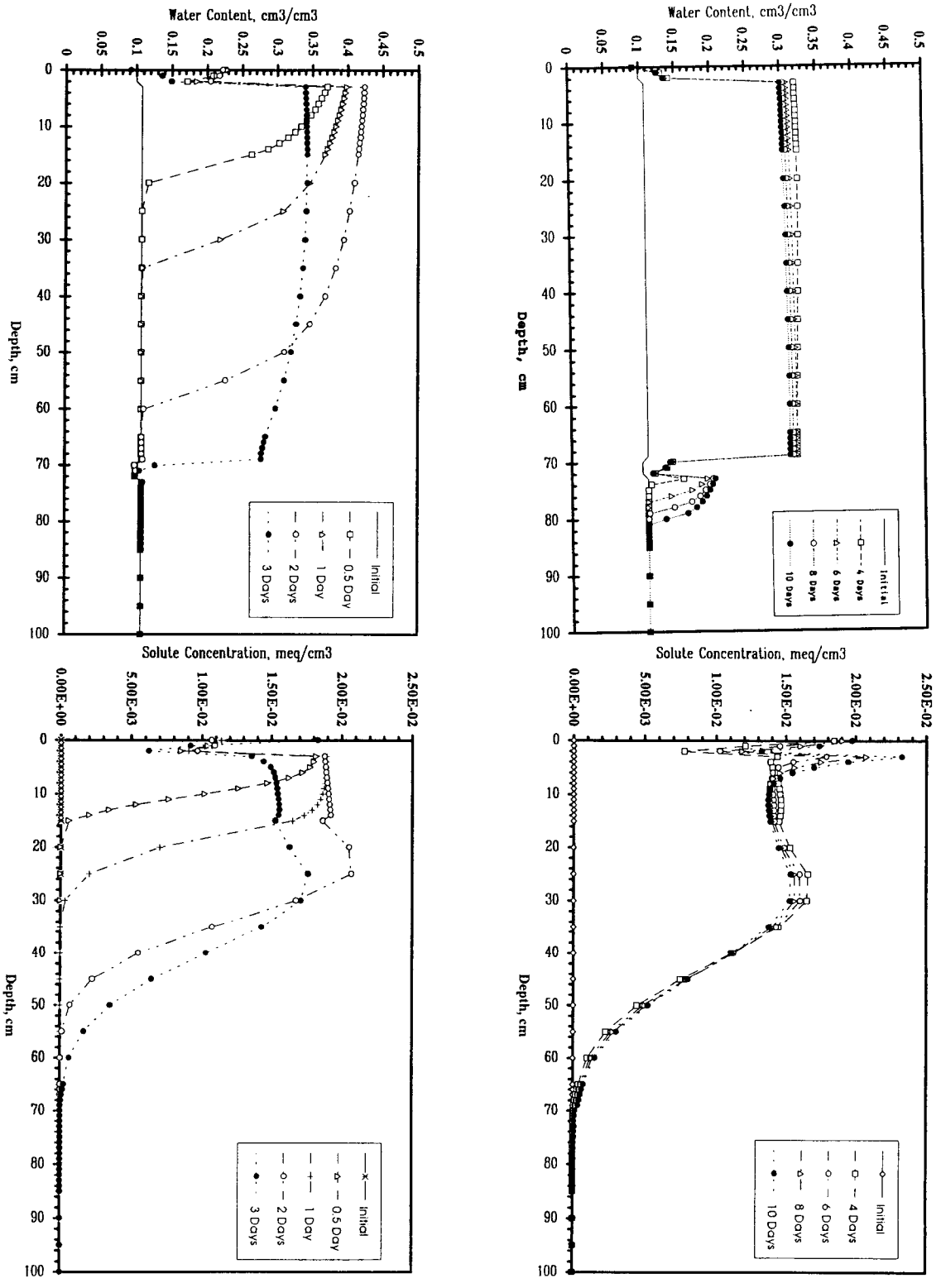

Figure C-27: Water and solute distribution.
(Treatment: 2.5 cm sand barrier and mulch layers - evaporation rate = 0.5 cm/day).

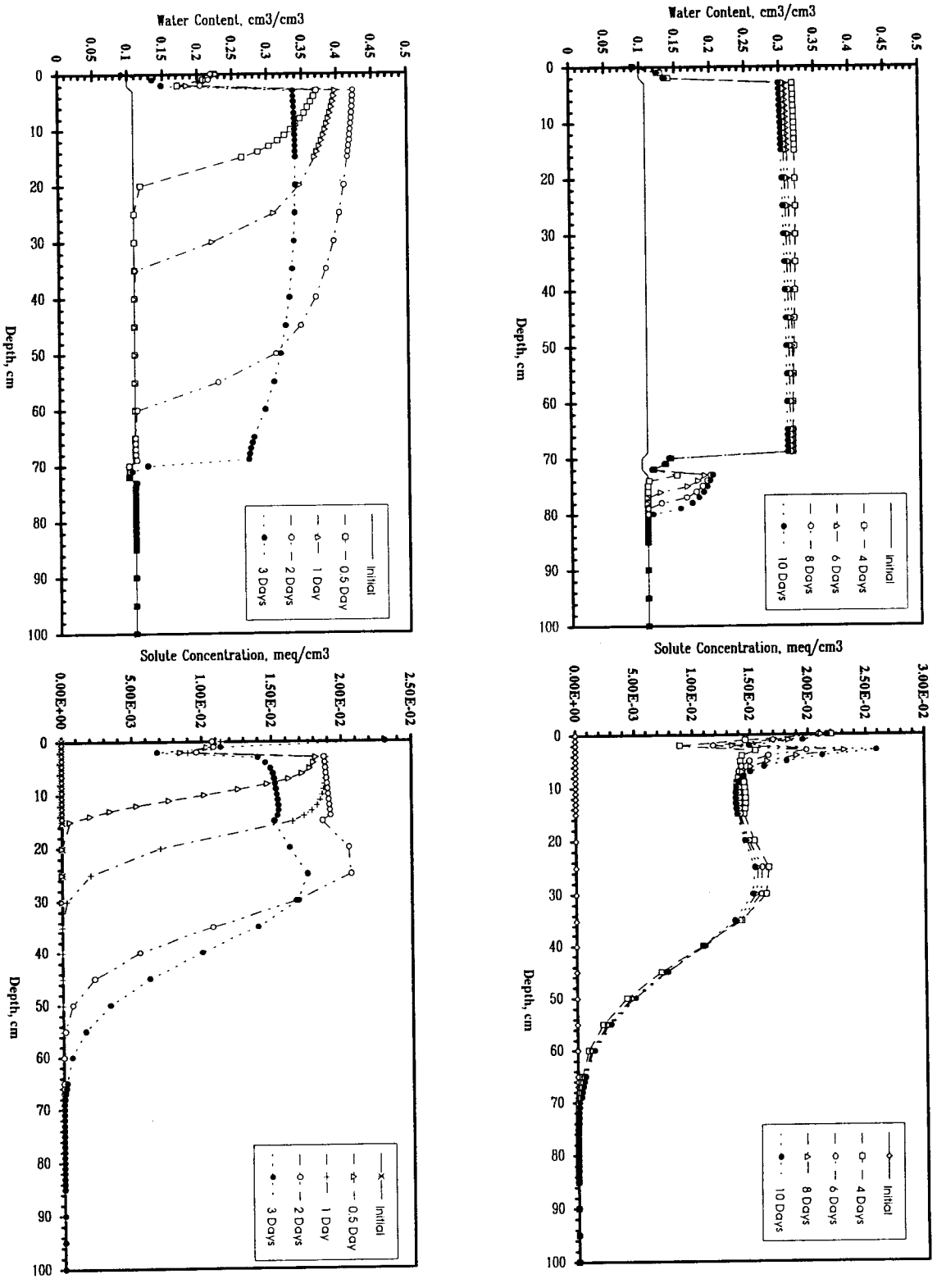

Figure C-28: Water and solute distribution.
(Treatment: 2.5 cm sand barrier and mulch layers - evaporation rate = 1.5 cm/day).

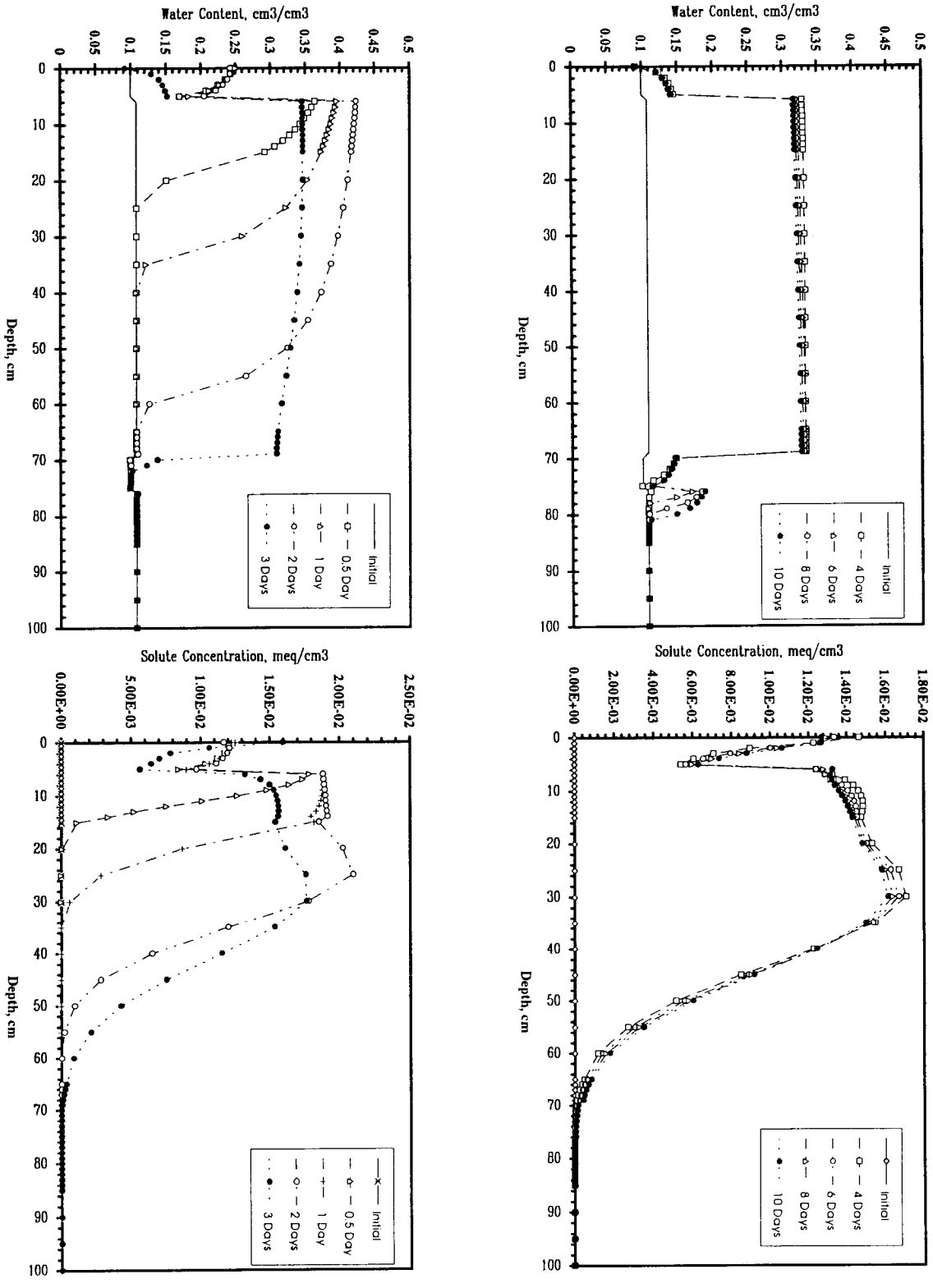

Figure C-29: Water and solute distribution.
(Treatment: 5.5 cm sand barrier and mulch layers - evaporation rate = 0.5 cm/day).

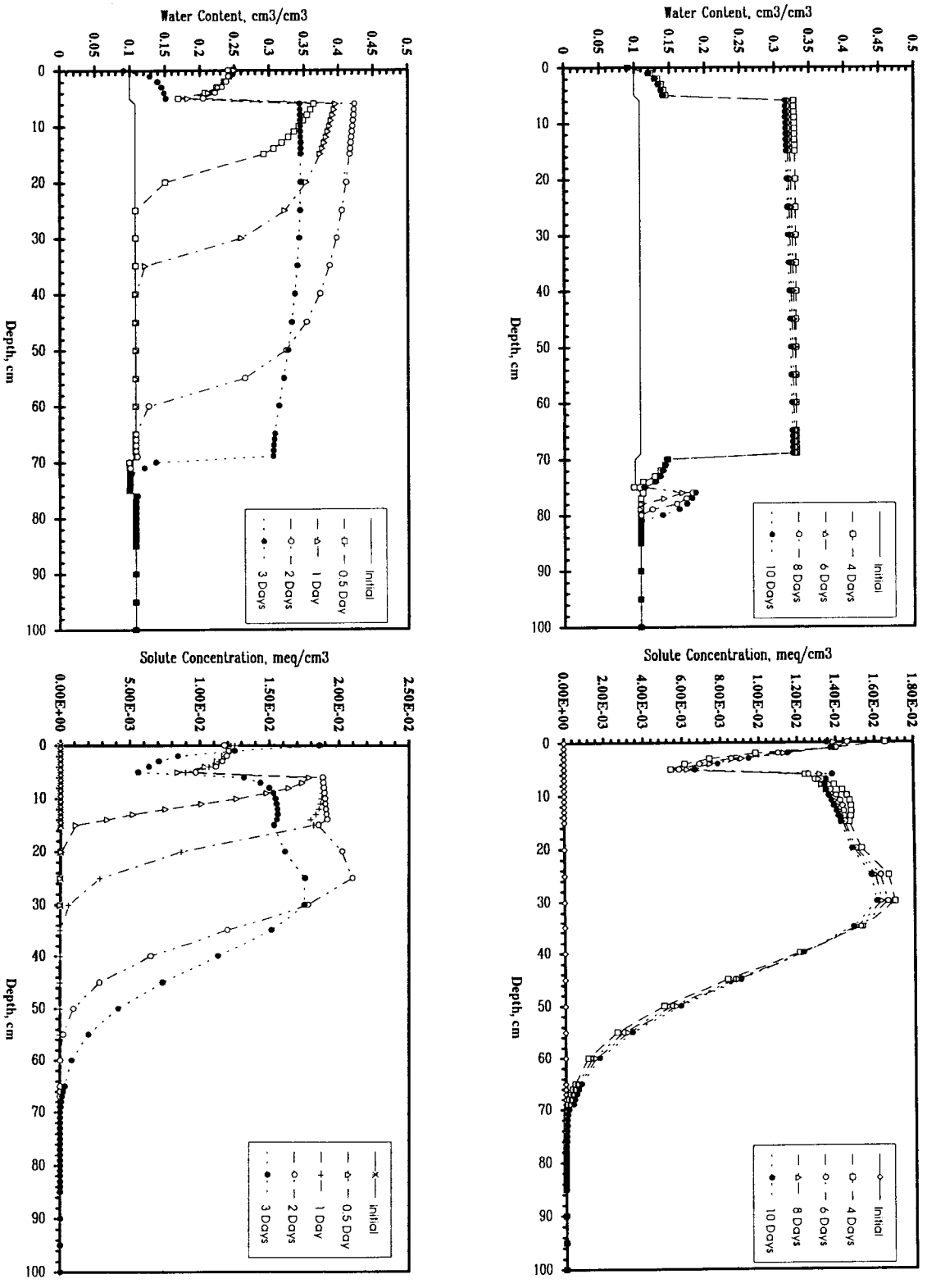

Figure C-30: Water and solute distribution.
(Treatment: 5.5 cm sand barrier and mulch layers - evaporation rate = 1.5 cm/day).

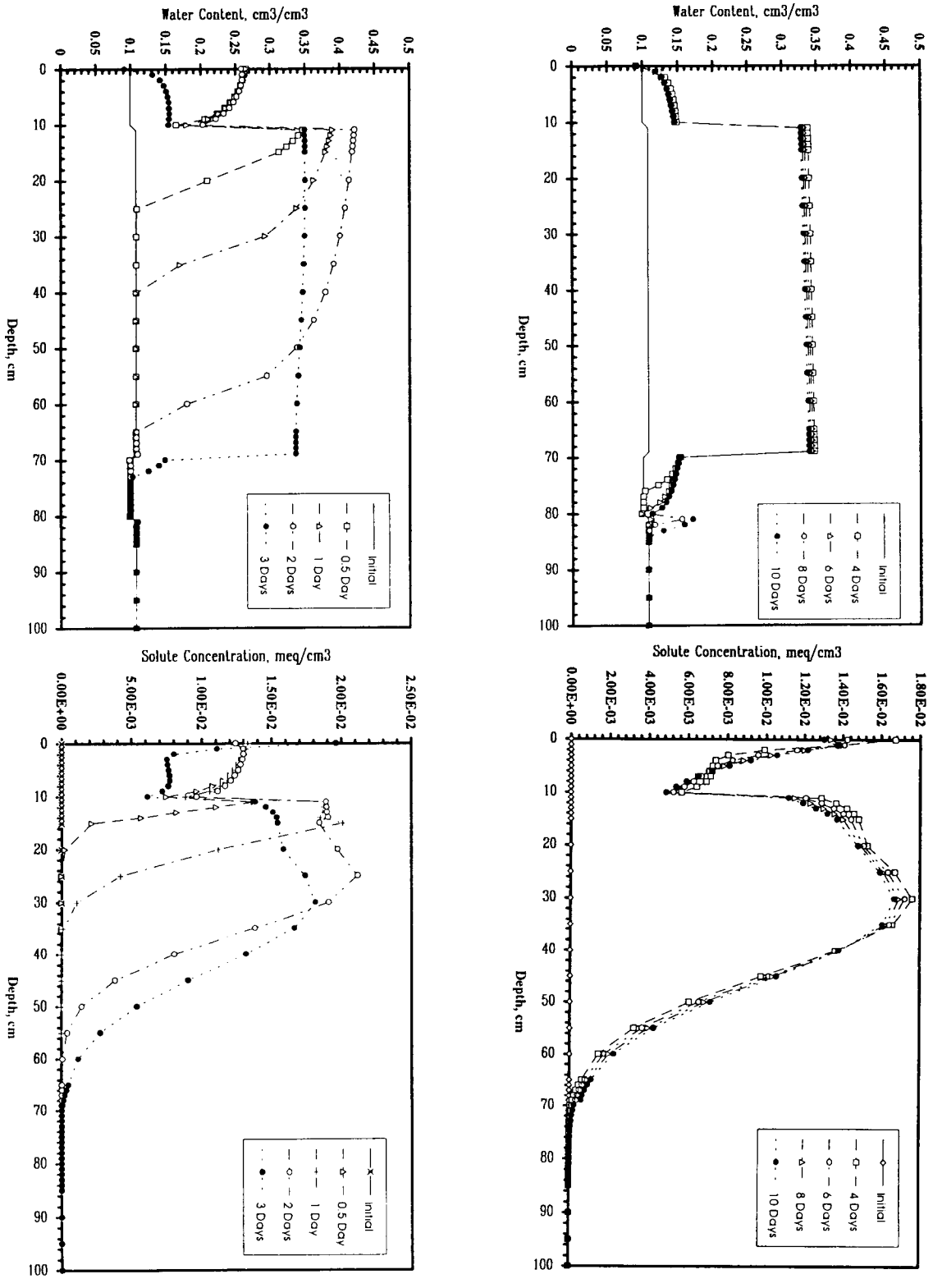

Figure C-31: Water and solute distribution.
(Treatment: 10.5 cm sand barrier and mulch layers - evaporation rate = 0.5 cm/day).

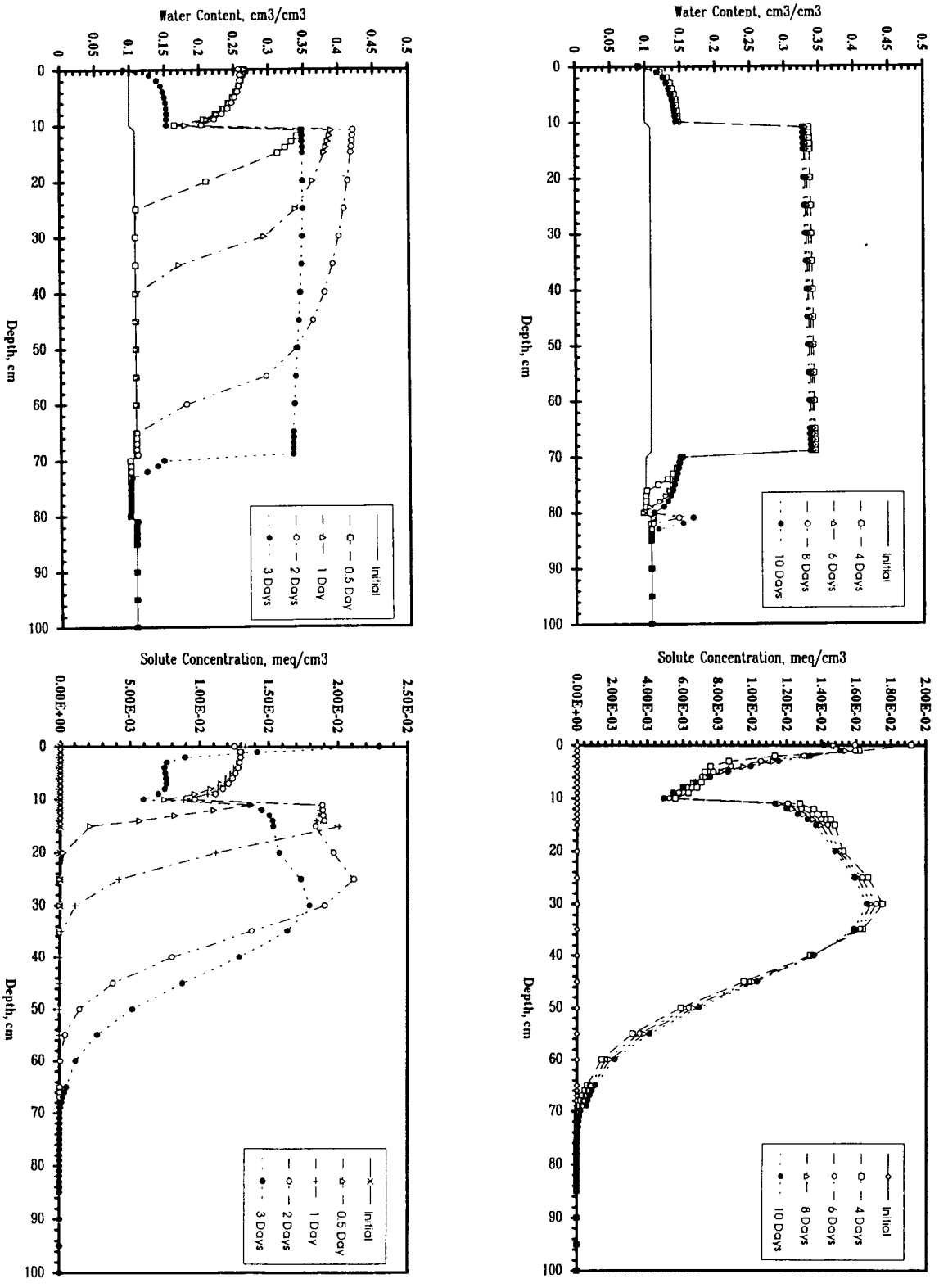

Figure C-32: Water and solute distribution.
(Treatment: 10.5 cm sand barrier and mulch layers - evaporation rate = 1.5 cm/day).

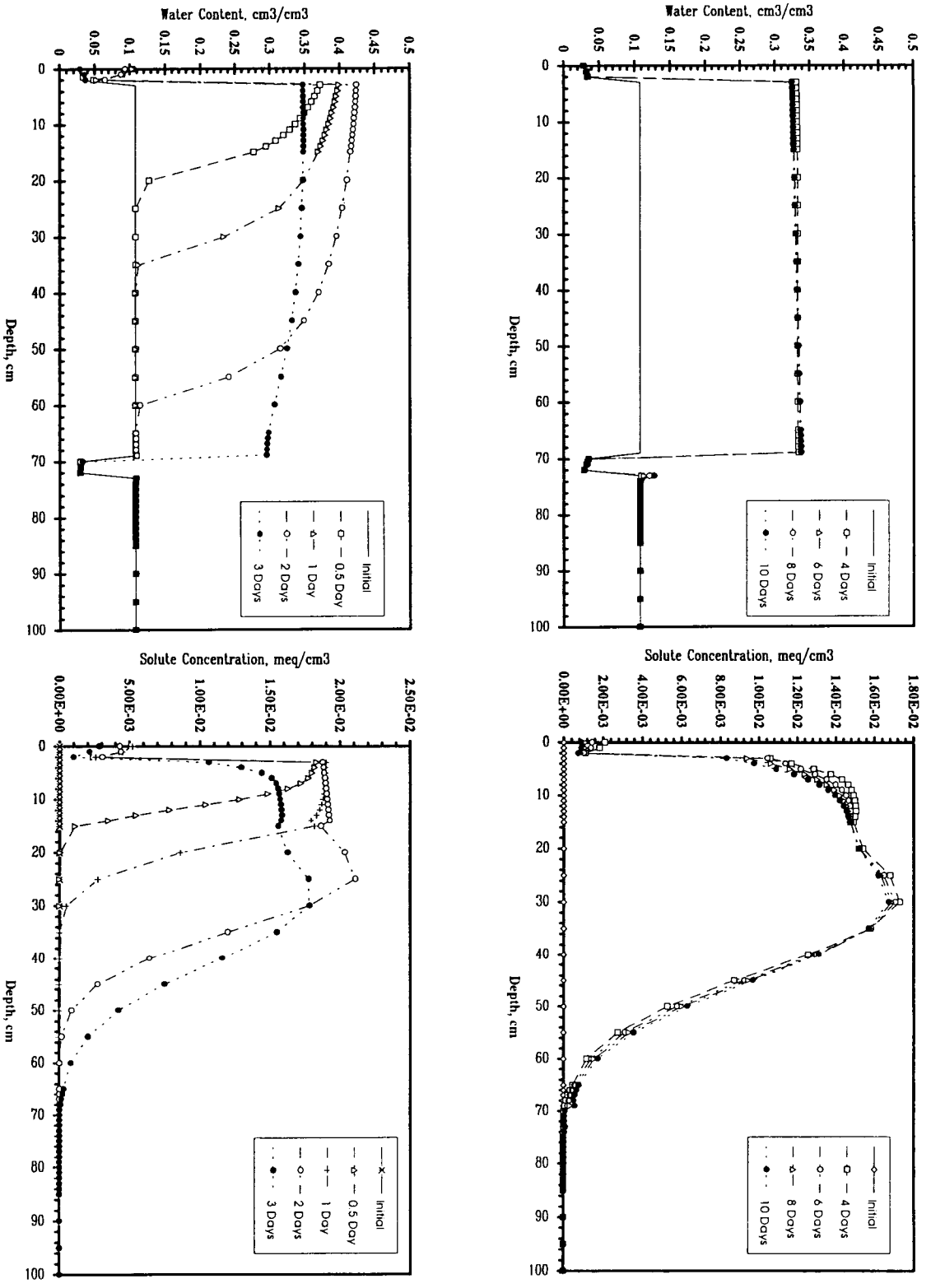

Figure C-33: Water and solute distribution.
(Treatment: 2.5 cm coarse sand barrier and mulch layers - evaporation rate = 0.5 cm/day).

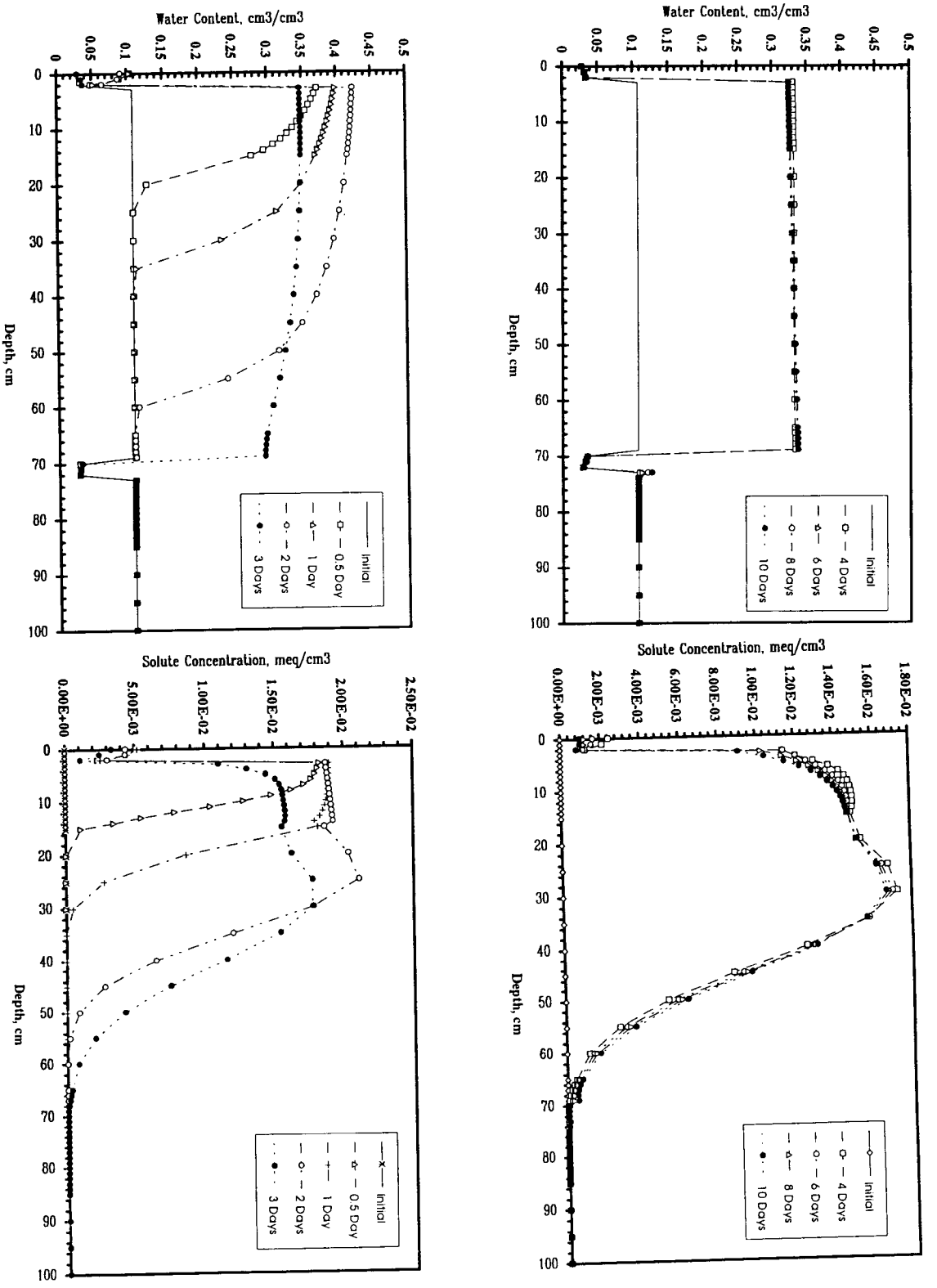

Figure C-34: Water and solute distribution.
(Treatment: 2.5 cm coarse sand barrier and mulch layers - evaporation rate = 1.5 cm/day).

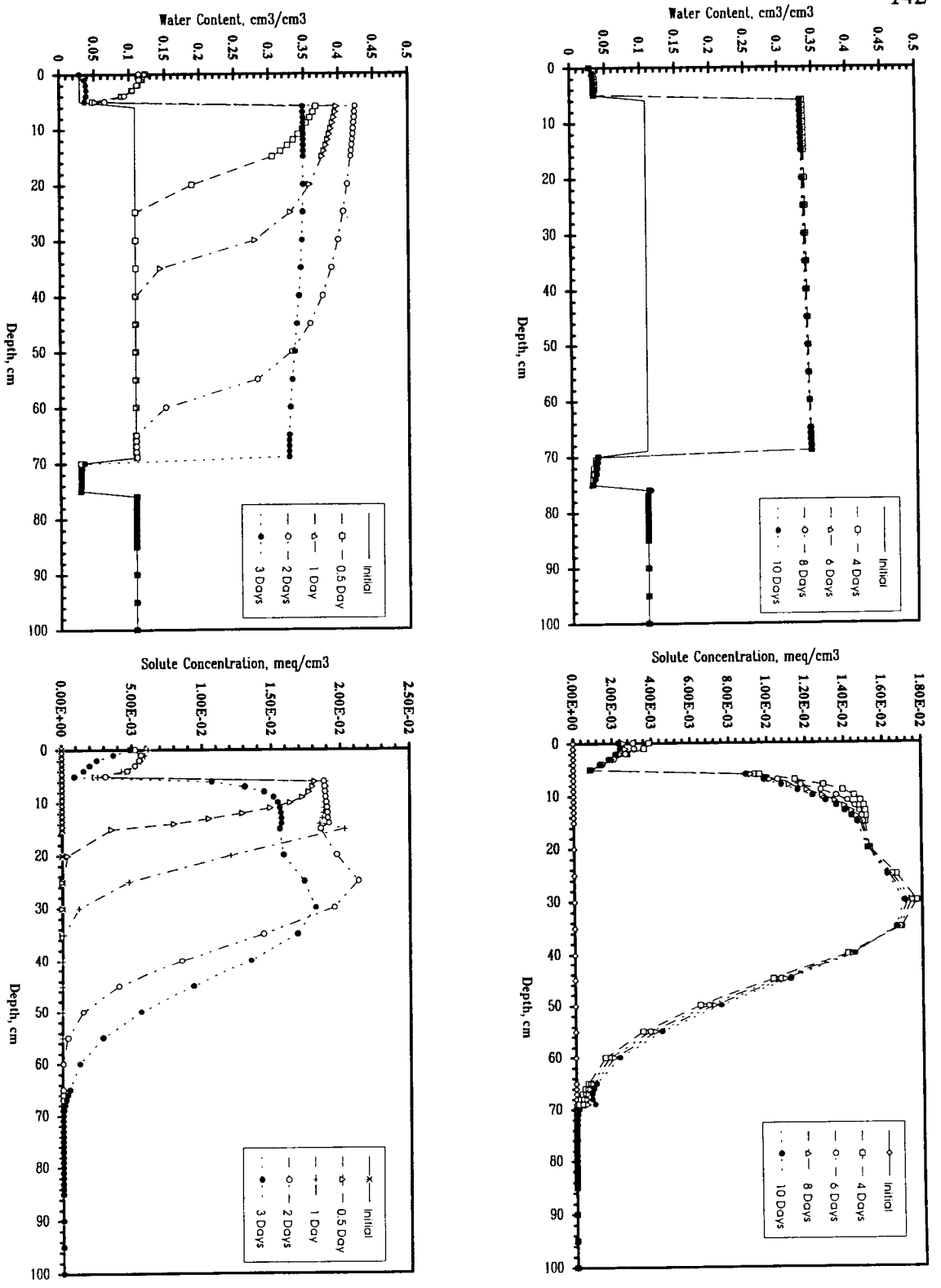

Figure C-35: Water and solute distribution.
(Treatment: 5.5 cm coarse sand barrier and mulch layers - evaporation rate = 0.5 cm/day).

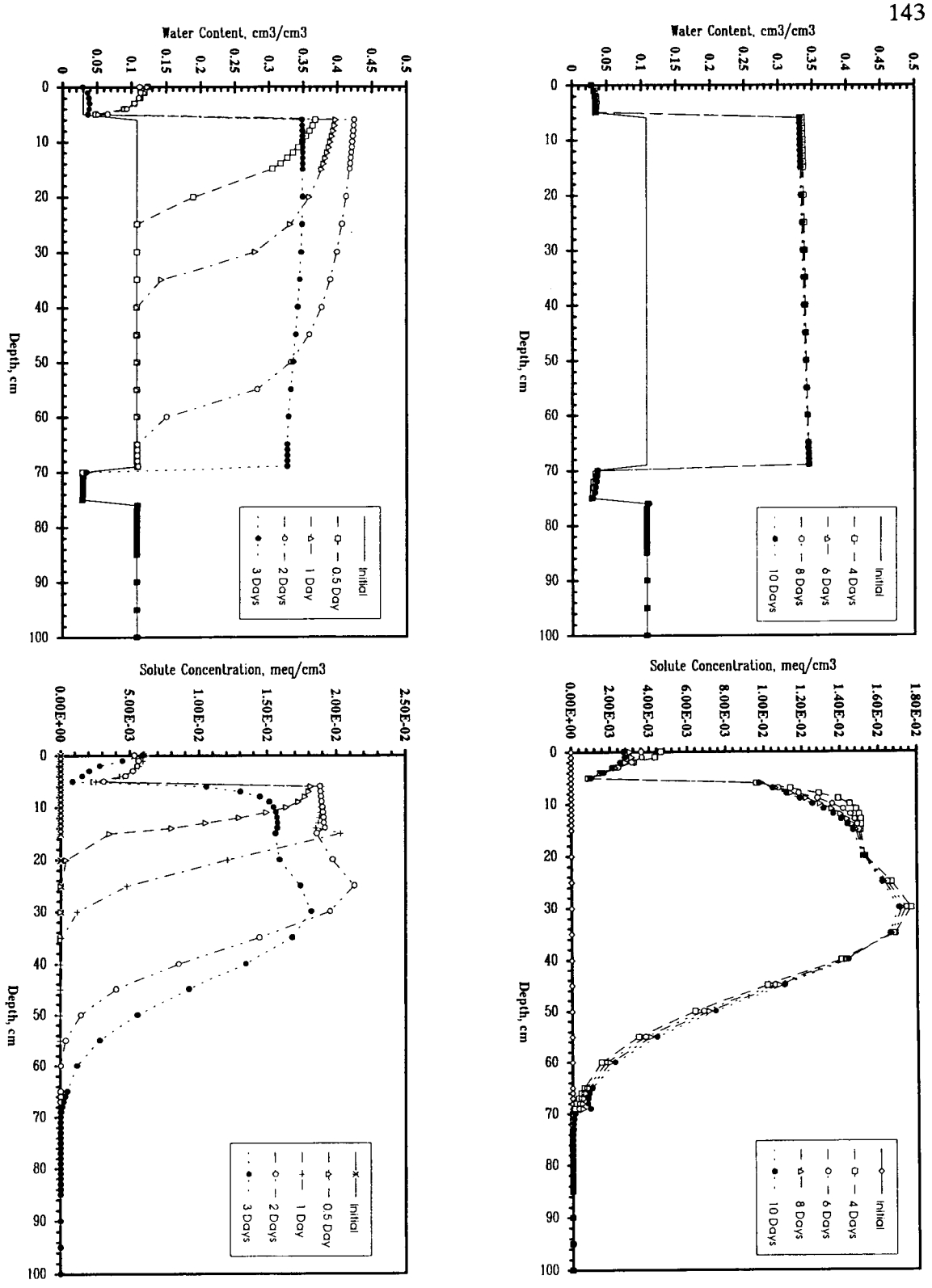

Figure C-36: Water and solute distribution.
(Treatment: 5.5 cm coarse sand barrier and mulch layers - evaporation rate = 1.5 cm/day).

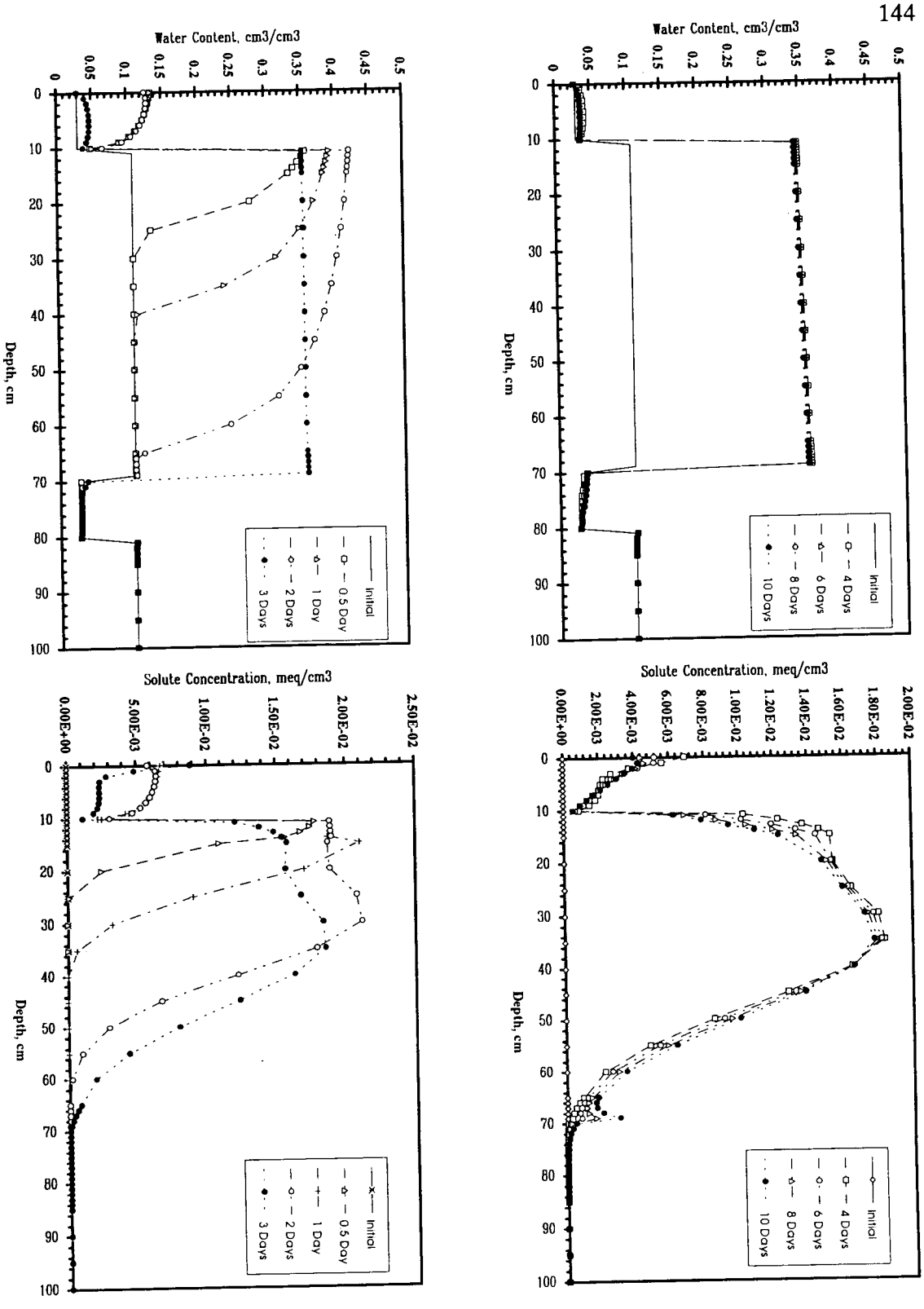

Figure C-37: Water and solute distribution.
(Treatment: 10.5 cm coarse sand barrier and mulch layers - evaporation rate = 0.5 cm/day).

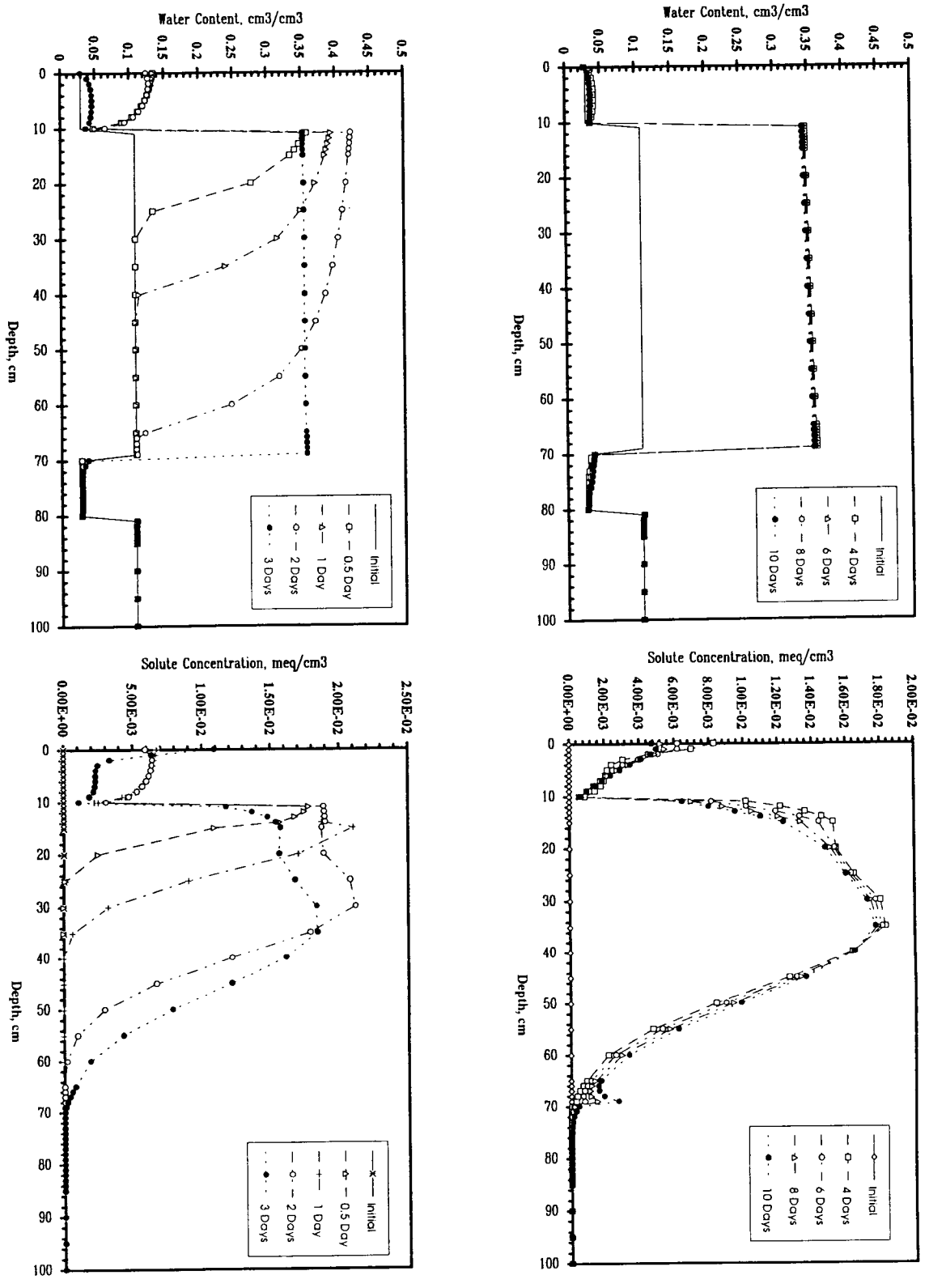

Figure C-38: Water and solute distribution.
(Treatment: 10.5 cm coarse sand barrier and mulch layers - evaporation rate =1.5 cm/day).